Energy and Environment Programme

"Feasibility Study for the Impact of Typhoon on Offshore Wind Farm Operation in China /EEP-PMU/CN/126077/RE003"

Oct.7th2008- Sep.30th2009

Final Technical Report

November 2009

Submission date: **5 November 2009**

Submitted to: **Mr. Frank Haugwitz**

Energy and Environment Project Manager

Submitted by: **National Climate Centre (NCC)**

China Meteorological Administration

Centre for Wind and Solar Energy Resources Assessment (CWERA)

Luo Yong, deputy director of Climate Centre

Zhongguancun South Street 46, Beijing, 100081

Tel : +86-10-68406488

Fax: +86-10-62176804

This project has been produced with the financial assistance of the European Union. The contents of this document are the sole responsibility of the National Climate Center (the beneficiary of this action) and can under no circumstances be regarded as reflecting the position of the European Union.

Prepared by:

Yan Junyue Project leader

Zhang Xiuzhi Key expert, Deputy leader

You Lijun System Developer

Zhang Rongyan Typhoon Expert (Fujian)

Gao Jianyun Wind Resource Expert

Li Qiang Junior Climatologist (1)

Sun Qizheng Junior Climatologist (2)

Wen Ming Zhang GIS Specialist

Yin Yizhou Project Manager 1

Lucie Vaucel Project Manager 2

Yang Xiaosheng Senior Windfarm Engineer

Qu Haibin Windfarm Economist

Xing Xuhuang Local Wind Resource Expert

Wu Jincheng Local Typhoon Expert

Lin Xiufang Local Typhoon Expert (Fujian 1)

Bao Ruijuan Local System Develop Expert (Fujian 2)

Chen Shengjun Local Typhoon Expert

Liang Zhiqiang Local Windfarm Engineer

Wang Xinwen Accountant

Lu Xinyan Project Secretary 1

Baoleer Qimuge Project Secretary 2

Preface and Acknowledgement

The EU-China Energy and Environment Programme (EEP; www.eep.org.cn) was established by a financing agreement between the European Community and the Government of the People's Republic of China signed on April 3rd , 2002. The Programme is designed for a period of 6.5 years of implementation, starting from May 2003 until November 2009.

The Executing Authority for the EU-China Energy and Environment Programme is the Ministry of Commerce of the People's Republic of China (MOFCOM). The Implementing Agencies are the National Development and Reform Commission (NDRC), the Ministry of Science and Technology (MOST), the Energy Research Institute (ERI), and the China National Petroleum Corporation (CNPC).

The overall strategic orientations that the EEP targets are:
(1) to foster the cooperation between Chinese and EU industries in China's energy markets;
(2) to strengthen the security of energy supply in both China and Europe;
(3) to protect the global environment in line with international objectives (in particular in the context of climate change), and to ensure sustainable development.

The EEP is designed to support these overall strategic orientations. Within this context, the EEP is conceptually represented by four components:
1. Energy policy development (EPD)
2. Energy efficiency (EE)
3. Use of Renewable energy (RE)
4. Use of Natural gas (NG)

The specific objectives of the renewable energy component of the EU-China Energy and Environment Programme are to:
(1) Develop policies that promote renewable energy
(2) Develop standards and certification procedures for renewable energy products
(3) Provide training on renewable energy power systems in selected areas
(4) Undertake feasibility studies and demonstration projects to introduce and disseminate relevant new technologies.
In 2007, the EEP had launched a call for proposals comprising purposes of four focal areas of the EEP's Renewable Energy component:
1. Strengthening policy development capacity

2. Development of biomass resources for rural energy provision
3. Development of China’s off-shore wind energy resources
4. Capacity building of village power development in Western China

Under the call, the renewable energy component award grants to support project purpose (2) Development of Biomass Resources for Rural Energy Provision, and project purpose (3) Development of Off-shore Wind Energy Resources.

The National Climate Center was awarded a contract under the priority 'Off-shore Wind Energy Technologies' and started implementing the 12 month action ''Feasibility study for the impact of typhoon on offshore wind farm operation in China' in October 2008. The final report in hands delivers the results of the EU-funded action.

This project has been produced with the financial assistance of the European Union. The contents of this document are the sole responsibility of the National Climate Center, the beneficiary of this action, and can under no circumstances be regarded as reflecting the position of the European Union.

This project would have not been feasible without the grant of the European Union and the active support of the EU-China Energy and Environment Programme (EEP) whose experts provided with constant assistance on both technical and administrative issues.

Abstract

Background

China's offshore area is an important economic development area. Energy shortage has been the bottleneck of its development. China has abundant coastal wind energy resources. The development of coastal wind energy resources is of utmost importance in order to alleviate the tension of electricity in offshore areas and to reduce the emission of greenhouse gases.

However, China's offshore area is an area with frequent tropical cyclones (TC) activities. Strong wind, ocean wave, storm tide, and other severe weathers caused by TC always damage wind farm and offshore projects. For example No.8 typhoon in 2006 "Saomai" landed at Cangnan County, Zhejiang Province. When it landed, the maximum wind power near its center was 68m/s(50 m high). Some vanes were broken and some tower drums just broke or collapsed. A loss of about 70 million Yuan was caused. Therefore, the influences of TC must be taken into account for wind power development in southeast coastal regions which have frequent TC activities. This is the major difference between Chinese climate and European climate.. The wind turbine and IEC standards should be adapted to the climate characteristics of China, especially in the Chinese areas influenced by TC.

Researching Goals

- Through the analysis and study of Tropical Cyclones (TCs) impacting China's coast and offshore from 1961 to 2007, get the frequency of occurrence of typhoon wind speeds in different wind turbine safety classes and design wind speeds of 1/50-year frequency, the maximum change of wind direction and wind vertical change during typhoon process;

- Using mesoscale model and microscale model, conduct wind speed, wind direction and turbulent flow simulation test in complicated landform and flat landform, study the wind field simulation method for the influence of the wind farm by typhoon, and provide scientific basis for site selection of the wind farm, wind turbine arrangement and losses evaluation;

- Compile an Anti-Typhoon Manual to guide managing personnel of the wind farm to reasonably defend the typhoon.

Estimated Results

- Obtain the wind speed of 1/50-year frequency of WTGS safety class on coastal measurement stations and offshore in resolution of 50km*50km, and provide references for wind turbine design, site selection for the wind farm and the risk of resisting typhoon by the wind farm;

- Obtain rule of wind direction change and wind vertical change during typhoon process, and provide scientific basis for site selection, wind farm operation and reasonable defending of typhoon by managing personnel of the wind farm;

- Establish the Retrieval System of typhoon at offshore wind farms in China. Users can search the TC extreme wind speed and engineering design maximum wind speed of 1/50-year frequency;

- Study wind speed, wind direction and turbulent flow characteristics in complicated landform and flat landform, study the wind field simulation method for the influence of the wind farm by typhoon, and provide scientific basis for site selection of the wind farm, wind turbine arrangement and losses evaluation

- Compile an Anti-Typhoon Manual to guide managing personnel of the wind farm to reasonably defend the typhoon.

The main results of the project

In-depth study was carried out according to the expected goals and working plan, as follows:

Result 1: Accomplish the statistics of the tropical cyclones affecting offshore and Coast region of China during 1971-2007, analyze the source region, moving paths, landing point and the characteristics of the wind field of tropical cyclone; Calculate TC wind field entering into the Coast of China at 0.5°×0.5° mesh point by using Asymmetric Typhoon Wind Field Mode, calculate the maximum wind speeds of 1/50-year frequency at all mesh points according to the gale series.

Result 2: Ground, 50m height and 70m height horizontal wind field, near ground turbulence intensities, vertical wind shear law under the influence of tropical cyclone, especially the wind field, turbulence intensity and characteristics of vertical wind shear of 3 typical tropical cyclones are analyzed

by using the observed data from more than 80 anemometer towers.

Result 3: Set up a searching system for TCs that affect wind-power development in offshore China.

Result 4: Using WRF meso-scale numerical model in topography sensitivity experiment, theoretically explain the changing mechanism of the intensity of tropical cyclone under the influence of Taiwan topography and sea surface flat landform.

Result 5: Compile a book “Effect of Typhoon on China Wind Power Development and Solutions”, 6 chapters in all , respectively:

Chapter 1 – Climate characteristics of tropical cyclone affecting China mainland coastal and offshore area

Chapter 2 – Characteristic analysis of tropical cyclone wind field

Chapter 3 – Effect of tropical cyclone on wind power development

Chapter 4 – Strategy resisting typhoon in coastal wind power development

Chapter 5 – Emergency management resisting typhoon in wind farms

Chapter 6 –Emergency management resisting typhoon in wind farms

Expected targets have been successfully fulfilled with the following innovative achievements in the project:

- Statistical analysis of the tropical cyclones landing on China mainland has been conducted in 8 regions, and the times of landing of the tropical cyclones in coastal areas of Zhejiang Province and those in the north of Fujian Province have obviously increased. An obvious decrease in times of landing thereof has taken place in offshore areas in the north of Zhejiang Province, and in central and southern parts of Fujian Province. The costal areas on the east of Pearl River estuary almost remains unchanged over the time, while a declining momentum has taken place in western Guangdong Province, Leizhou

Peninsula and Hainan islands area.

- The maximum in-process wind series of the tropical cyclones at the mesh points 50km×50km in offshore areas of China have been calculated by the asymmetrical wind field model of typhoon, as well as the distribution of the maximum wind speeds of the strongest wind in 50 years and the frequencies of the occurrence of wind speeds in various operational levels of the wind turbines. .

- The horizontal wind fields, the vertical shear of winds, strength of turbulent flow during 19 periods under the influence of tropical cyclones have been analyzed with the data of 85 wind towers and a great deal of ground meteorological data, and the characteristics of variation in the vertical shear of winds and strength of turbulent flow in case of various distances to the center of the tropical cyclones, various terrains, various lower surfaces and wind directions.

- It can be seen that typhoon moves quickly in case of no terrain factor with the meso-scale numerical model WRF and test of terrain sensibility. The terrain of Taiwan causes typhoon to weaken about 3 hours before landing, and the power and source of heat of typhoon on which it depends for maintenance or development are influenced by the terrain there after landing of the typhoon, which renders the power and structure of thermal field asymmetrical. The higher the terrain is, the more obvious the asymmetry is, the faster and fiercer the “eye area” is filled and the more incomplete the structure of the “eye wall” is.

“Influences of Typhoon on Offshore Wind Power Development in China and Countermeasures” addresses the scientific issues and demands of coastal and ocean wind power development, and conducts gradual in-depth presentation of the climatic characteristics of the tropical cyclones influencing coastal areas and offshore areas of China mainland. It expounds the characteristics of the wind field of tropical cyclones and analyzes the influences of tropical cyclones on wind power development, the countermeasures against typhoon in costal wind development and emergency control of typhoon wind power fields through integrating the experience of the typhoon experts and wind power experts. In addition, it features novel contents, a well-knit structure with both illustrations and texts of both informativeness and readability.

Contents

Feasibility Study for the Impact of Typhoons on Offshore Wind Farm Operation in China

1 BASIC SITUATIONS OF THE PROJECT

1.1 Background

The offshore of China is an important economic development area. Energy shortage has been the bottleneck of its development. China has abundant coastal wind energy resources. The development of coastal wind energy resources is an important way in alleviating the tension of electricity in offshore areas and in reducing the emission of greenhouse gases.

However, the offshore of China is the area with frequent tropical cyclones (TC) activities. Strong wind, ocean wave, storm tide, and other severe weathers caused by TC always damage wind farm and offshore projects. For example, No.13 typhoon "Dujuan" was formed on August 29, 2003. It grew stronger in its way to the west. At 19:50 on September 2, it landed at Huidong at the west bank of Honghai Gulf. When it is landed, the maximum wind power at its center is grade 12, which is the strongest wind at Shanwei area in the last thirty years. Thirteen of the twenty-five wind turbines in Honghai Gulf Wind Farm which was just constructed and put into production were damaged in different degrees. No.8 typhoon "Saomai" was formed in the southeast coastal region of Guandao on August 5, 2006. It was landed at Mazhan Town, Cangnan County, Zhejiang Province at 17:25 on August 10. When it was landed, the maximum wind power near its center was 68m/s(50 m high), which is the strongest typhoon since the founding of new China. The center of this typhoon directly stroke Cangnan Wind Farm at 17:25 on August 10. Some vanes were broken and some tower drums are broken or collapsed. A loss of about 70 million Yuan was caused (Influences and Inspiration of Saomai Typhoon, Wu Jincheng, China Wind Power No.2 in 2008). Therefore, the influences of TC must be taken into account for wind power development in southeast coastal regions which has frequent TC activities. This is the major difference between the climate of China and the climate of Europe.

Facing with the fast increase for the development of coastal wind farm and the offshore wind farm, the wind turbine and IEC standards should adapt to the climate

characteristics of China, especially the one influenced by TC. Developers of wind power in southeast coastal and offshore regions should get to know its extreme design wind conditions when developing wind farm. They should master TC preventive measures and scientific defending methods during the operation of the wind farm. A series of studies will be unfolded for the above problems in this task to provide scientific basis for site selection of wind farm and wind turbine design, to provide basic methods and preventive measures for correctly resisting the attack of the wind farm by typhoon, and to provide scientific methods for reasonably evaluating the influences of typhoon to the wind farm.

1.2 Researching goals and estimated results

Researching Goals

- Through the analysis and study of Tropical Cyclones (TCs) impacting China's coast and offshore from 1961 to 2007, get the frequency of occurrence of typhoon wind speeds in different wind turbine safety classes and design wind speeds of 1/50-year frequency, the maximum change of wind direction and wind vertical change during typhoon process;

- Using mesoscale model and microscale model, conduct wind speed, wind direction and turbulent flow simulation test in complicated landform and flat landform, study the wind field simulation method for the influence of the wind farm by typhoon, and provide scientific basis for site selection of the wind farm, wind turbine arrangement and losses evaluation;

- Compile an Anti-Typhoon strategy Manual to guide managing personnel of the wind farm to reasonably defend the typhoon.

Estimated Results

- Obtaining the wind speed of 1/50-year frequency of WTGS safety class on coastal measurement stations and offshore in resolution of 50km*50km, and provide references for wind turbine design, site selection for the wind farm and the risk of resisting typhoon by the wind farm;

- Obtaining rule of wind direction change and wind vertical change during typhoon process, and provide scientific basis for site selection, wind farm operation and reasonable defending of typhoon by managing personnel of the wind farm;

- Establishing the Retrieval System of typhoon at offshore wind farms in China. Users can search the TC extreme wind speed and engineering design maximum wind speed of 1/50-year frequency;

- Studying wind speed, wind direction and turbulent flow characteristics in complicated landform and flat landform, study the wind field simulation method for the influence of the wind farm by typhoon, and provide scientific basis for site selection of the wind farm, wind turbine arrangement and losses evaluation

- Compiling an Anti-Typhoon strategy Manual to guide managing persons of the wind farm to reasonably defend the typhoon.

2 RESULTS 1 CALCULATION OF DESIGN WIND SPEED OF 1/50-YEAR FREQUENCY ON COASTAL MEASUREMENT STATIONS AND OFFSHORE

2.1 Basic characteristics of TC influencing China's coast

2.1.1 Occurrence frequency of TC at coastal regions of China

By using the data of TC central locations, air pressures and wind speeds from 1961 to 2007 obtained from Shanghai Typhoon Institute of China Meteorological Administration, make statistics of TCs in the range of 15°N - 45°N and 105°E - 130°E. It is found out that 579 TCs entered into this region from 1961 to 2007. The intensity of TC is represented by maximum wind speed at the center of TC. Its grade is classified according to new standard of WMO (table 2.1). From table 2-1, we can see that, typhoon and severe topical storms occur the most with the frequencies of 23.7% and 21.6%, and the total frequency is 45.3%. The frequencies of super typhoon and severe typhoon account for 15.2% and 12.1%, separately. TC with this intensity will bring damages to the wind farm and other coastal projects.

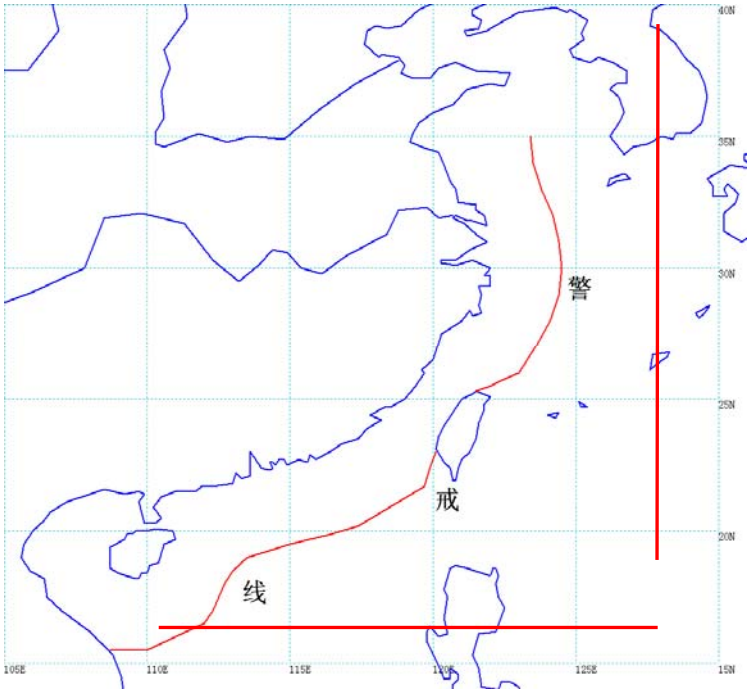

Figure 2.1 the map of study area

To fully understand the distribution of TCs which enter this region, 579 TCs in this area are selected. Their frequencies of occurrences are accounted according to 0.5°×0.5° mesh. The frequencies of occurrences of TCs with different intensities are provided (see Fig.2.1). From Fig. 2.1a and 2.1b, we can see that, the most TC and TC with the intensity of stronger than tropical storms occur over the ocean of the east of Taiwan, and over the sea of the north of Guangdong and east of Hainan (Fig. 2.1c). the most super typhoon occur on the ocean of the east of Taiwan, and most times they enter into the offshore at the east of Guangdong, Taiwan island, south and north of Fujian, and offshore at the south of Zhejiang (Fig.2.1d).

Table 2-1 Intensity grade standard and occurrence frequency of TCs entering into the selected region

Wind speed (m/s)	Wind power (grade)	Name	15° - 45°N，105° - 130°E	The frequency entering warning area	Landing frequency
≥51	≥16	Super typhoon (super TY)	**88**	**34**	**5**
41.5-50.9	14~15	Severe typhoon (severe TY)	**70**	**58**	**27**
32.7-41.4	12~13	Typhoon (TY)	**137**	**144**	**111**
24.5-32.6	10~11	Severe tropical storm (severe TS)	**125**	**110**	**119**
17.2-24.4	8~9	Tropical storm (TS)	**58**	**44**	**53**
10.8－17.1	6~7	Tropical depression (TD)	**101**	**38**	**46**

2.1.2 Characteristics of TC tracks at offshore of China

For coastal wind farm, it is really challenging to defend severe TCs. Therefore, thorough analysis of TC movement law has great significance to the safety operation of wind farm.

The dominate tracks of TCs with different intensities entering into the researching region are shown in Fig.2.2. We can see that, super typhoons are mainly generated on northwest Pacific Ocean and landed at the south and north of Fujian coast (Fig.2.2a). Severe typhoons are mainly TCs which are generated on northwest Pacific Ocean (Fig.2.2b). There three common tracks are directly entering into Zhejiang coast from northwest Pacific Ocean, or entering into Fujian central coast while passing from Taiwan, or generated on Nanhai Sea, landed at Hainan and then Leizhou Peninsula. Three common movement tracks of TCs with typhoon intensity are generated on southwest Pacific Ocean and landed at the west of Guangdong, or generated on Nanhai Sea and landed at Hainan, or went north from southwest

Pacific Ocean, passing through Taiwan island and entering into Fujian coast (Fig.2.2c). TCs with the intensity of severe tropical storm include southwest Pacific Ocean TCs and Nanhai Sea TCs. TCs generated on southwest Pacific Ocean entered into Nanhai Sea through Philippines (Fig.2.2d), and most of them are landed at the west of Guangdong and Hainan.

2.1.3 Characteristics of TCs landed at coast region of China mainland

Taken the maximum wind speed within six hours before the landing as the intensity of landed TC and divided into 14 regions according to land lots (see table 2.2), the frequencies of occurrences of landed TCs with various intensities are accounted.

From the table we can see that, the region with the most landed TCs is Hainan, which accounts for 25.81% of the total landed TCs in the whole country. The frequency of super typhoon and severe typhoon is 2.15%, and the frequency of typhoon and severe tropical storm is 13.17%. The secondary place is the east of Guangdong (including those landed at Zhujiang estuary), which accounts for 20.43% of the total landed TCs in the whole country. The frequency of super typhoon and severe typhoon is 1.61%, and the frequency of typhoon and severe tropical storm is 13.17%.

The frequency of super typhoon landed at central south of Fujian, south of Zhejiang, east of Guangdong, and Hainan coast is large. Enough attentions should be paid to the construction of wind farm.

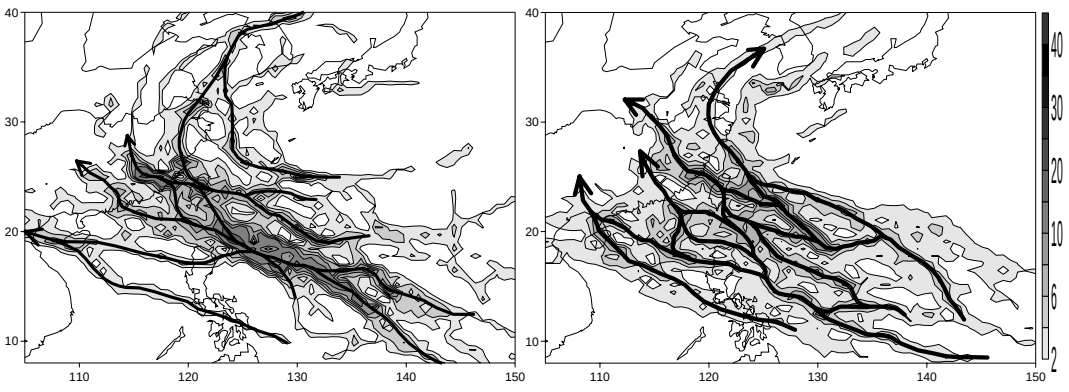

(a)Super typhoon (b)Severe typhoon

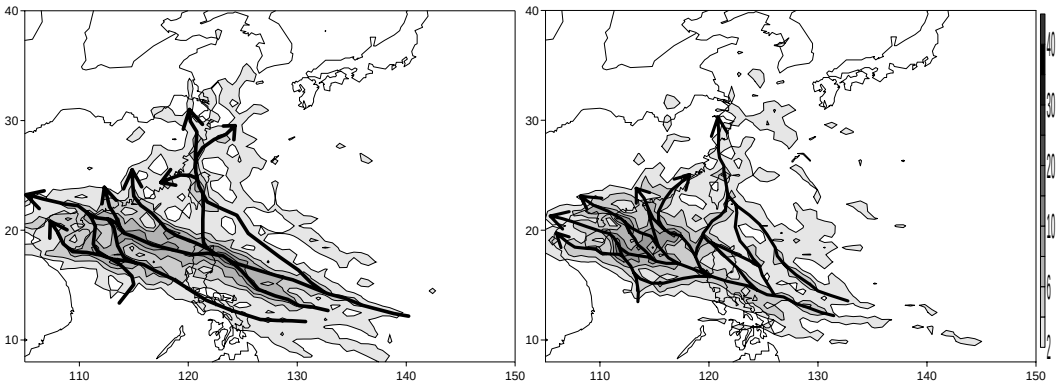

(c)Typhoon (d) Severe tropical storm

Fig.2.2 Dominate tracks of TCs with various intensities

Table 2.2 Intensities and frequencies of TCs landed at various regions (%)

region	Super typhoon	Severe typhoon	Typhoon	Severe tropical storm	Tropical storm	Total
Hainan	0.54	1.61	7.26	5.65	2.96	2.15
Leizhou Peninsula	-	0.81	1.61	2.69	1.08	0.81
West of Guangdong	-	0.54	3.76	5.65	2.42	0.54
Zhujiang estuary	-	0.54	2.15	1.34	1.34	0.54
East of Guangdong	0.27	0.81	4.57	5.65	1.61	1.08
South of Fujian	-	0.54	0.81	0.27	1.08	0.54
Central of Fujian	0.27	0.27	5.11	2.69	2.69	0.54
North of Fujian	-	0.54	1.08	2.96	0.27	0.54
Zhejiang	0.27	1.61	2.96	2.69	0.81	1.88
Shanghai	-	-	0.27	0.27	-	-
Jiangsu	-	-	0.27	0.27	-	-
Shandong	-	-	-	1.34	-	-
Liaoning	-	-	-	0.27	-	-
Guangxi	-	-	-	0.27	-	-
Total	1.34	7.26	29.84	31.99	14.25	100

2.2 Calculating TC wind field entering into the coast of China by using asymmetric typhoon wind field model

TC strong wind series at certain sea area was obtained through directly choosing the maximum wind speed at the center of TC passing that area. TCs with strong intensity, large gale diameter, passing through this sea area but has great influences to that sea area are always missed. Therefore, gale distribution of all mesh points in the scope affected by the TC marching process is calculated by using typhoon wind field mode and the variation law of TC gale at all mesh points is accounted.

The research shows that, when TC is moving on an open ocean, its gale distribution is close to circular symmetry. With its approaching to the land, the wind field becomes asymmetric distribution from the original circular symmetry. Therefore, it is very important to select a reasonable typhoon wind field distribution model which is easy to calculate.

2.2.1 Introduction of asymmetric typhoon wind farm model

By comparing more than ten existed typhoon wind field models, the asymmetric typhoon model improved by Hu Banghui[2,3] is selected. This model can preferably describe the characteristics of asymmetric typhoon wind field. Main equations of this model include:

Taken the center of tropical cyclone as the origin, the horizontal movement equations in plane polar coordinates of one air particle in tropical cyclone region by taking into account of sea surface friction are:

$$\frac{dv_r}{dt} - \frac{v_\theta^2}{r} - fv_\theta = -\frac{\partial P}{\rho \partial r} + F_r \qquad (2\text{-}1)$$

$$\frac{dv_\theta}{dt} + \frac{v_r v_\theta}{r} + fv_r = -\frac{\partial P}{\rho \partial \theta} + F_\theta \qquad (2\text{-}2)$$

F_r and F_θ represent the friction forces at r direction and θ direction. Assume the tropical cyclone is in stable state and the pressure field is round, yields:

$$-\frac{v_\theta^2}{r} - fv_\theta = -\frac{\partial P}{\rho \partial r} + F_r \qquad (2\text{-}3)$$

$$\frac{v_r v_\theta}{r} + fv_r = F_\theta \qquad (2\text{-}4)$$

Applying Fujita Formula to the pressure field in tropical cyclone region, the air pressure at one point and the variation of air pressure are:

$$P = p_\infty - (p_\infty - P_0)\left[1 + 2\left(\frac{r}{R}\right)^2\right]^{\frac{1}{2}} \qquad (2\text{-}5)$$

$$\frac{\partial P}{\partial r} = \frac{2(p_\infty - P_0)r}{R^2}\left[1 + 2\left(\frac{r}{R}\right)^2\right]^{-\frac{3}{2}} \qquad (2\text{-}6)$$

Applying state equation $P = \rho k_c T$ and (2-6) into equation (2-3), gives:

$$\frac{v_\theta^2}{r} + fv_\theta = \frac{A}{r} - F_r \qquad (2\text{-}7)$$

Where, $$A = 2k_c T(P_\infty - P_0)\left[1 + 2\left(\frac{r}{R}\right)^2\right]^{-\frac{3}{2}} r^2 \Big/ \left\{P_\infty - (P_\infty - P_0)\left[1 + 2\left(\frac{r}{R}\right)^2\right]^{-\frac{1}{2}}\right\} R^2 \qquad (2\text{-}8)$$

When tropical cyclone moves with the speed v_s, the relation of curvature radius r of static tropical cyclone and curvature radius r of moving tropical cyclone at any point in the region is:

$$\frac{r'}{r} = \frac{v_\theta}{v_\theta + v_s \sin\alpha} \qquad (2\text{-}9)$$

$$v_\theta = v'_\theta - v_s \sin\alpha \qquad (2\text{-}10)$$

$$v_r = v'_r - v_s \cos\alpha \qquad (2\text{-}11)$$

Where, α is the angle between the movement direction of tropical cyclone and the connecting line from the discussed point to the center of cyclone, and the direction of counterclockwise is positive.

Combining (2-4) (2-8) (2-9) (2-10) (2-11), we can get:

$$\frac{v_\theta^2}{r} + \frac{v_\theta v_r \sin\alpha}{r} + fv_\theta = \frac{A}{r} - F_r \qquad (2\text{-}12)$$

$$\frac{v_r v_\theta}{r} + \frac{v_r v_\theta \sin\alpha}{r} + fv_r = F_\theta \qquad (2\text{-}13)$$

Where,

$$v_\theta = v\sin\alpha \qquad (2\text{-}14)$$

$$v_r = v\sin\beta \qquad (2\text{-}15)$$

$$F_\theta = kv\cos(\varphi+\beta) \qquad (2\text{-}16)$$

$$F_r = kv\sin(\varphi+\beta) \qquad (2\text{-}17)$$

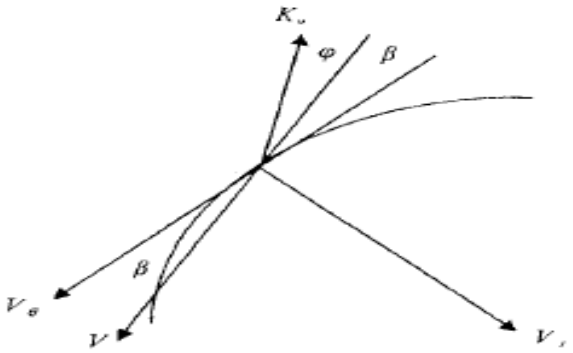

Fig.2.3: Basic relations among β , φ and actual wind

Applying (2-14) to (2-17) into (2-12) and (2-13), and eliminating v, we can get:

$$y^3 + zy + q = 0 \qquad (2\text{-}18)$$

Where, $q = 2\left[\frac{A - k^2 r^2 \cos^2\varphi}{3kr\cos\varphi(v_s \sin\alpha + kr\sin\varphi + fr)}\right]^3 - \frac{A + 2k^2 r^2 \cos^2\varphi}{3kr\cos\varphi(v_s \sin\alpha + kr\sin\varphi + fr)}$;

$$z = 1 - \frac{1}{3}\left[\frac{A - k^2 r^2 \cos^2\varphi}{kr\cos\varphi(v_s \sin\alpha + kr\sin\varphi + fr)}\right]^2$$

$$y = \frac{A - k^2 r^2 \cos^2\varphi}{3kr\cos\varphi(v_s \sin\alpha + kr\sin\varphi + fr)} + \tan\beta \qquad (2\text{-}19)$$

From equation (2-18), we can get:

$$y_1 = 2\sqrt[3]{r}\cos\theta;$$

$$y_2 = 2\sqrt[3]{r}\cos(\theta + 120^\circ);$$

$$y_3 = 2\sqrt[3]{r}\cos(\theta + 240^\circ)$$

Where,

$$r = \sqrt{-(\frac{z}{3})^2},$$

$$\theta = \frac{1}{3}\arccos\left(-\frac{q}{2r}\right)$$

According to (2-19)and (2-13), we can obtain the calculating formulas of wind direction inner deflection angle of moving tropical cyclone and the wind speed:

$$\beta = \arctan[y - \frac{A - k^2 r^2 \cos^2 \varphi}{3kr \cos\varphi(v_s \sin\alpha + kr \sin\varphi + fr)}] \tag{2-20}$$

$$v = \frac{kr\cos(\varphi+\beta) - v_s \sin\alpha \sin\beta}{\sin\beta\cos\beta} - \frac{fr\sin\beta}{\sin\beta\cos\beta}] \tag{2-21}$$

If the maximum wind speed $V_{\max}$ of tropical cyclone is given, we can obtain the maximum wind speed diameter and corresponding wind direction inner deflection angle:

$$\beta = \arcsin(-\frac{b}{2a} \pm \frac{\sqrt{b^2 - 4ac}}{2a}) \tag{2-22}$$

$$R = \frac{A_\alpha - v_s v_\alpha \sin\alpha \sin\beta}{kv_\alpha \sin(\varphi+\beta) + fv_\alpha \cos\beta} - \frac{v^2{}_\alpha \cos^2\beta}{kv_\alpha \sin(\varphi+\beta) + fv_\alpha \cos\beta} \tag{2-23}$$

Where,

$$a = A_\alpha{}^2 (k\sin\varphi + f)^2 + k^2 \cos^2\varphi (A_\alpha - v_\alpha{}^2)^2 ;$$

$$b = 2kA_\alpha v_\alpha v_s \sin\alpha \cos\varphi (k\sin\varphi + f)$$

$$c = k^2 v_\alpha{}^2 v_s{}^2 \sin^2\alpha \cos^2\varphi - k^2 \cos^2\varphi (A_\alpha - v_\alpha{}^2)^2$$

In the calculation, if considering the nonlinear action of sea surface, the calculating formula of friction coefficient will be $k = k_s \left[1 + 7\frac{r}{R}\exp(-\frac{r}{R})\right]$.

The maximum wind speed (V_α) of typhoon at any direction is composed by two parts which are maximum circumfluence wind speed ($V'_{\max}$) and typhoon moving speed

(V_s). The maximum circumfluence wind speed has nothing to do with the wind direction. Therefore, the maximum wind speeds at all directions are the same in static. Assuming the maximum value ($V_{\max}$) of maximum wind speeds at all directions are given during the moving process, and the direction is the same with the moving direction, the maximum circumfluence wind speed can be expressed as:

$$V'_{\max} = V_{\max} - V_{\alpha}$$

The maximum wind speed at any α direction can be expressed as:

$$V_{\alpha} = \sqrt{V_{\theta}^2 + V_r^2}$$

$$V_{\theta} = V'_{\max} \cos\beta - V_s \sin\alpha$$

$$V_r = V'_{\max} \sin\beta - V_s \cos\alpha$$

β is the wind speed inner deflection angle at the maximum wind speed radius of static tropical cyclone.

2.2.2 Calculation

Calculation is conducted by using the above asymmetric typhoon wind field model, and the data of air pressure and wind speed at the center of TCS (TCs) from 1961 to 2007 obtained from Shanghai Typhoon Institute of China Meteorological Administration. The temperature (T) in formula (2-8) is the GISST monthly average temperature from 1961 to 1977 obtained from Hadley Centre, and the temperature data for every six hours in reanalyzing data from 1978 to 2007 from Japan Meteorological Agency. 25km×25km landform data are used as the frictional resistance during the movement process of typhoon. The TC wind field at 0.5°×0.5° mesh point at the coast of China is calculated at last. Due to the smallness of the mesh point, the phenomena of without data at the mesh points always occur for TC with fast moving speed if calculating for one time in each six hours. Therefore, the linear interpolation of two hours is conducted in the calculation process, and TC central air

pressure, wind speed data and temperature data in each two hours are obtained. Atmosphere pressure (p_∞) is related to the season, and it is set according to the average value of sea surface climate in different months.

2.2.3 Comparison with observed wind field

Calculate the wind speed of No.9 typhoon "Matsa" (Fig.2.4b) in 2005 and the wind speed of No.15 typhoon "Khanun" (Fig.2.4d) by using the asymmetric typhoon model, and compare them with the actual observed wind fields of typhoon "Matsa" (Fig.2.4a) and typhoon "Khanun" (Fig.2.4c). The comparison shows that, gale region on Fig.2.4a and Fig.2.4c appear at the right of typhoon movement path, and the wind power at the right is obviously stronger than the left. We can clearly see in Fig.2.4b and Fig.2.4d that, the gale region is at the right of typhoon movement direction and the wind power at the right is obviously stronger than the left. The calculated values are consistent with the actual observed typhoon wind field.

2.2.4 Comparison with wind speed observed by the meteorological stations

Selecting No.9 and No.16 typhoons in 2007, collecting observed data of the affected region from the meteorological stations (refer to 2.3 observed values at the automatic station), the maximum wind speeds of these stations while affected by tropical cyclone by using asymmetric typhoon wind field model were calculated, and testing the reasonability of the asymmetric typhoon wind field model. We can see from table 2.2 that, the calculated values of the model are relatively close to the observed values at the observation stations. This indicates that the calculating results of the model are relative reasonable. We can see from Fig.2.5a and Fig.2.5b that, the wind field calculated from the model shows its asymmetric property at offshore, which is consistent with the asymmetric property of typhoon when approaching to the land. From the aspect of structure, it is complied with asymmetry of tangential wind speed, and the maximum wind speed region in semi-lune is at the right of the typhoon.

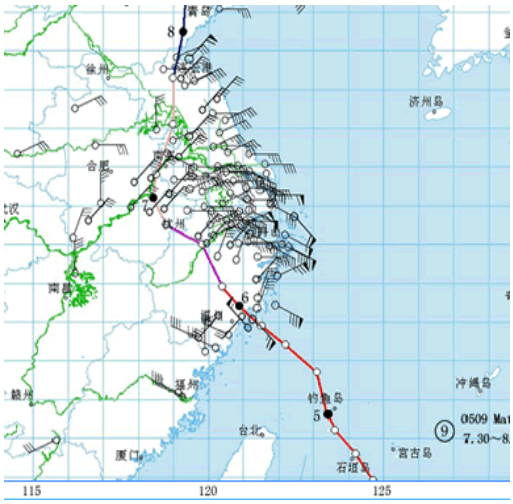

a Actual observed wind field

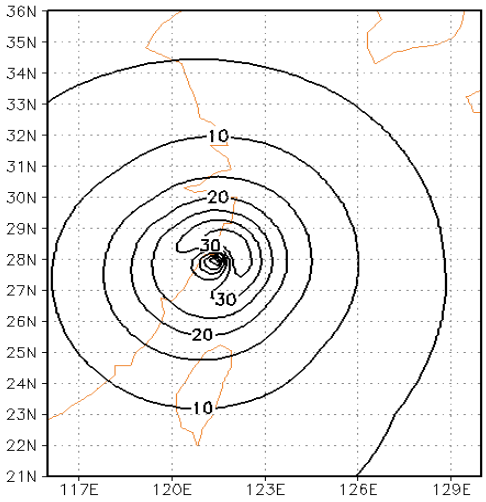

b Wind field by the model

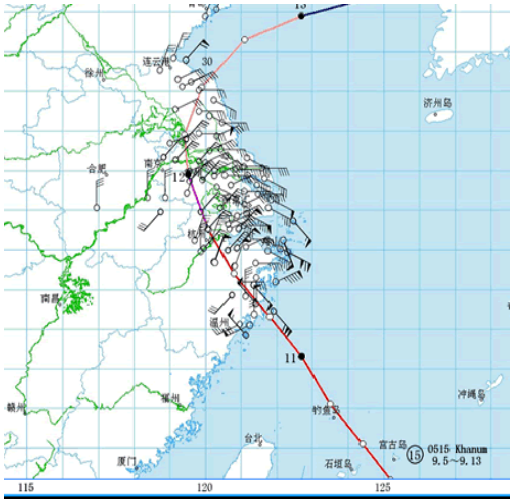

c Actual observed wind field

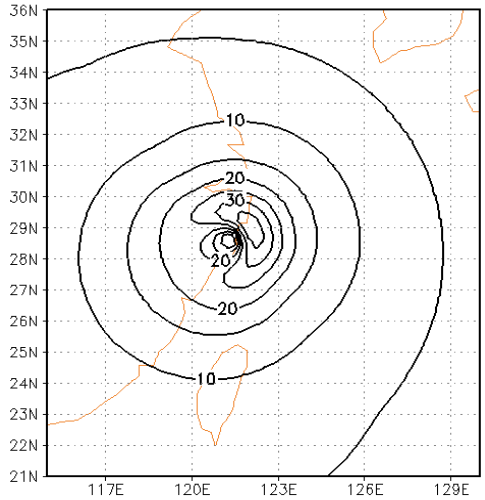

d Wind field by the model

Fig.2.4 Wind field of typhoon “Khanun” in 2005

Table 22a: Comparison of model values and observed values of No.9 typhoon wind speed in 2007

Latitude (°N)	Longitude (°E)	Calculated values from the model(m/s)	Observed values from the automatic station (m/s)
26. 20	119. 68	19. 7	17. 0
25. 63	119. 51	25. 7	30. 6
26. 60	119. 94	14. 3	12. 8
26. 30	119. 90	16. 4	17. 9
25. 88	116. 14	10. 7	10. 1
26. 30	119. 70	16. 9	17. 4
26. 96	120. 32	11. 9	8. 6

Table 2.2b: Comparison of model and observed of No.16 typhoon wind speed in 2007

Latitude (°N)	Longitude (°E)	Calculated values from the model(m/s)	Observed values from the automatic station (m/s)
27.24	119.94	10.6	11.8
25.09	119.12	12.6	10.9
27.38	118.10	9.2	7.3
25.40	119.60	14.8	15.2
25.25	119.36	14.1	14.1
27.23	119.88	11.6	9.9
27.28	120.03	10.7	9.8
25.72	118.10	12.1	11.1

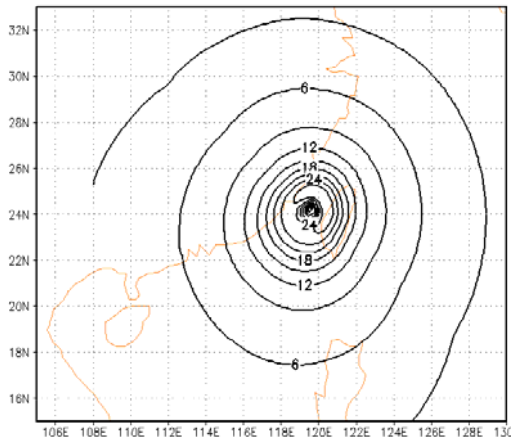

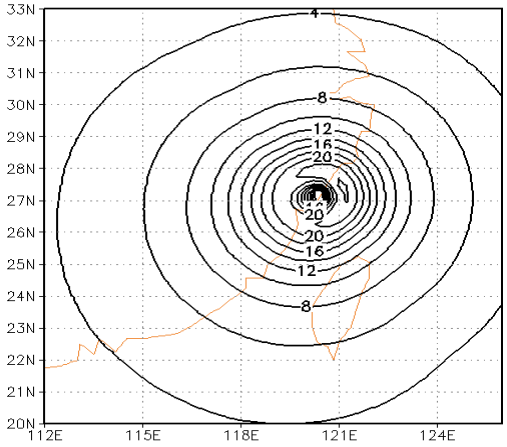

Fig.2-5a: Distribution of wind speeds calculated from the model corresponding to table 2a

Fig.2-5b: Distribution of wind speeds calculated from the model corresponding to table 2b

2.3 Calculation of extreme maximum wind speeds at all mesh points under the influences of typhoon

To guarantee the safety operation of wind turbine generator systems (WTGS), the International Standardization Committee established the IEC61400-1:1999WTGS safety requirements. This standard divides the extreme maximum wind speeds of 1/50-year frequency into four grades: 30, 37.5, 42.5 and 50m/s. The extreme

maximum speed is deduced through probability statistics.

The climate extreme value of return period T actually refers to a specific value of climate extreme value which appears for one time in T years (such as 50 years, 100 years, etc.). The probability for the occurrence of this value is 1/T. T is named as the return period of this specific value.

If specific value x represents the annual maximum value of a certain climate factor, according to the probability distribution, the probability exceeding this maximum value is

$$P(X \geq x) = 1 - F(x) = \frac{1}{T(x)}$$

Therefore, the return period of maximum value can be expressed by the following formula: $T(x) = \frac{1}{1 - F(x)}$

It represents the extreme wind speed load which might be occurred in the region of the project with T years in the future.

2.3.1 Poisson-Gumbel joint probability distribution model

The tracks, intensities and times of TCs in each year are random. Therefore, in the TC gale series of certain mesh point calculated from the asymmetric typhoon wind field model, some years may have many gale values while others may not have the gale values at all. Therefore, conventional probability distribution model can not be used for calculation, for example, Weibull Probability Distribution and Gumbel Probability Distribution require one maximum wind speed in each year. Poisson-Gumbel Joint Probability Distribution can satisfy its requirements. Assuming that the occurrence times of TC in each year can satisfy the discrete distribution Poisson Distribution, the maximum wind speeds under the influences of TC can form continuous distribution Gumbel Distribution , Poisson-Gumbel can reckon the distribution function G(x) of maximum wind speed when the probability distribution of TC occurrence frequency n is P_k.

Assume the TC influenced frequency n complies with Poisson Distribution,

denoted as $$p_k = e^{-\lambda}\frac{\lambda^k}{K!}$$

Where, $\lambda = \frac{N}{M}$, N is TC influenced total times, and M is total years.

Assuming TC influenced wind speed complies with Gumbel Distribution, denoted as

$$G(x) = \exp\{-\exp[-\alpha(x-\delta)]\}$$

We can obtain the distribution function of Poisson—Gumbel compound extreme distribution

$$F(x) = \sum_0^k p_k[G(x)]^k = \exp\{-\lambda[1-G(x)]\} = P$$

Then

$$G(x) = 1 + \frac{1}{\lambda}\ln P$$

$$\exp\{-\exp[-\alpha(x-\delta)]\} = 1 + \frac{1}{\lambda}\ln P$$

Taking logarithm for two times, we can get

$$\alpha(x-\delta) = -\ln\left[-\ln\left(1+\frac{1}{\lambda}\ln P\right)\right]$$

Therefore, the gale extreme value when the probability is P is

$$Vp = \delta + \frac{-\ln[-\ln(1+\frac{1}{\lambda}\ln P]}{\alpha} = \delta + \frac{-\ln[-\ln(1+\frac{1}{\lambda}\ln(1-\frac{1}{T}))]}{\alpha}$$

Where, $\alpha = 1.28255/\sigma$, $\delta = \bar{x} - 0.57722/\alpha$, $\bar{x}$ is the average of sampling sequence, and σ is the standard deviation of sampling sequence.

The following two items must be satisfied while using Poisson-Gumbel Joint Probability Distribution to calculate the maximum wind speed of 1/50-year frequency:

I. Samples in strong wind speed series are independent

II. The occurrence frequency of TC in each year should be complied with Poisson Distribution, and χ^2 is usually used for testing.

2.3.2 Analysis of calculating results

Gumbel Distribution requires the sample values in the series to be independent. To guarantee the independence of maximum wind speeds of each mesh point, only one process maximum wind speed value will be used for each mesh point after the calculation of wind fields at all times during each TC movement process. The TC influenced maximum wind speed series of 0.5×0.5 latitude and longitude mesh points at the offshore of China from 1961 to 2007 is finally formed. By using the above Poisson-Gumbel Joint Probability Distribution Model, the maximum wind speed series, and the distribution diagram (Fig.2.6) of extreme wind speeds of 1/100-year, 1/50-year, 1/30-year and 1/20-year frequencies which influence the offshore of China are obtained.

We can see from Fig.2.6c that, the 1/50-year frequency maximum wind speed, the wind speeds at Donghai Sea and Huanghai Sea are gradually reducing from south to north, in which Huanghai Sea is 20-30m/s and Donghai Sea is 35m/s-50m/s. Due to the less influence of Beihai Sea, Huanghai Sea and Bohai Sea area by typhoon, the credibility of calculated maximum wind speed in multi-year return period is relatively low, and detailed analysis is not conducted. From Beibu Gulf to Bashi Channel, the maximum wind speed is increasing from west to east, and the wind speed changes from 30m/s - 60m/s.

The costal sea area of China is the main development and construction region of offshore wind farm, nuclear power plant, port projects, and other coastal projects. The influences of typhoon are especially important. The maximum wind speed of 1/50-year frequency at offshore of Jiangsu varies from 20 to 30m/s and at Hangzhou

Gulf and Yangtse River Estuary varies from 30m/s to 35m/s. The gale induced by TC at the offshore of central and south of Zhejiang and north of Fujian is the strongest with the speed varies from 40m/s to 45 m/s. Due to the obstruction and diminution to typhoon by Taiwan island, the influencing degree of typhoon to the offshore at the central and south of Fujian is obviously smaller than south and north adjacent sea areas, and the maximum wind speed varies from 30 m/s to 40 m/s. The wind speed at the offshore at the north of Nanhai Sea is stronger than 35 m/s. The influencing degree of typhoon to southeast sea area at Hainan Province and offshore at the east of Guangdong is relatively greater than other sea areas, and its wind speed of 1/50-year is stronger than 40m/s. Due to the weakening by Leizhou Peninsular and Hainan Island, the maximum wind speed of 1/50-year frequency at Beibu Gulf sea area is less than 35m/s.

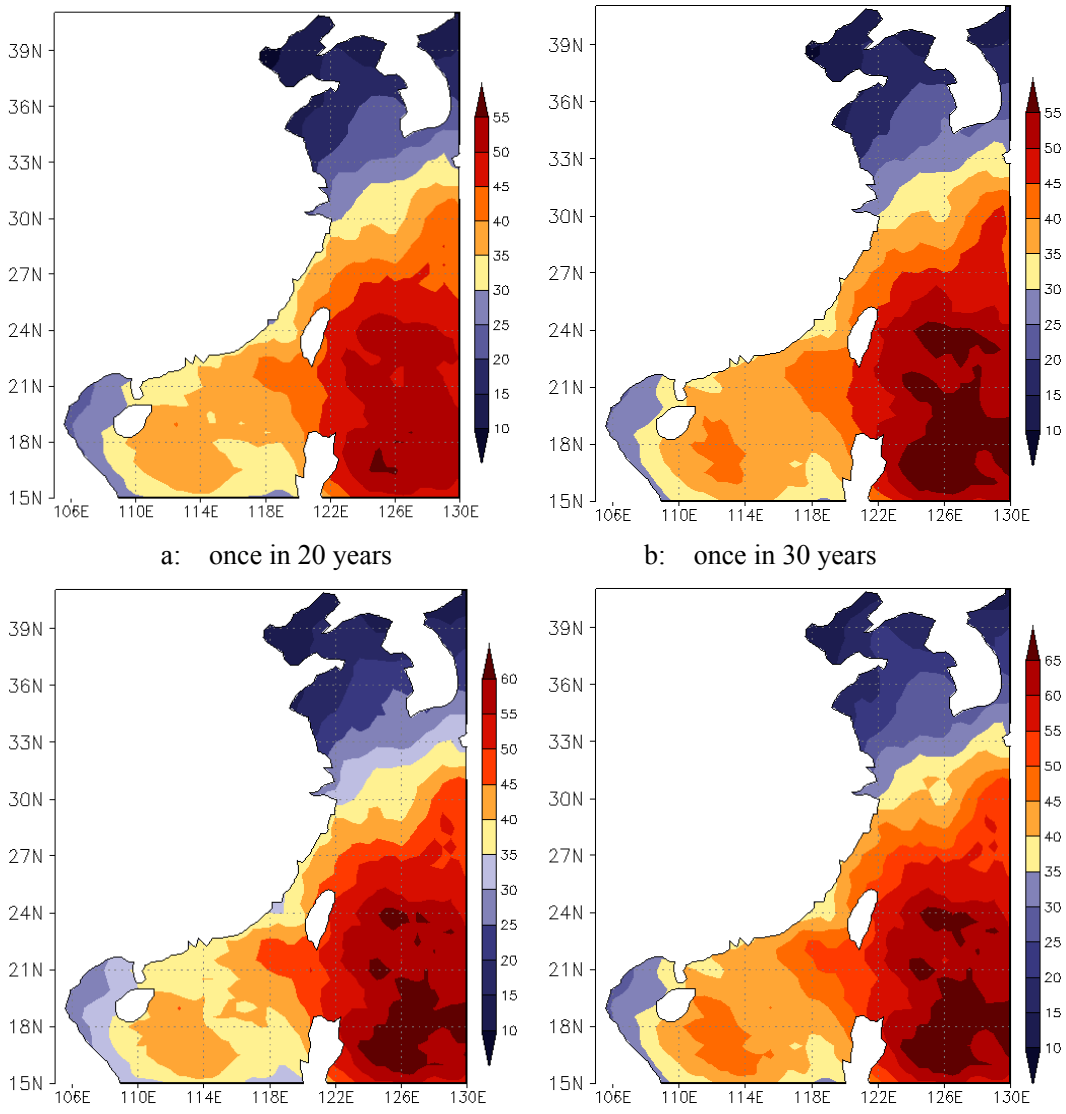

a: once in 20 years b: once in 30 years

c: once in 50 years d: once in 100 years

Fig.2.6 Maximum wind speed frequency under the influence of TC

2.3.3 Calculation by using Weibull extreme distribution model

Weibull Probability Distribution is the method which is widely used in extreme calculation in the world at present. To make the calculation results more reliable, the extreme wind speeds of 1/100-year, 1/50-year, 1/30-year and 1/20-year frequencies of each mesh point are calculated by using Weibull Probability Distribution. Weibull Probability Distribution and its probability density function forms are as follows:

$$F(x) = 1 - e^{-\frac{(x-r)^m}{\alpha}}$$

$$f(x) = \begin{cases} \dfrac{m}{\alpha}(x-r)^{m-1} e^{-\frac{(x-r)^m}{\alpha}} & (x \geq r) \\ 0 & (x < r) \end{cases}$$

According to Weibull distribution function F(x), we can obtain the function form of maximum value return period T(x), that is

$$T(x) = \frac{1}{1-F(x)} = e^{\frac{(x-r)^m}{\alpha}}$$

Therefore, the gale extreme when the probability is P is:

$$Vp = (\alpha \cdot \ln T)^{1/m} + r$$

Using the above formula for maximum value estimation, parameters of m, α, r should be calculated at first.

We form the maximum wind speed series in 47 years from 1961 to 2007 by selecting the maximum wind speed of each mesh point under the influence of TC in each year and using the minimum value of this mesh point in other years as substitute for years without TC influences. The extreme wind speeds (Fig.2.7) of 1/100-year, 1/50-year, 1/30-year and 1/20-year frequencies are calculated by using Weibull extreme distribution model.

Comparing with Fig.2.6 and Fig.2.7, we can see that, the calculating results by using

annual maximum wind speed time series are really close to the results calculated by Poisson-Gumbel Joint Extreme Distribution for the series composed by many TC influenced wind speeds in each year. It shows that, it is reasonable and correct to use Poisson-Gumbel Joint Extreme Distribution to calculate the extreme wind speed in multi-year return period in the sea areas influenced by TCs.

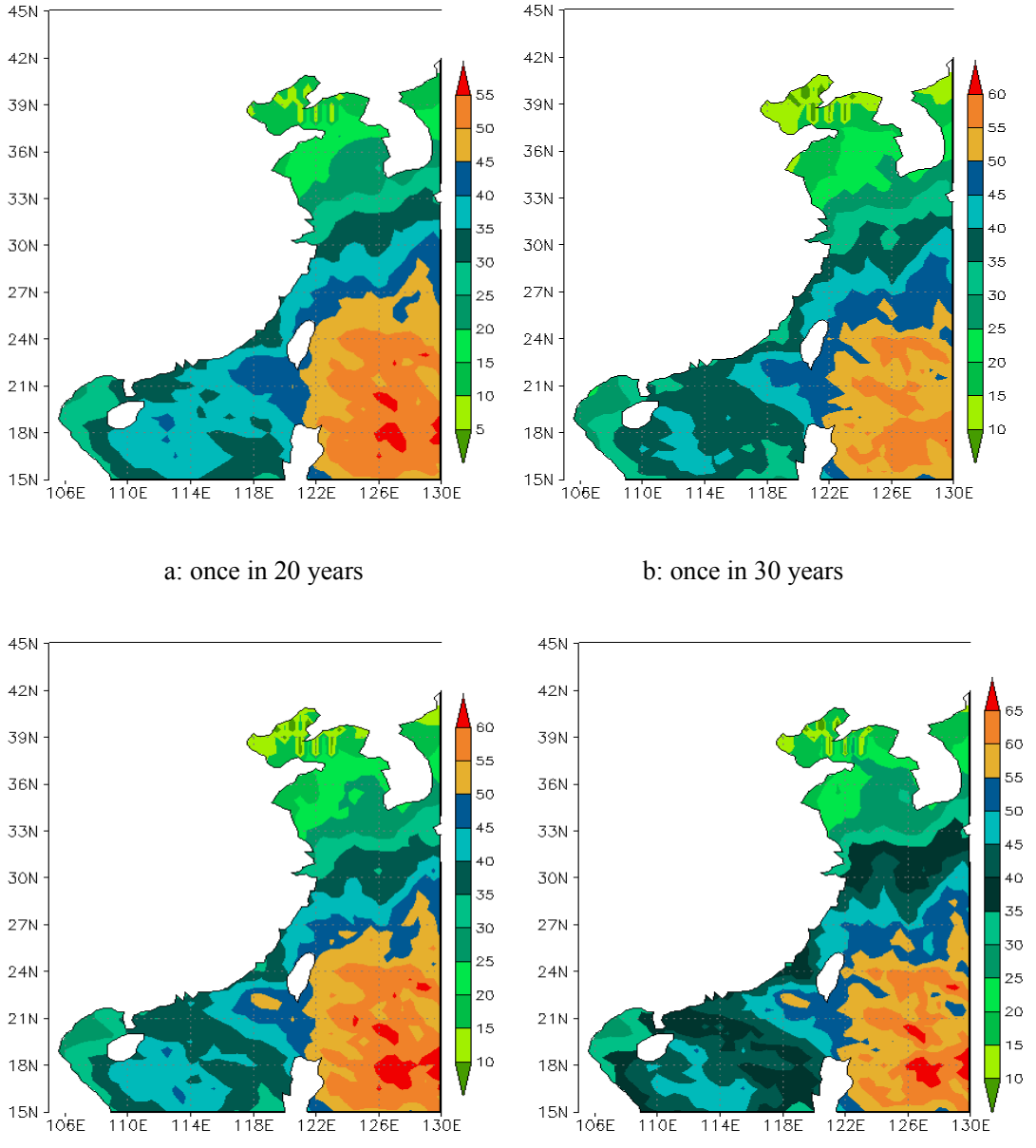

a: once in 20 years

b: once in 30 years

c: once in 50 years

d: once in 100 years

Fig.2.7 Maximum wind speed frequency under the influence of TC

2.4 Calculation of maximum wind speed of 1/50-year frequency in coastal observing stations

The maximum wind speeds of TCs landed in China and during its influencing period are recorded at the coastal meteorological stations. Shanghai Typhoon Institute provided the gale data of all meteorological stations from 1961 to 2006. The maximum wind speed at costal meteorological stations since there is observation and the maximum wind speed of 1/50-year frequency are analyzed by using these data.

2.4.1 Distribution of maximum wind speed of all coastal meteorological stations since there is observation

Fig.2.8 shows the maximum wind speed recorded at coastal meteorological stations caused by TC which is influencing the coast of China from 1961 to 2006. We can see that, most of the wind speeds at the south coast of Hangzhou Gulf are stronger than 25m/s (wind with 10th grade), and at the north coastal area are less than 25m/s. In the region with the wind grade of 10, the wind speed at the offshore of central Fujian (except island) is obviously less than other areas. The region with the wind speed of 40m/s (13th grade) or more is concentrated at the offshore of Guangdong at the east of Zhujiang Estuary and at the east coast of Hainan.

2.4.2 Maximum wind speed of 1/50-year frequency at all coastal observing station

By using Poisson－Gumbel Joint Probability distribution, the extreme maximum wind speed of 1/50-year frequency at all meteorological stations under the influences of TC were calculated. Fig.2.9a shows the maximum wind speed distribution of 1/50-year frequency. The wind speeds in 53.3% of the total stations over the southeast coastal regions are less than 25m/s, which means that most areas are safe. The maximum wind speeds of 1/50-year frequency in 9.4% of the total stations are stronger than 37.5m/s. The maximum wind speed is 54.0m/s (Nanjishan in Zhejiang). The speed of 51.5m/s at Zhelang of Guangdong is the second strongest, and the speed of 45.0m/s at Shengshan of Zhejiang is the third strongest. The wind speed at south coast of Fujian is obviously less than other areas.

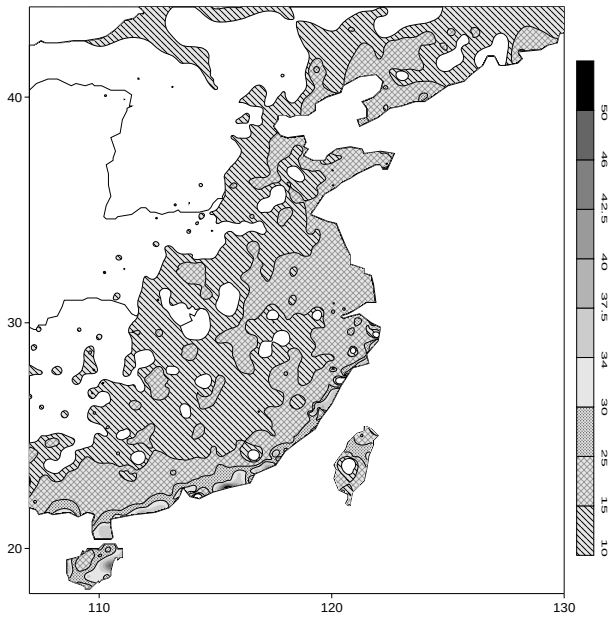

Fig.2.8 Distribution of wind speeds of TCs influencing the coast of China

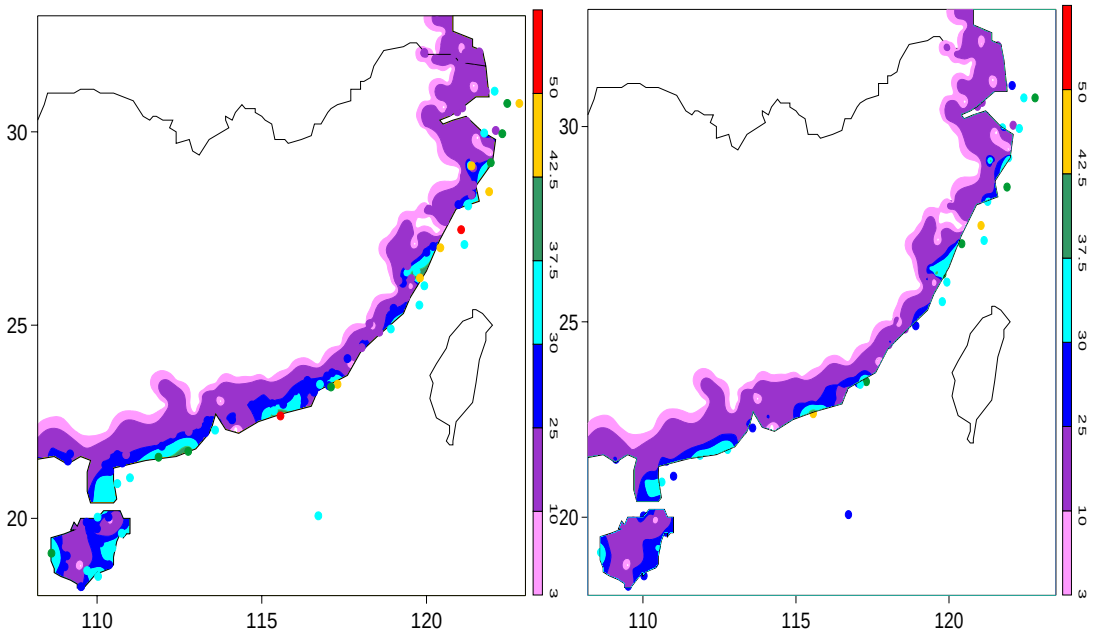

(a) (b)

Fig.2 Average maximum wind speed of 1/20-year (a) and 1/50-year (b) in 10min

2.5 Conclusion

1) During 1961-2007, totally 579 tropical cyclones (TC) had affected offshore China. Of these, most were typhoons and severe tropical storms, of which the frequency of super and severe typhoons accounted for 27.3%, occupying 8.6% of the total landing TCs.

2) The maximum wind velocities, with a return period of 50 years, caused by TCs were 40m/s-45 m/s, 30 m/s-40 m/s, and <35 m/s in the paralic areas of the central and south Zhejiang, the northeast Fujian, the east Guangdong and the east Hainan Island, in the paralic areas of the central and south Fujian and the west Guangdong, and to the north of the mouth of Changjiang River, respectively.

3 RESULT 2: WIND VARIATION STUDY UNDER THE INFLUENCE OF TROPICAL CYCLONE

The variations of air pressure, wind speed and direction, wind vertical shear and turbulence intensity of 19 tropical cyclones were analyzed according to the observation data collected by anemometer tower and meteorological station. Three typical typhoons represented different intensities, influence ranges and movement features were calculated. Among which the No. 8 typhoon "Morakot " in 2009 features the typical route of traversing Taiwan, landing at the coast of Fujian province and then moving southward via Zhejiang and Jiangsu to the sea. The No. 13 super typhoon "Vipha" in 2007 had the route of traversing the sea area to the south of Taiwan and directly moving southward to land at the coast of boundary of Fujian and Zhejiang province. No. 18 typhoon "Dawei" in 2005 was generating at west Pacific and moving westward to land at the middle of Nanhai island. We analyze their horizontal wind field characteristics by use of the MM5 modelling data, satellite cloud pictures and data of anemometer tower and meteorological station. We also analyze the variation characteristics of different wind directions, topographies, underlying surfaces, distances to typhoon centre, orientations, wind speeds, wind directions, wind vertical shears and turbulence intensities by using the data of anemometer tower.

3.1 Data collection and treatment of mast tower

Now the data related to tropical cyclone of 85 mast towers have been collected, which mainly come from the wind power enterprises, local development and reform commission and weather bureaus. Firstly we carry out the quality inspection to the observed wind data, and then sort the relative anemometer tower data according to influence period of tropical cyclones; conducting the comparative analysis for the anemometer tower data during the influence period of each cyclone, weeding out irrational data and finally establishing 17 tropical cyclone data documents.

3.2 No.8 typhoon "Morakot"

"Morakot" is a tropical typhoon featuring the typical route of traversing Taiwan, landing at the coast of Fujian province and then moving southward via Zhejiang and Jiangsu to the sea. The "Morakot" typhoon generated over the west Pacific at 02 o'clock in August 4 in 2009, then moved westward and landed at Hualian of Taiwan at 45 minutes past 23 o'clock, after that entered the Taiwan Strait at 8 o'clock in August 8, landed again at the coast of Beibi of Xiapu of Fujiang (when landing, the minimum

air pressure near the centre was about 955 hectopascal and maximum wind was of grade 12 (33m/s); then passed through Zhejiang, Jiangsu after landing and entered the sea at Sheyang of Jiangsu (Figure 3.1).

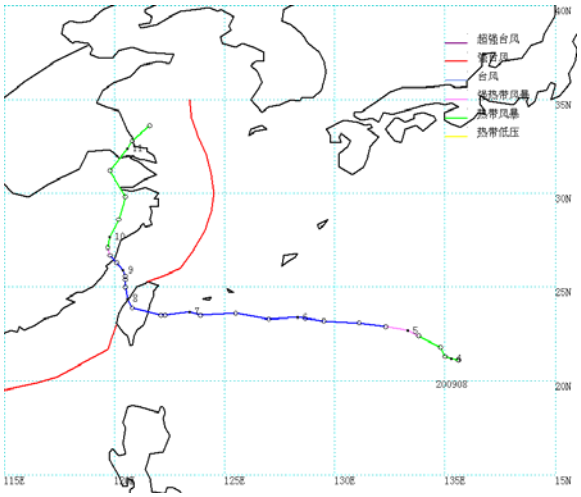

Figure 3.1 Typhoon Route Diagram of No.8 “Morakot” in 2009

3.2.1 Distribution characteristics of horizontal wind fields of ground and 50m height

The wind field of tropical cyclone is the basic information for the wind farm to utilize and protect from the typhoon. The area away from the harmful wind speed range of tropical cyclone is favorable for the wind power generations. For the harmful wind speed range, it can minimize the loss by identifying the wind field structures with the various tools and taking effective protection measures. Each tropical cyclone has its unique ground field structure, it is related to both typhoon intensity and passing underlying surfaces. At a clear sea surface with less roughness, the wind field structure is of symmetrical and round shape; while at large islands and coast line of different directions, the wind field becomes asymmetrical and of oval with the effect of ground friction. The hazardous large wind zone is located at the front right of moving route of tropical cyclone and the range at left is less than that at right.

(1) Ground wind field

At August 7, when the typhoon centre approached the coast at middle of Taiwan, the Guangdong, Fujian and south of Zhejiang have been controled by the peripheral wind

of typhoon (Figure 3.2a). From the MM5 data simulated results (Figure 3.2b), the typhoon is approximately of round shape and the strong wind area at north is large than that at south. From the continental shore land, the Grade 6 strong wind area range extended to north of Jiangsu and middle of Fujian. The diurnal maximum wind speed from the coast of Zhejiang to middle of Fujian can reach 15 to 26.8m/s (Figure 3.2c) with the northeastward direction, in which the maximum wind speed in Yuhuan and Cangnan Heding Shan exceeded 25m/s.

At August 8, the typhoon traversed Taiwan Island to entered Taiwan Strait. The typhoon cloud is looser than that in 7th, which shows the typhoon intensity weakened after traversed Taiwan, and it is approximately of oval (Figure 3.3a、b). The wind force at sea coast increased: the wind force at Jiangsu sea coast reached grade 6 and grade 9 for Zhejiang and Fujian, and both sides of typhoon had strong wind area (Figure 3.3c). The stations of wind speed more than 25m/s included Yuhuan, Cangnan Hedingshan, Xiapu, Lianjiang, Pingtan and Fuqing and the maximum wind speed occurred at Xiapu (30m/s) and Fuqing Donghan (30.1m/s).

At August 9, the asymmetry of typhoon structure was more apparent and the intensity significantly reduced (Fig 2.4a and b). Under the topographic influence (Figure 3.4c), the wind forces of northern Jiangsu and the middle coast of Fujian reduced and those of middle Zhejiang and northern Fujian further increased which was normally 15 to 22m/s. At the right side of typhoon moving route, the range of wind speed of larger than 25m/s extended northward to Shipu of Zhejiang with the Northeastward direction; at the left side, the wind speed is obviously less than that in August 8 and normally less than 20m/s. The maximum wind speed at the station of left side occurred when typhoon approaching, so the wind direction in the area close to typhoon centre represented as northeast wind; while that in the area south away from typhoon centre of northwest or west; the wind speed of Xiapu Dongchong near the typhoon centre reached 31m/s. the typhoon landed at Xiapu Beibi at 16:20 in 9th.

At August 10, the typhoon entered Zhejiang province and penetrated into the interior continent and the wind force significantly reduced (Figure 3.5a). The Zhejiang coast at right front side of Typhoon route was of strong wind area with maximum wind speed of 17 to 24m/s and direction of southeast to northeast; while Fujian coast at the rear of typhoon feathered with maximum wind speed of grades 6 to 7 and direction of southwest; the Jiangsu coast at north of typhoon circulation was of wind force of grades 6 to 7 with direction of northeast (Figure 3.5b), which was favorable for wind power generation.

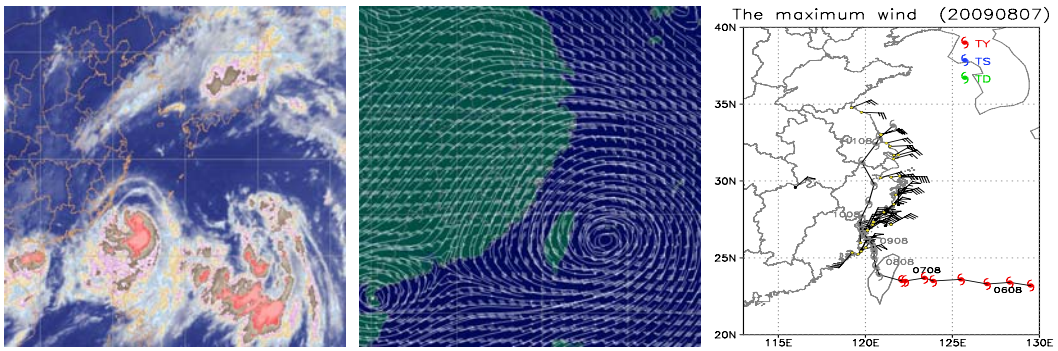

(a) (b) (c)

Figure 3.2 Meteorological satellites cloud picture (a), MM5 data simulated 925 hPa wind field (b) and ground observed diurnal maximum wind speed (c) in August 7 of 2009

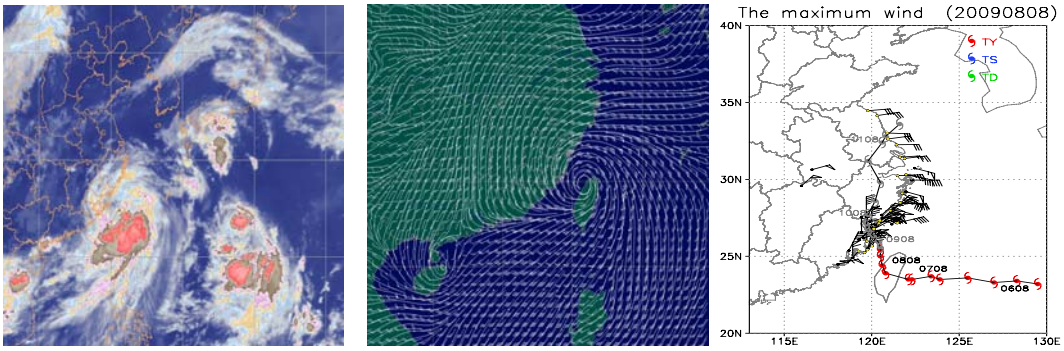

(a) (b) (c)

Figure 3.3 Meteorological satellites cloud picture(a), MM5 data simulated 925 hPa wind field (b) and ground observed diurnal maximum wind speed (c) in August 8of 2009

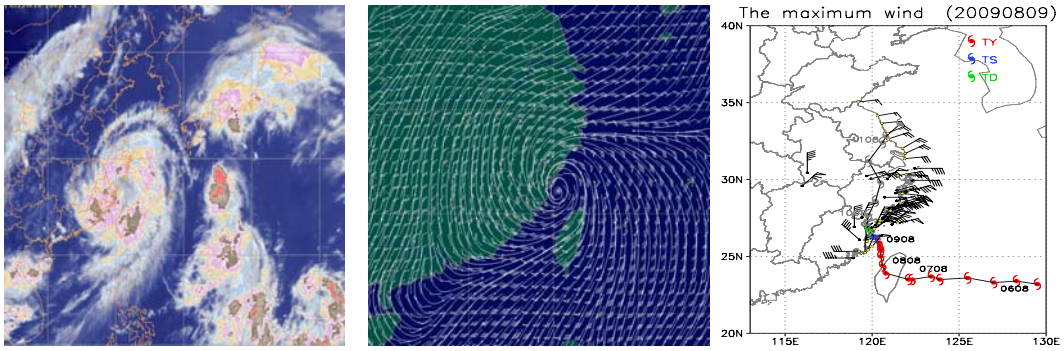

(a) (b) (c)

Figure 3.4 Meteorological satellites cloud picture(a), MM5 data simulated 925 hPa wind field (b) ground observed diurnal maximum wind speed (c) in August 9 of 2009

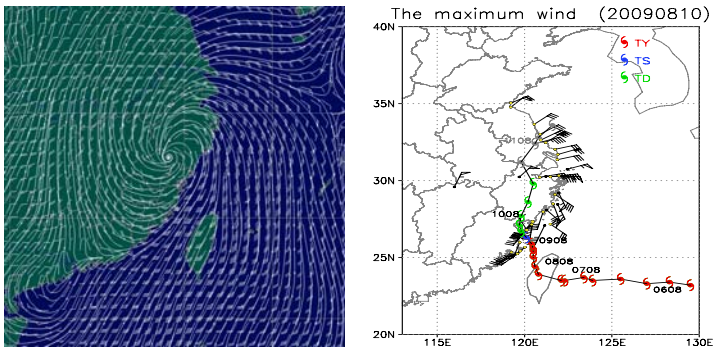

(a) (b)

Figure 3.5 MM5 data simulated 925 hPa wind field (a) and ground observed diurnal maximum wind speed (b) in August 10 of 2009

(2) Wind field at 50 meter height

Figure 3.6 is the time variation diagram of 50m height wind field of anemometer tower during the influence period of "Morakot" typhoon. The Y coordinate are the series numbers of mast towers indicating from north to south with 1 to 20 separately. There are 4 typhoon symbols for every day in the figure, which separately represent the four hours sequence of 02, 08, 14 and 20 o'clock, and the special location of mast towers and corresponding station names refer to figure 3.7。

As shown in figure 3.6, at 6 hours before landing of typhoon, the coast at south of No. 12 tower (Zhejiang Cangnan Hedingshan) were of strong northeast wind, which means that the mast towers were at the left side of typhoon and the typhoon was still on the sea; at 02 o'clock of 9th, the typhoon moved northwestward to the latitude of Pingtandao and the direction of Nanridao and Houwen became northwest. It means that these areas had fallen behind the typhoon and the wind speed reduced to grade 6; however, the areas at the north of same latitude as the typhoon still were of north to northeast wind.

With the typhoon moving northward and approaching the continent, the wind direction of tower at south of typhoon rotates anticlockwise from northwest to southeast through west wind; while the wind direction of towers at north of typhoon rotates clockwise from northeast to southeast via east wind with earlier conversion time and the wind speed reduces to less than 10m/s during wind direction conversion. At 16:20 of 9th, the typhoon landed at Beibi of Xiapu of Fujian. There lasted low speed wind for relatively long time at Dongchong (No. 15 tower) and Jiangtian (No. 16 tower) near the northern and southern side of typhoon centre (Fig3.7), but when moving southward or northward, the wind speed begins to increase for southward

high wind, southwest wind for the south side and southeast wind for the northern side. The strong wind at the south extends to Ninghai (No. 8 tower) and the wind force were able to reach grade 8. The typhoon kept moving northward after landing and there occurred long time strong southward wind at the coast of Zhejiang for its location at the right side of typhoon.

The analysis of tower data in Jiangsu province showed, the wind speed was less when the typhoon was far away from Jiangsu (August 8) with the direction of east to southeast; after typhoon landed in August 9. The wind speed in north of Jiangsu increased more than 12 m/s when the typhoon entered Jiangsu province in August 11. The wind speed in south rapidly decreased and that in north increased, but the direction still was anticlockwise for left side and clockwise for right side. The typhoon reached the sea in August 11, of which the wind speed of No. 1 and 2 mast towers were up to grade 8 with the direction of north to northeast. The wind speed at the north decreased to 6 to 7 m/s with north to northeast directions.

In short, the wind direction at left side of typhoon route rotated anticlockwise while clockwise for right side, and the wind force were able to reach more than grade 11. when the typhoon was about to land, the wind direction rapidly changed and the wind speed reduced to less than grade 6. After the typhoon landed, the strong southward wind of grade 8 might occur. Before the typhoon reached the sea, for the wind field at nearby area, the wind was able to reach grade 8 at the north while only 6 to 7 m/s at the north. The technicians in wind farm can judge the location of typhoon center according to the variations of wind speed and direction and then determine the protection and utilization measures to be taken.

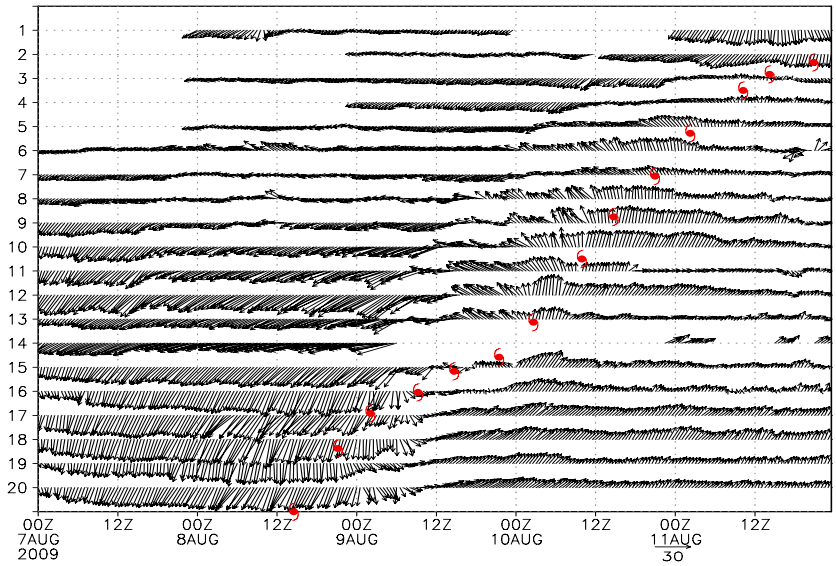

Figure 3.6 The time – conversion diagram of “Morakot” typhoon at 50m height

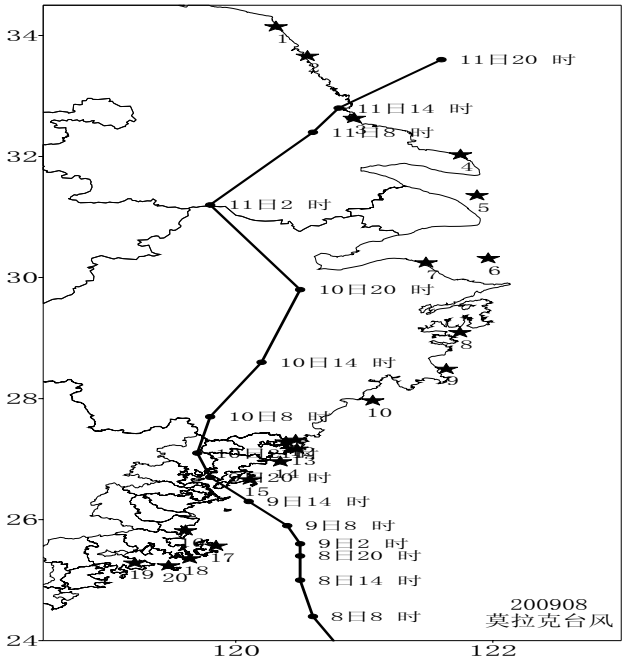

Figure 3.7 Anemometer tower sites around the typhoon route

3.2.2 Turbulence intensity

(1) Relationship between turbulence intensity and wind direction

The analysis of wind data of 15 mast towers at the coasts of Zhejiang, Jiangsu and Fujian provinces during the influence period of "Morakot" typhoon (Figure 3.8), the wind direction kept stable during the strong northward wind before typhoon landed and the strong southward wind after landed, and the turbulence intensity between high and low layers had less variation, of which the magnitude depended on the underlying surface characteristics. However during the excessively rapid variation of wind direction and reduction of wind speed, the inconsistent sudden increase of turbulence intensity occurred at both high and low layer, and the increment at high layer was sometimes larger than that of low layer, which enabled the turbulence intensity of high layer exceeds that of low layer. Taken the 70m height as an example, when the varied angle of wind direction within short time (less than 6 hours) exceeds 45°, the turbulence intensity might increase by 0.1 to 0.5 in 10 minutes and the maximum turbulence intensity might reach 1.5. After that, it may suddenly decreased. So it shown the sudden frequent variation. This case normally occurred before and after the typhoon landing. The anemometer tower nearer the typhoon landing point would show more apparently (Figure 3.8a).

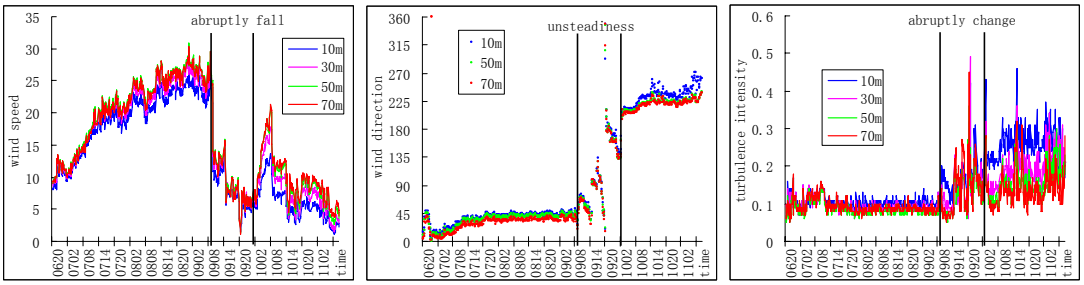

Wind speed wind direction turbulence intensity

(a) Xiapu Dondchong

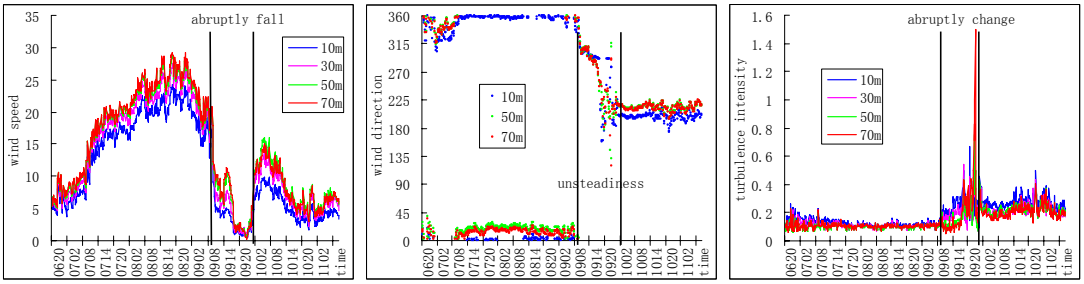

Wind speed wind direction turbulence intensity

(b) Changle Jiangtian

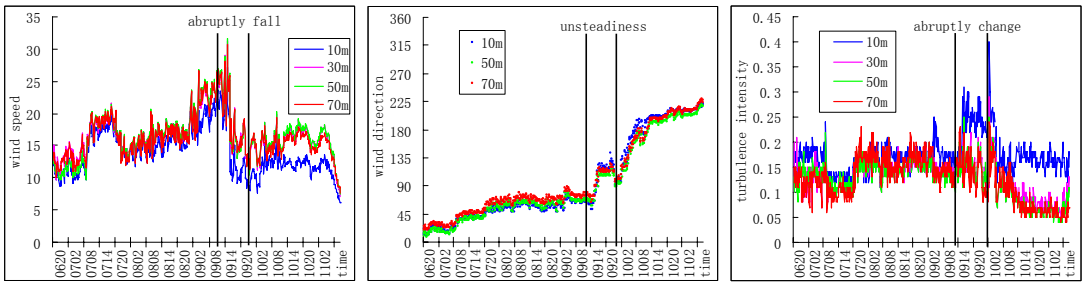

Wind speed wind direction turbulence intensity

(c) Dongtou Damendao

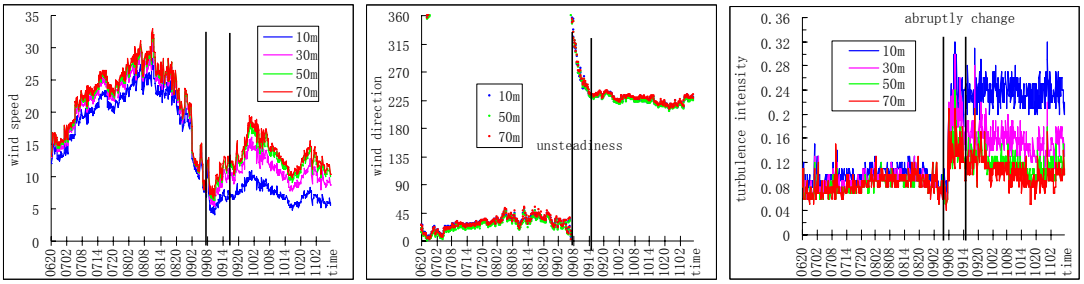

Wind speed wind direction turbulence intensity

(d) Pingtan Liushui

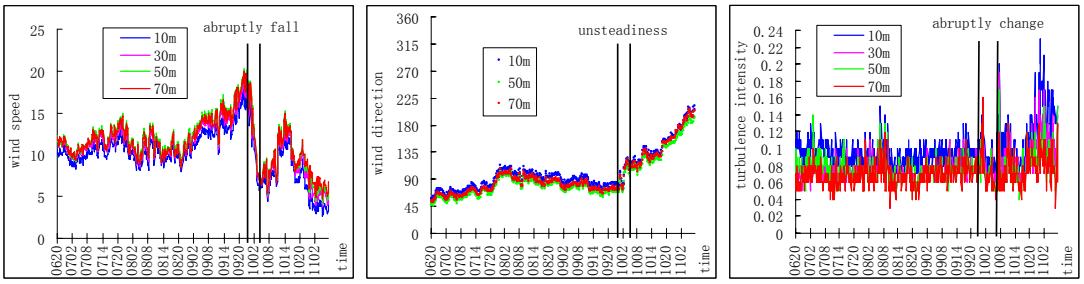

Wind speed wind direction turbulence intensity

(e) Ningbo Cixi

Figure 3.8 Relationships between turbulence intensity, wind speed and wind direction for the anemometer tower at different locations from typhoon landing point

(2) Relationship between turbulence intensity and underlying surface

Normally the turbulence intensity will increase with the increase of toughness and the increment depends on the topography condition.

Flat sand field, such as Xiapu Dongchong, Changle Jiangtian and Pingtan Liushui (Figure 3.8a, b and d): during the northeast wind, the turbulence intensity variation at all heights kept stable and decreased with the height. The maximum turbulence intensity was about 0.12, because the wind came from the sea with less roughness of underlying surface. When the wind speed increased, the difference of turbulence intensity between the upper and lower layers reduced and the turbulence intensity were almost the same; when the wind direction was extremely unstable due to typhoon approaching, the turbulence intensity magnitude significantly increased and might exceed 0.46; when the wind direction kept stable as the southward wind, the turbulence intensity became stable again; the wind came from the land to make the

lower layer influenced by the underlying surface, and the lower layer turbulence intensity could reach 0.22, the difference between the upper and lower layer could be up to 0.16 and the turbulence intensity trends to decrease with the height increasing.

Trees around the tower, such as Putian Nanridao (Figure 3.9a): the turbulence intensity reduced with the height increasing during northeast wind period. While the windbreak with a 10m height located at the south of the tower, the lower layer wind speed and turbulence intensity were significantly influenced by underlying surface, so the wind speed reduced and magnitude of turbulence intensity increased to be up to about 0.28; but the high layer was not affected, it was about 0.12, and the larger the wind speed is, the turbulence intensity would be more stable; when the wind direction was unstable, the sudden variation of turbulence intensity occurred; during the southeast wind period, the south of tower was open and the wind would not be affected by the trees; in addition, the wind speed decreased, so the turbulence intensity represented reduction at the lower layer and increased at the higher layer, but it still decreased with the height increasing.

Coteau and hill, such as Fuding Jiayang (altitude of more than 700m, Figure 3.9b): a certain distance from the sea; the turbulence intensity increased with the increase of wind speed during a northward wind period, while decreased during the southward wind period. The variation rules with the height was: it did not decrease with the height, the turbulence intensity at 70m high layer was larger than the 50m middle layer during a northward wind period, but it might be correspondent to that of 10m height, and the turbulence intensity at 70m height might exceed 0.16 and reach 0.26; during the southward wind, the turbulence intensity at 70m height would not correspond to that of 10m height and the turbulence intensity of more than 30m height were similar and lower than that of 10m height.

In conclusion, the variation of turbulence intensity is related to both underlying surface and distance from typhoon landing point. At the location near the typhoon landing point, the extremely instability of wind direction leads to an instability of underlying surface characteristics, so that it may lead to sudden variation of turbulence intensity; the turbulence intensity at the high layer is relatively larger and often in connection with a sudden decrease of wind speed. When the wind direction keeps stable, the underlying surface attribute is simple, and the variation of turbulence intensity depends on the wind speed. The larger wind speed is, the less turbulence intensity, and the difference between the high and low layers reduces, vice versa. It is worth to mention that at coteau and hill area, the variation of turbulence intensity with the height change does not comply with the normal rule, i.e., decrease with the height increasing.

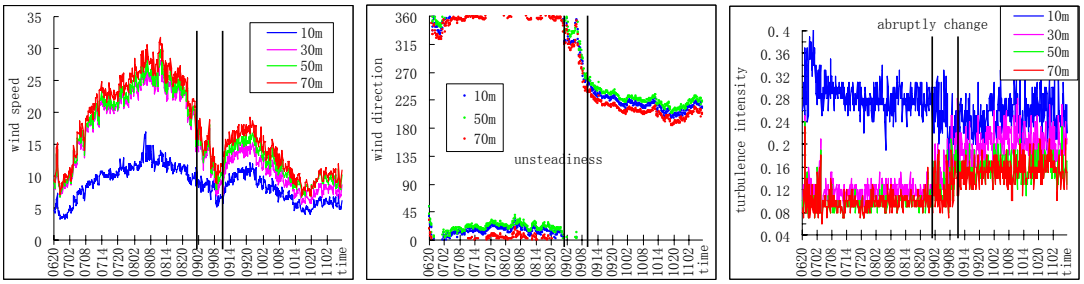

Wind speed wind direction turbulence intensity

(a) Putian Nanridao

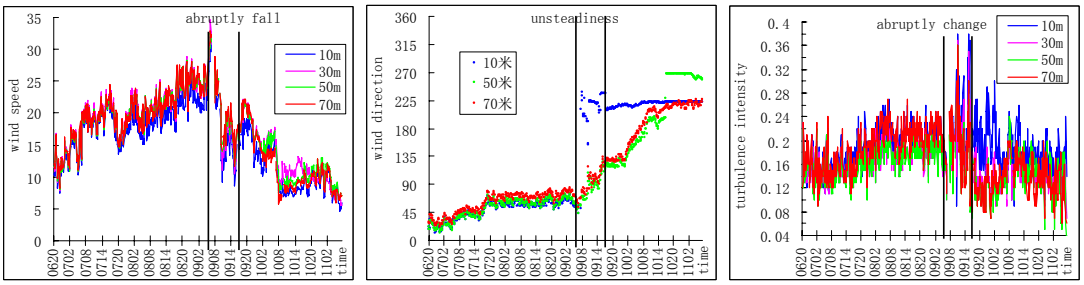

Wind speed wind direction turbulence intensity

(b) Fuding Jiayang

Figure 3.9 Relationship between turbulence intensity of anemometer tower and wind speed and wind direction for different underlying surface

3.2.3 Wind speed vertical shear

At the peripheral area of typhoon, the wind shear intensity was only related to underlying surface, such as Congming, Dongyuan and Yuantuojiao (Figure 3.10); near the landing point of typhoon, the vertical shear of wind speed was more complicated, which was not only related to the wind speed and underlying surface, but also the typhoon circulation position of anemometer tower, which defined the approaching direction of wind.; the topography passed by the wind directly influenced the wind speeds at various heights of anemometer tower. Here separately describe the observation facts of mast towers at the coast of north of Zhejiang to middle of Fujian near the landing point during typhoon influence period.

The statistical results of anemometer tower data show as the following, during the rapid decrease period before typhoon landing, the wind speed was small and normally less than 12 m/s; the variation of exponent sign had the common features and its

variation magnitude was the maximum value of the whole typhoon process; sometimes the negative and positive shear might alternatively occur with the positive shear for sudden increase and negative for sudden decrease. During other periods under the influence of typhoon, different location might have the different characteristics .

(1) Wind coming from the sea and sand beach topography

Before typhoon approaching, such as Changle Jiangtian, Pingtan Liushui (Figure 3.11): wind direction was northward and of sea wind; the vertical variation of wind speed was of positive shear which meant that the wind speed increased with the height and the exponent sign was in inverse correlation to the wind speed and decreased with the height; the wind speed difference between the upper and lower layers was less; when the wind speed was larger than 10m/s, the exponent sign was about 0.1; when it was less than 10 m/s, its exponent sign would be little larger but not more than 0.2; the maximum wind speed difference between the upper and lower layers was 3.8m/s at 10m to 30m height, 2.1m/s at 30 to 50m, 0.9m/s at 50 to 70m; After typhoon landed**,** such as Xiapu Dongchong, Pingtan Liushui: wind direction was southwestward and of sea wind, the vertical variation of wind speed was of positive shear which meant that the wind speed increased with the height and the exponent sign was in inverse correlation to the wind speed and decreases with the height; it was larger than that of the northward wind and between 0.3 to 0.4; the maximum wind speed difference between the upper and lower layers was 5.3m/s at 10m to 30m height, 3.1m/s at 30 to 50m, 1.1m/s at 50 to 70m.

(2) With trees or shrubs near the tower

Such as Fuding Yushandao and Putian Nanridao, before the typhoon approaching, wind direction was northward and of sea wind; the vertical variation of wind speed was of positive shear; the lower layer was affected by the underlying surface and the exponent sign was especially large (see figure 3.12) and might exceed 0.7, while that of upper layer was small and not more than 0.1. the maximum wind speed difference between the upper and lower layers was 22.8m/s at 10m to 30m height, 13.6m/s at 30 to 50m, 2.1m/s at 50 to 70m; After typhoon landed, wind direction was southwestward; at Nanridao, due to the open underlying surface of the south, the exponent sign of lower layer decreased; but that of high layer increased under the influence of typhoon circulation to be 0.1 to 0.3; the maximum wind speed difference between the upper and lower layers was 3.8m/s at 10m to 30m height, 2.8m/s at 30 to 50m, 1.7m/s at 50 to 70m.

(3) Wind coming from land

Before the typhoon landed, such as Xiapu Dongchong (see figure 3.11), the northeastward wind passed the mountainous area; the wind speed at 10 to 50m height was of positive shear and that at 50 to 80m height was of negative shear; the layer of maximum wind speed was at about 50m height. The exponent sign difference was within about 0.1 to 0.2. The maximum wind speed difference between the upper and lower layers was 2.8m/s at 10m to 30m height, 1.8m/s at 30 to 50m, -0.8m/s at 50 to 70m; After typhoon landed, such as Changle Jiangtian, wind direction became southwestward and the wind came from the land, the wind speed at the height of less than 50m increased with the height, while contrary for that of above 50m, so the high layer was of negative shear and the magnitude was ±(0.3～0.4) larger than that before typhoon landing. The maximum wind speed difference between the upper and lower layers was 3.9m/s at 10m to 30m height, 2.9m/s at 30 to 50m, -1.6m/s at 50 to 70m.

(4) Coteau with high altitudes

Such as Fuqing Donghan, Fuding Jiayang and Cangnan Hedingdhan (see figure 3.13): before typhoon landing, the wind direction was northward and the exponent sign was between about 0.2 and 0.3. The variation of wind speed with the height was inconsistent. The wind speed decreased or increased with the heights above 30m; except for the 10m height, the wind speed difference between the upper and lower layers was small and between -1.2 and 1.1 with the negative exponent sign. After the typhoon landed, wind direction became southwestward and the exponent sign variation suddenly increased and swang between -0.8 and +0.6. The wind speed difference between the upper and lower layers was large.

The maximum wind speed difference between upper and lower layer was 4.7m/s at 10m to 30m height, -3.3m/s at 30 to 50m, -3.4m/s at 50 to 70m, which was due to the smooth slope at the north of tower and steep slope at the south.

In conclusion, the exponent sign shows obvious sudden increase or decrease before and after the typhoon landing. Near the typhoon landing point, when the wind direction comes from the sea, the wind speed increases with the height. The exponent sign of northward wind before typhoon approaching is smaller than that of southward wind after landed, and not more than 0.2; the exponent sign of southward wind is normally twice of that of northward wind; the exponent sign is most unstable with largest fluctuation before and after typhoon landing and the positive and negative exponent sign may alternatively occur. When the wind comes from the land, the layer

of maximum wind speed mainly occurs at 50m height, that of more than 50m height is of negative shear and that of less than 50m height is of positive shear. The exponent sign of southward wind is twice larger than that of northward. On the high mountains, the negative shear exists before and after the influence of typhoon due to the slope influence, and the positive and negative shear differences will increase with the increment of gradient.

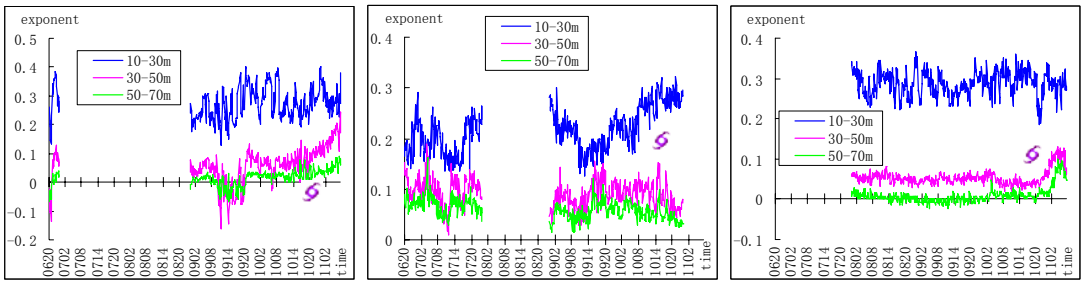

Qidong Dongyuan Qidong Yuantoujiao Congming Hengshadao

Figure 3.10 Typhoon peripheral anemometer tower exponent sign

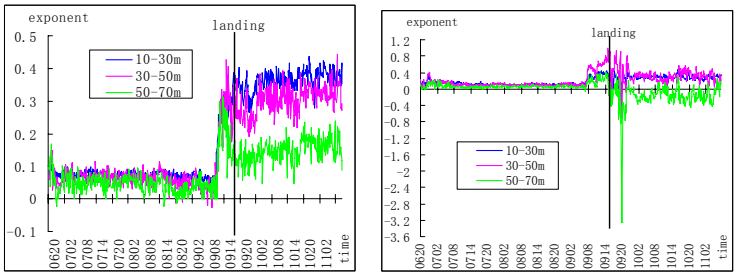

Pingtan Liushui Changle Jiangtian

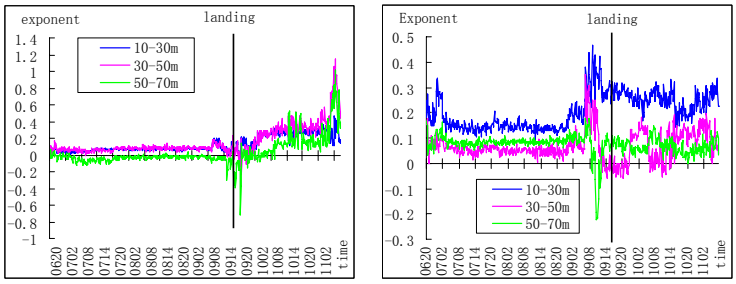

Xiapu Dongchong Putian Houwen

Figure 3.11 Exponent sign at sand beach topography anemometer tower

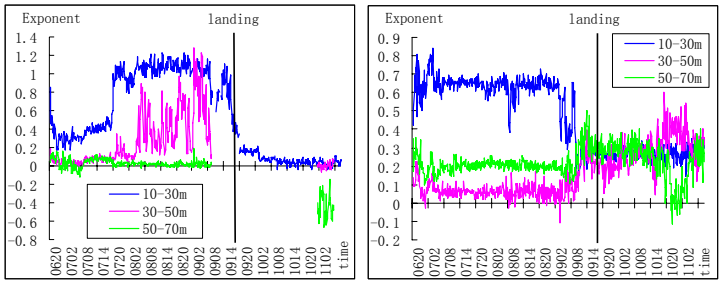

Fuding YushanDao Putian Nanri

Figure 3.12 Exponent sign at shrub topography anemometer tower

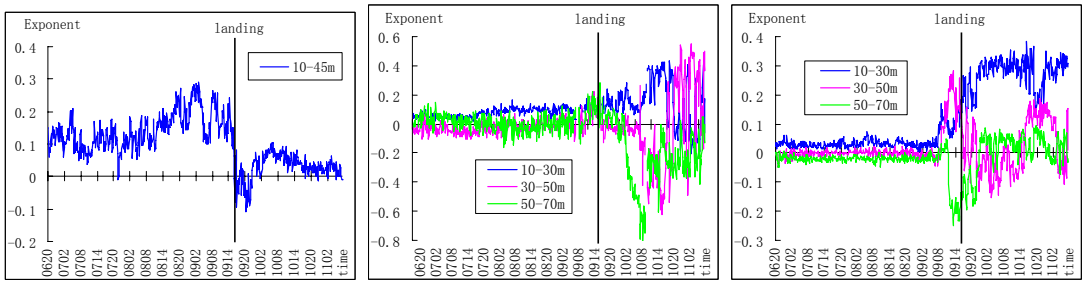

Cangnan HedingShan Fuding Jiayang Fuqing Donghan

Figure 3.13 Exponent sign at coteau and mountainous terrain topography anemometer tower

3.3 Turbulence intensity of surface layer of tropical cyclone

By collecting the data of 85 mast towers of the coastal area from Jiangsu to Hainan selected the data affected by the tropical cyclones (including both landing typhoons and offshore turning ones) .Nineteen tropical cyclones were obtained for case study by statistically, arranging in order and generalizing.

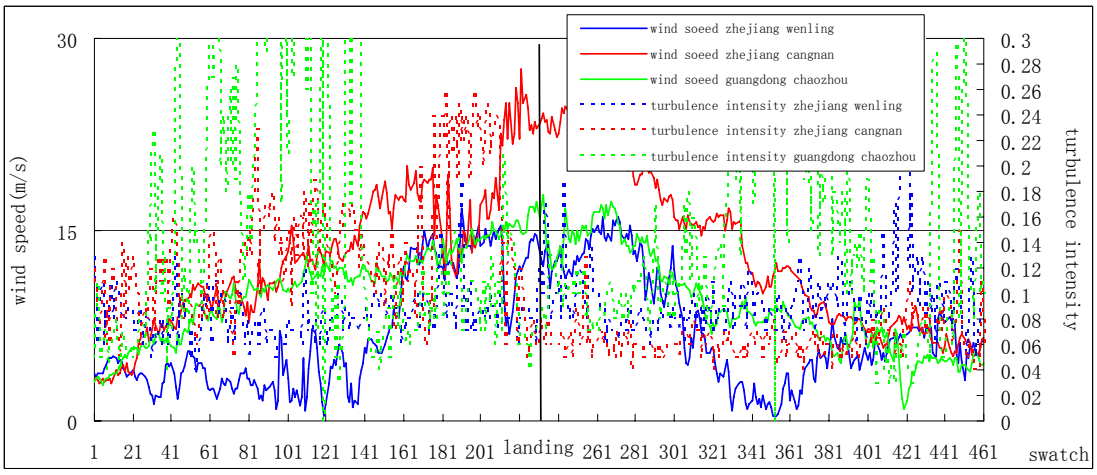

Fig. 3.14 The time evolution diagram of wind speed and turbulence intensity at the 70m-height anemometer tower on both sides of Typhoon Talim (200513)

All the case studies have shown that the properties of the underlying surfaces would become unstable with the abrupt turning of wind when the tropical cyclones approached the mast towers, often leading to a sharp increase in turbulence intensity, accompanied with a sharp decrease in wind speed. The wind speed would decrease when the landing of a tropical cyclone and at that time the change in turbulence intensity would not follow the law of its decreasing with increase in height. Generally, wind turbine can resist the intense turbulence under a weak wind speed. However, sometimes the wind speed was still very strong before and after the landing of a tropical cyclone, and at the height of 70m the intense turbulence with a strong wind speed was unfavorable to the existence of the wind turbine designed in accordance with the existing IEC standard. For example, Typhoon Vipha, Typhoon Talim (200513)(figure 3.14) which landed at Putian, Fujian and Typhoon Sepat (200709).

What we concern is whether the turbulence intensity is greater at the height of over 30m when wind speed is relatively strong. In this study, under the wind speeds of 15～25m/s (the wind speed range of a wind turbine with full output) and ≥25m/s (the wind speed range of wind turbine shut-down) have been analyzed, showing the characteristics of turbulence intensity of southward and northward winds.

When the wind speed ranges of 15～25m/s at the height of 70m the wind turbine works and the enhanced turbulence intensity will influence the operational life span of the wind turbine . By statistically analyzing the nineteen tropical cyclones, the result showed that the average turbulence intensity was approximately for the southward and northward wind. The decreasing rate of the turbulence intensity was not great at the height of 10m～70m .The turbulence intensity changed the ranges in 0.05～0.02(figure 3.15) at the height of 10m～70m ,according to 71% of the tropical cyclones ,and 16% ranges in 0.09～0.04 ,only the turbulence intensity at the height of 10m～70m at Dongshan Aojiao mast towers ranged in 0.12～0.03.

The extremum of turbulence intensity at the range of this wind speed were more than 0.16 that was the IEC level of intense turbulence. In the mountainous areas of complicated terrain (e.g. Shachengtai Peak at Fuding and Xiapuxiahu), the values could maximize up to 0.28 at the height of 70m ,with insignificant difference between the southward and northward winds occupying by 32% (figure 3.15). The extremum of turbulence intensity of northward wind was greater than the southward wind occupying by about 32%(figure 3.16). The extremum of turbulence intensity of northward wind was smaller than the southward wind occupying by about 16% (figure3.17) ,and became apparent under 40m .Moreover, when the anemometer tower, lands on the north side of the tropical cyclone the turbulence intensity was more intense than that when it lands on the south side of the tropical cyclone; when the anemometer tower was located around the tropical cyclone center, the turbulence

intensity of northward wind was greater than that of southward wind.

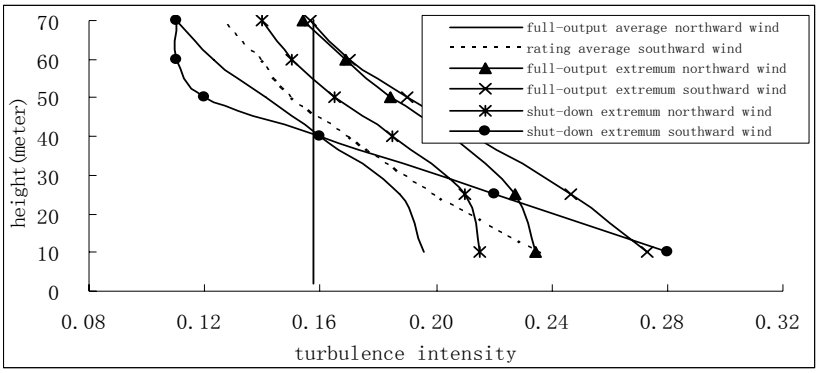

Fig. 3.15 Turbulence intensity in different wind-speed ranges at Pinghai of Putian, Fujian

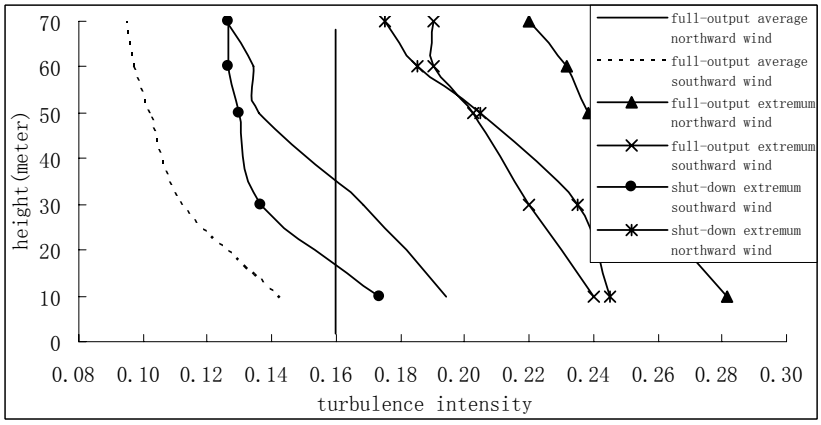

Fig. 3.16 Turbulence intensity in different wind-speed ranges at Cangnan of Zhejiang

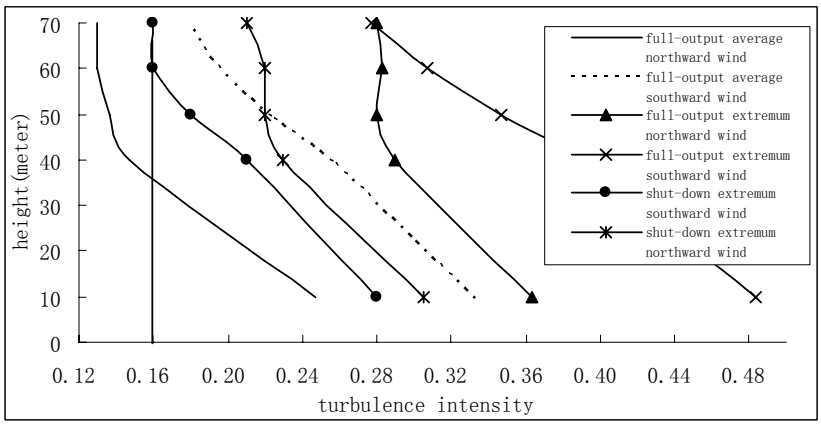

Fig. 3.17 Turbulence intensity extremum in different wind-speed ranges at Shachengtai Peak of Fuding, Fujian

When the wind speed was more than 25m/s at the height of 70m, about 87% of the turbulence intensity extremum was smaller than that of 15～25m/s. For the isolated cases with the northward wind, it would be turbulence intensity extremum of

15～25m/s (figure 3.18).

The characteristic of the change of the turbulence intensity extremum with the increase of height at the speed of over 25m/s : at the range of 10m～70m, there are only 3 that have insignificant difference ,including 2 strong northward wind and 1 strong southward wind, respectively. Majority of the turbulence intensity extremum at the height of over 40m had the insignificant difference, it was greater under 40m than upper 40m,. The turbulence intensity extremum under the strong northward wind at 40m and 10m differs were 0.02-0.04 occupying by 57%, 0.05-0.10 occupying by 29%，>0.10 occupying by 14%, respectively. The turbulence intensity extremum under the strong southward wind at 40m and 10m differs were 0.02-0.04, occupying 43%，0.05-0.10 occupying 36%，>0.10 occupying 29%, respectively。

The comparison of the turbulence intensity extremum of both strong northward wind and southward wind, the southward strong wind was greater than the northward strong wind for 3 times (figure 3.19), the southward strong wind was smaller than the northward strong wind for 2 times (figure 3.16 and figure 3.17), the southward strong wind was smaller at the height of over 40m than that of northward strong wind, it was opposite under 40m(figure 3.15). This inhomogeneous turbulence intensity change led to the negative effects on the wind turbine.

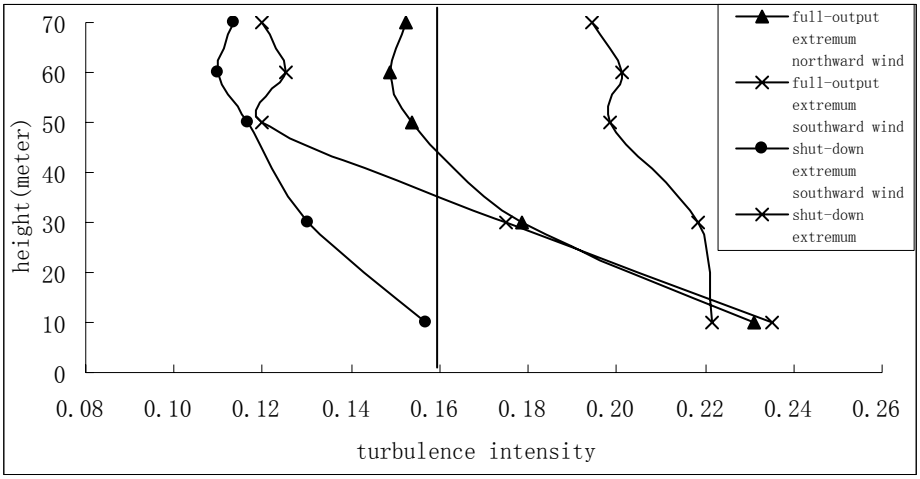

Fig.3.18 Mean turbulence intensity of different wind-speed ranges during the influence of tropical cyclone at Wenling, Zhejiang

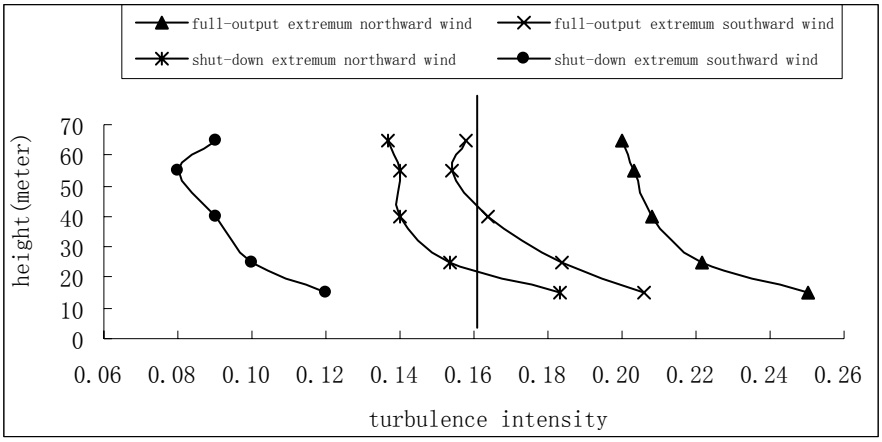

Figure 3.19 Extreme turbulence intensity of different wind-speed ranges at Xianjincun of Pingtan , Fujian

3.4 Vertical Shear Law of Wind Speed under the Influence of Tropical Cyclone

Based on the data of 85 coastal mast towers, the vertical shear of wind speed from 10 to 70m is analyzed. It is found out that the shear index of both wind speed between 15 and 25m/s and more than 25m/s were positive. However, the difference among indexes in different topographic conditions was great: the shear index on a flat beach was the smallest in several topographic conditions. Its average shear index varied from 0.11 to 0.20. The extreme value of 10min index could reach to 0.11 to 0.33 (refer to table 3.1 Zhejiang Wenling and Fujian Pingtan). The shear index of north wind is larger than that of south wind. On mountainous region with the elevation of more than 100m, such as Fujian Fuding Shachengtaifeng, Dongshan Aojiao and Guangdong Chaozhoutuolin Town in table 3.1, the index could exceed 0.6 due to the influence of topographic slope. In seaside areas with low elevation, mast towers with trees and shrubs at the surrounding, such as Fujian Lianjiang Beijiao and Hainan Danzhou EmanLongmen in table 3.1, the average index was between 0.24 and 0.45, and the extreme value of 10min index could reach to 0.27 to 0.94. This shows that under the influence of tropical cyclone, the vertical shear indexes of typhoons were larger than that of international criterion GB50009-2001 with the same topographic conditions, and there is obvious difference in wind direction.

Table 3.1 Vertical shear of wind speed below the height of 70m for typical topography

Name of tower	Environment	Elevation	Wind speed section	Wind direction	Average power index of the whole layer	Extreme value of power index of the whole layer
Zhejiang Wenling	Shoal	8	15-25m/s	North wind	0.17	0.28
				South wind	0.14	0.27
			≥25m/s	North wind	0.20	0.33
				South wind	0.14	0.22
Fujian Pingtan	Beach	30	15-25m/s	North wind	0.19	0.29
				South wind	0.15	0.3
			≥25m/s	North wind	0.16	0.23
				South wind	0.11	0.11
Fujian Fuding Shachengtaifeng	Hilly and mountainous area	267	15-25m/s	North wind	0.24	0.43
				Southerly wind	0.30	0.44
			≥25m/s	North wind	0.22	0.36
				South wind	0.24	0.32
Fujian Dongshan Aojiao	Costal hills		15-25m/s	North wind	0.80	0.91
				South wind	0.67	0.9
			≥25m/s	North wind	0.66	0.7
Guangdong Chaozhoutuolin Town	Hill	107	15-25m/s	North wind	0.29	0.58
				South wind	0.40	0.64
			≥25m/s	North wind	0.34	0.49
				South wind	0.31	0.51
Liangjiang Beijiao	Coastal low hills	50	15-25m/s	North wind	0.36	0.83
				South wind	0.45	0.94
			≥25m/s	North wind	0.43	0.75
Hainan Danzhou EmanLongmen	Plain	23	15-25m/s	North wind	0.34	0.68
				South wind	0.34	0.47
			≥25m/s	North wind	0.24	0.28
				South wind	0.25	0.27

Based on the analysis of shear indexes at all heights, it is found out that there were the negative shear phenomena (table 3.2) on some mast towers at the height of 60 to 70m or 50 to 70m. This indicates that during the period under the influence of tropical cyclone, some places were not fully complied with the index law. We can also see from the table that the shear index of coastal low hills at the height between 10 to 30m

or 10 to 40m was large, at the height between 50 and 70m was relatively reduced, while the difference in other topographies was relatively small. In addition, the analysis of typical cases in sections 3 to 5 of this chapter shows that the wind direction and wind speed were very unstable while the tropical cyclone was closing or before and after it was landed. This led to the unsteadiness of the shear index. Most of the negative shear indexes occurred at this period.

Table 3.2 Vertical shear indexes of wind speed at different heights

Name of tower	Environment	Elevation	Wind speed section	Wind direction	Height (m)			
					10 - 30	30 - 50	50 - 60	60 - 70
Zhejiang Wenling	Shoal	8	15-25m/s	North wind	0.20	0.14	0.16	-0.02
				South wind	0.14	0.15	0.12	0.14
			≥25m/s	North wind	0.25	0.18	0.15	-0.08
				South wind	0.14	0.15	0.10	0.16
					10 - 40	40 - 50	50 - 60	60 - 70
Liangjiang Beijiao	Low hills	50	15-25m/s	North wind	0.43	0.13	0.02	0.21
				South wind	0.57	0.10	-0.09	0.06
			≥25m/s	North wind	0.52	0.13	0.05	0.23
					10 - 40	40 - 50	50 - 60	60 - 70
Xiapu Xiyang Island	Small sea island	39	15-25m/s	North wind	0.08	0.16	0.16	0.00
				South wind	0.31	0.03	0.30	-0.12
			≥25m/s	North wind	0.08	0.02	0.02	-0.13
					10 - 30	30 - 50	50 - 65	65 - 70
Hainan Wenchang 41	Seaside	5	15-25m/s	North wind	0.22	0.11	0.11	-0.14
				South wind	0.14	0.10	0.19	-0.61
			≥25m/s	North wind	0.13	0.09	0.11	-0.27

4 RESULT 3: SET UP A SEARCHING SYSTEM FOR TCS THAT AFFECT WIND-POWER DEVELOPMENT IN OFFSHORE CHINA

4.1 Structure of retrieval system of tropical cyclones affecting China offshore wind power development

Retrieval system of tropical cyclones affecting the Chinese offshore wind power development can be divided into 3 subsystems, i.e., tropical cyclone path, statistical characteristics and extreme wind speed, as well as system instructions (see Figure 4.1). Tropical cyclone path subsystem consists of monthly tropical cyclone path, path of tropical cyclones with different intensity, and path of tropical cyclones landing on different areas. Statistical characteristics subsystem consists of frequency of tropical cyclones with different intensity affecting the Chinese offshore, and frequency of intensity of tropical cyclones landing on different areas. Extreme wind speed subsystem consists of distribution of extreme maximum wind speed of tropical cyclones affecting the Chinese coast, distribution of maximum wind speed once in the multiple years of tropical cyclones affecting Chinese coast, distribution of extreme maximum wind speed of tropical cyclones affecting China offshore, and distribution of maximum wind speed once in the multiple years of tropical cyclones affecting the Chinese offshore.

4.2 Technical requirements of retrieval system

The system takes Windows as platform of operation system, visual basic 6 as program developing language, SuperMap as GIS system platform, and access as assistant database system. Document output adopts VB for an Application technology, calling programming interface provided by word to implement automatic control for whole course to generate documents.

4.3 Function of retrieval system

Through software, real-time and batch update of tropical cyclone data, path query and statistical chart query automatically come true. The system mainly consists of five functions, i.e., data management, path query, statistical chart query, output and help. Detailed instructions for all function modules are as follows:

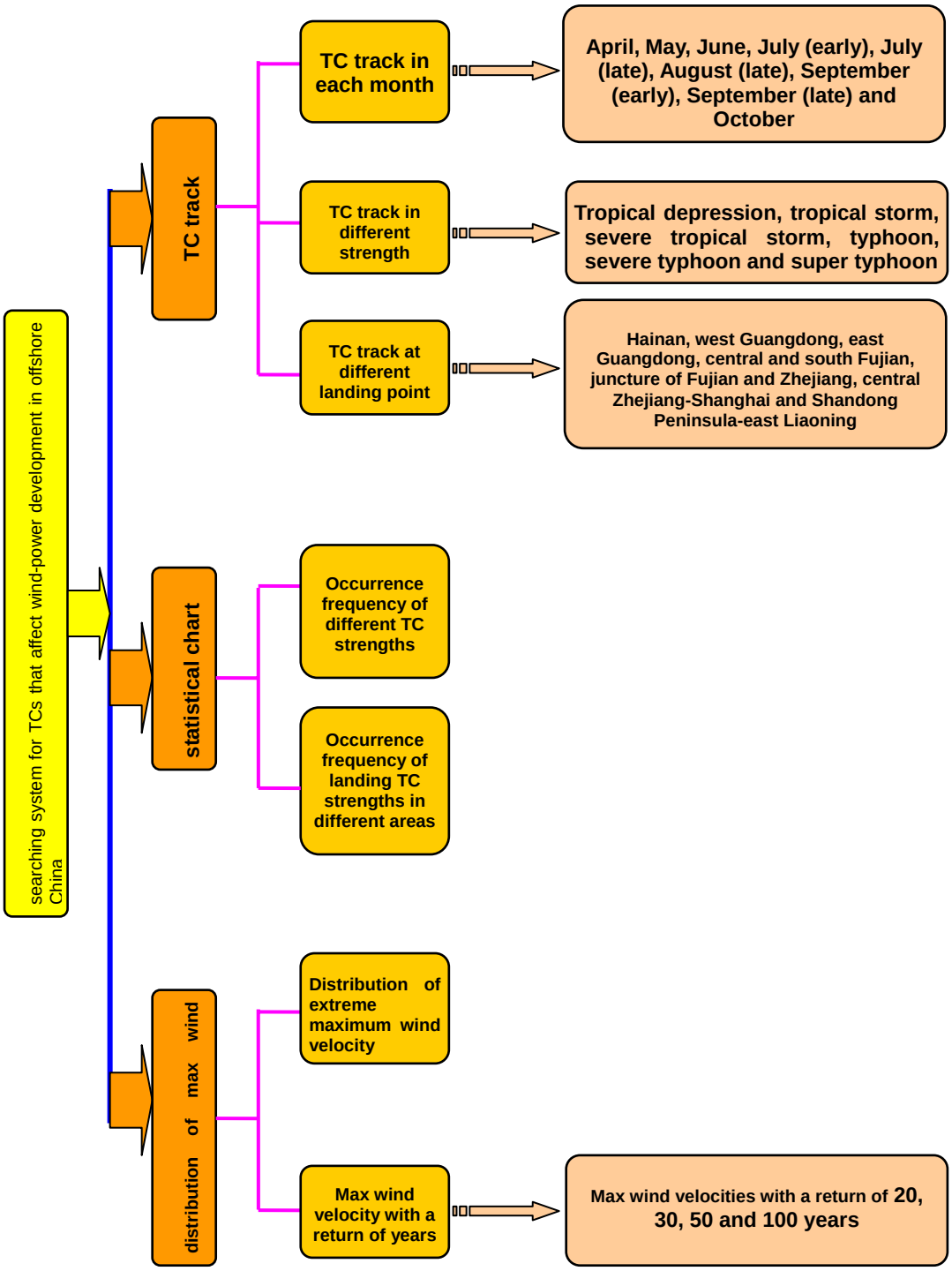

Fig. 4.1 The framework chart of the searching system for TCs that affect wind-power development along the offshore of China

4.3.1 Data management module

Providing real-time and batch update functions of typhoon data. Real-time update sub-module decodes from ground station code and typhoon path message, and adds path information into accessory database of GIS platform. Batch update sub-module is used to cover non-audited information acquired through monitor in former years with audited path information or newly path information every year, or to add information.

4.3.2 Tropical cyclone path query module

Providing space query and attribute query sub-modules. Space query sub-module is used to enter typhoon in a defined region by means of arbitrary circle, arbitrary rectangle, arbitrary polygon, fixed point circle and fixed point rectangle queries. Attribute query sub-module provides a screening condition builder for the user to generate a character string corresponding to where clause in SQL statement, so as to obtain the typhoon to be inquired about.

Screen display provides zoom in, zoom out, panorama, free shift, stepless zoom with middle key of mouse and other functions. In status bar, information on longitude and latitude where mouse is located can be automatically displayed. Under path attribute query status, name, maximum wind speed, lowest air pressure and other information of this typhoon can be displayed in status bar by clicking path line. Visibility or non-visibility, color, line mode and others of layers can be freely selected by means of multi-layer controller.

4.3.3 Statistical characteristic query module

Providing charts, tables, literal statement and other query functions,.including frequency of tropical cyclones with different intensity affecting the Chinese offshore, frequency of intensity of tropical cyclones landing on different regions, landing frequency intensity, typical typhoon process and other obtained by project statistical analysis.

4.3.4 Extreme wind speed module

Providing query function for extreme maximum wind speed, maximum wind speed in 100 years, 50 years, 30 years, 20 years, 2 years of tropical cyclones on the sea and land by project calculation and analysis, respectively.

4.3.5 Output module

It provides the saving function for a current graphic screen, function of saving current isoline, as well as function of printing according to selected graphics and literal.

4.3.6 Help

This searching system provides system operation instructions, including system installation, directory structure, input/output files, and specific operation instructions of individual sub-modules.

4.4 Usage instructions of retrieval system of tropical cyclones affecting China offshore wind power development

The usage instructions of retrieval system of tropical cyclones affecting the Chinese offshore wind power development are divided into 5 parts.

4.4.1 Functions and characteristics

The system possesses functions of real-time and batch update of tropical cyclone data, path query and statistical chart query, including 5 functions of data management, path query, statistical chart query, output and help. The system displays query results in graphics, tables and literal, with friendly operation interface, provides installer and help file. The system utilizes developable module of GIS platform to implement accurate time and space query for typhoon path.

4.4.2 Requirements for software and hardware

Hardware requirements: CPU basic frequency > 3G, EMS memory > 1G, hard disk > 80GB, color display > 15". If necessary, various common blacks and white or color printers may be equipped.

Software requirements: Windows 2000/XP, GIS platform SuperMap

4.4.3 Operation instructions

(1) General rules

Software adopts a common main window – sub-window structure. All functions of software can be used through main menu. For some frequently used functions, tool bar shortcut mode is provided.

(2) Main interfaces of tropical cyclone path

This interface provides:

- Year selection (1949-2008)
- Selection for path and extreme value of wind speed numbered (with international number and Chinese number) tropical cyclones every year
- Selection for saving and clear screen
- Information appending

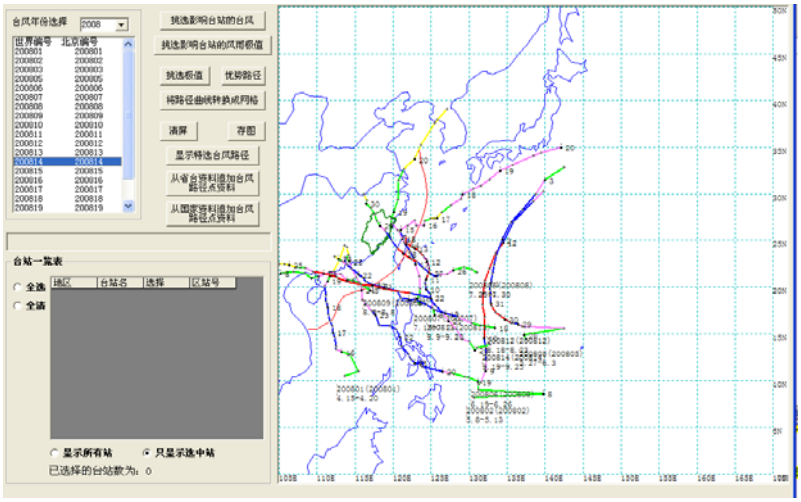

By means of numbered menus, any one or more necessary tracks and related information on tropical cyclone can be inquired.

(3) Main interfaces of statistical characteristic query

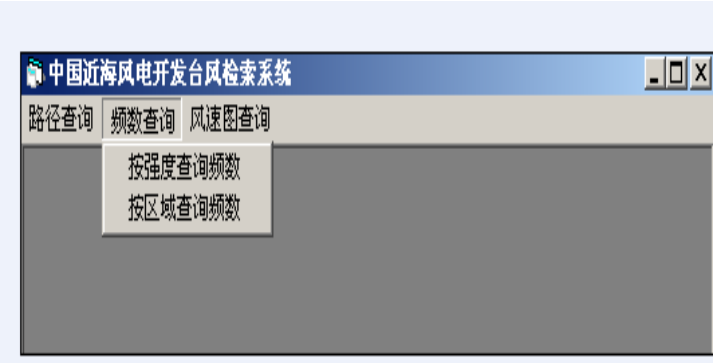

By means of this interface, occurring frequency of tropical cyclones affecting the Chinese offshore, tropical cyclones landing on different areas, horizontal wind field of typical typhoon, turbulence intensity, wind vertical shear exponent charts and so on can be inquired.

风速（米/秒）	风力（级）	名称	15° N - 45° N， 105° E - 130° E	进入警戒区	登陆
≥51	≥16	超强台风	88	34	5
41.5—50.9	14～15	强台风	70	58	27
32.7—41.4	12～13	台风	137	144	111
24.5—32.6	10～11	强热带风暴	125	110	119
17.2—24.4	8～9	热带风暴	58	44	53
10.8—17.1	6～7	热带低压	101	38	46

(4) Main interfaces of extreme wind speed query

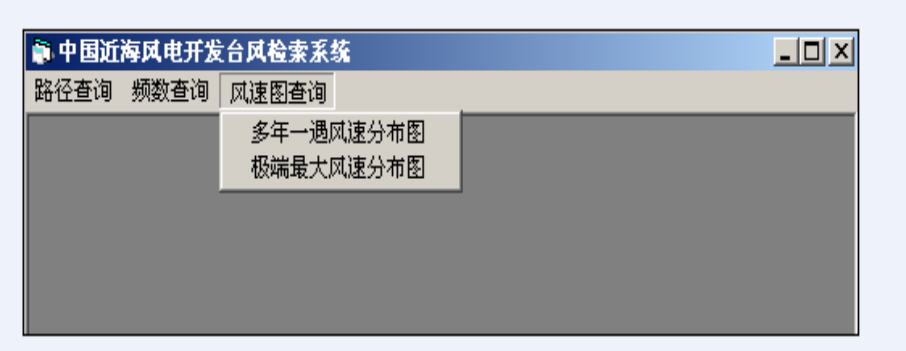

By means of this interface, distribution of extreme wind speeds of tropical cyclones affecting the Chinese offshore can be inquired.

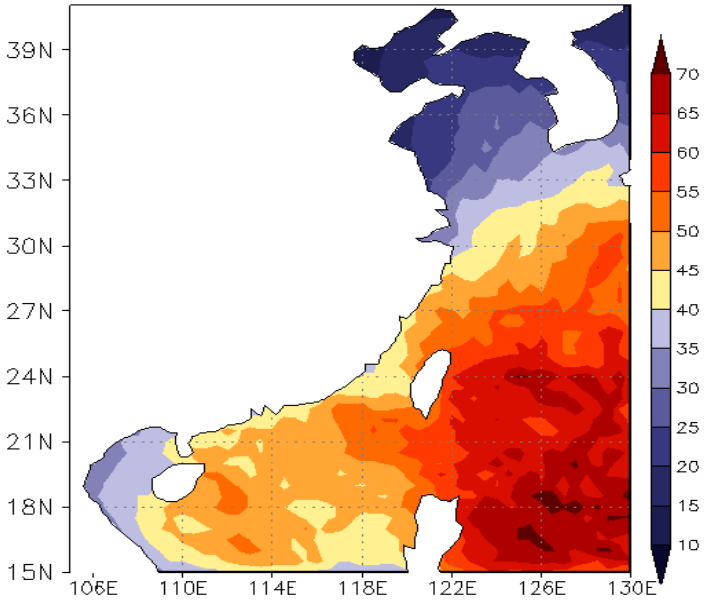

Maximum wind speed frequency once in 50 years

5 RESULT 4: THE STUDY ON THE CHARACTERISTICS OF VARIATION IN TYPHOON INTENSITY UNDER COMPLICATED AND PLAIN LANDFORMS

From Figure 2.6 we know that the maximum wind speed once in 50 years in the middle south offshore of Fujian is less compared with the sea areas in the south and the north. We know in Table 5.1 that the super typhoons landing on Taiwan took by 35% of the total 48 years, severe typhoon took by 22%, and stronger than all areas in the mainland China. The cause may be that the intensity of tropical cyclone during passing Taiwan Island weakened. In this research project, No.8 tropical cyclone in 2008 “Fungwong” is selected as a research object. The reasons to select “Fungwong” are mainly based on the following. First, “Fungwong” was a westbound (northbound) tropical cyclone formed on the northwest Pacific Ocean, and is representative, because most TCs hitting Taiwan have had such features. Secondly, intensity of “Fungwong” passing Taiwan Island was stronger, and it was severe typhoon (45m/s) when lading on Taiwan Island, in favor of comparison and analysis. Thirdly, the landing site of “Fungwong” is located in the middle of Taiwan where there are higher mountains and more complex topography, in favor of conformation of topography sensitivity experiment and comparison and analysis with the true situations. WRF meso-scale numerical model is used for the simulation of the effect of Taiwan Island on typhoon intensity.

Table 5.1- Frequency of different intensity TCs landing on Taiwan Island

Super severe typhoon	Severe typhoon	Typhoon	Severe tropical storm	Tropical storm	Tropical depression
31	19	16	12	8	2

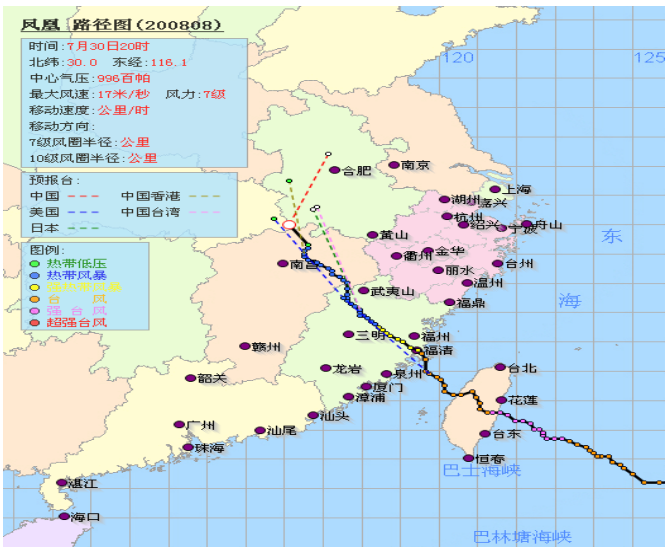

Figure 5.1 – Typhoon “Fungwong” path

(From Zhejiang Province typhoon path real-time issuing system, http://www.zjwater.com/typhoneweb/

5.1 Introduction to WRF meso-scale numerical model

WRF (Weather Research Forecast) model is a new generation of medium-scale weather forecast model and assimilation system which was cooperatively researched and developed by scientists from many research institutions and universities in USA. The development of the system is to provide a public model framework for the idealized dynamic research, weather forecast of all physical processes, air quality forecast and regional climatic simulation.

WRF model commits itself to improve the forecast precision of weather characteristics of different scales from cloud to weather scales and is mainly focused on the horizontal grid of 1-10 km. This model has been combined with the advanced numerical methods and data assimilation techniques, has adopted the improved physical process schemes, and has the ability to the multinest and locate at the different geographic positions easily.

WRF model belongs to a completely compressible and non-hydrostatic model and F90 language is used for programming. Horizontally, Arakawa C grid points are used (Fig. 5.2), whereas vertically two selections have been provided: one is height coordinate (Eulerian height coordinate), i.e. the ground is 0 m high and then gradually increases up to the atmospheric top; the other is mass coordinate (Eulerian mass coordinate), established on the base of η coordinate, i.e. the ground is 1 while the

model top is 0 (Fig. 5.3). In time integral scheme, the three-level Runge-Kutta is used. This model not only can be used for the case simulations of real weather, but also can use its inclusive module sets as the theoretical bases for exploration of basic physical processes.

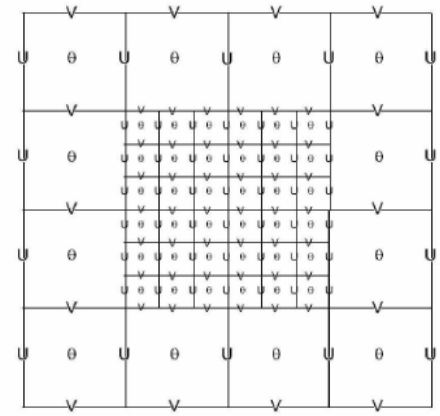

Fig. 5.2: Arakawa C Grid Sketch Map

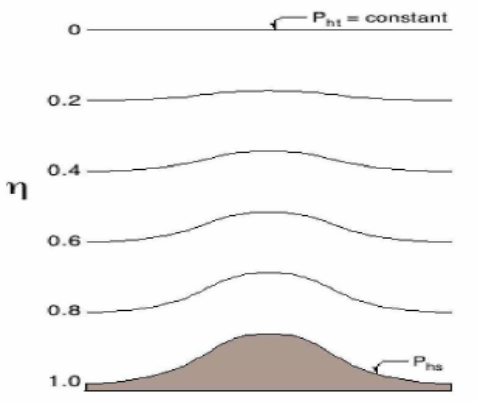

Fig.5.3: Coordinate Sketch Map

Table 5.2: WRF Physical Scheme

Microphysical	Kessler Scheme (warm rain scheme), the scheme by Lin et al. (vapor, rain, snow, cloud water, ice and hail), WSM 3-class simple ice scheme, WSM5 scheme, Ferrier (new Eta) microphysical scheme (vapor and cloud water), WSM6 hail scheme, the scheme by Thompson et al. etc.
Cumulus convection	Kain-Fritsch Convective (new Eta) scheme, Betts-Miller-Janjic scheme, Grell-Devenyi aggregated scheme and simplified Arakawa-Schubert scheme
Long-wave radiation Short-wave radiation	RRTM scheme, GFDL (Eta) scheme Dudhia scheme, Goddard scheme, and GFDL (Eta) scheme
Disturbance	TKE forecast, Smagorinsky, stable diffusion
Boundary layer scheme	MRF, MYJ, YSU
Ground layer	Monin-Obukhov scheme, MYJ scheme, NCEP's global forecast system scheme
Land surface	5-layer soil model, RUC land model, Noah uniform land model

5.2 Main WRF modules and their functions

In Fig 5.4, WRF modeling system flow chart can be actually simplified three parts into as WPS + WRF-ARW Model + Post Processing.

WPS pre-processing consists of three parts: geogrid, ungrib and metgrid. Of these, geogrid is used for establishment of "static" ground data, ungrib is used for decompression of GRIB meteorological data, metgrid is used for horizontal interpolation of meteorological data into modeling domains, and metgrid output files are used as input ones for WRF modeling.

The main body of WRF-ARW Model consists of real.exe and wrf.exe. real.exe is used to form the initial field and boundary condition required for integration, but the real integration is completed through wrf.exe.

In this study, GRADS software is mainly used for visualization processing of the output data from WRF model.

Presently, the debugging of WRF medium-scale numerical model has been completed and it is being used for simulation test with severe typhoon 'Phoenix' of 2008.

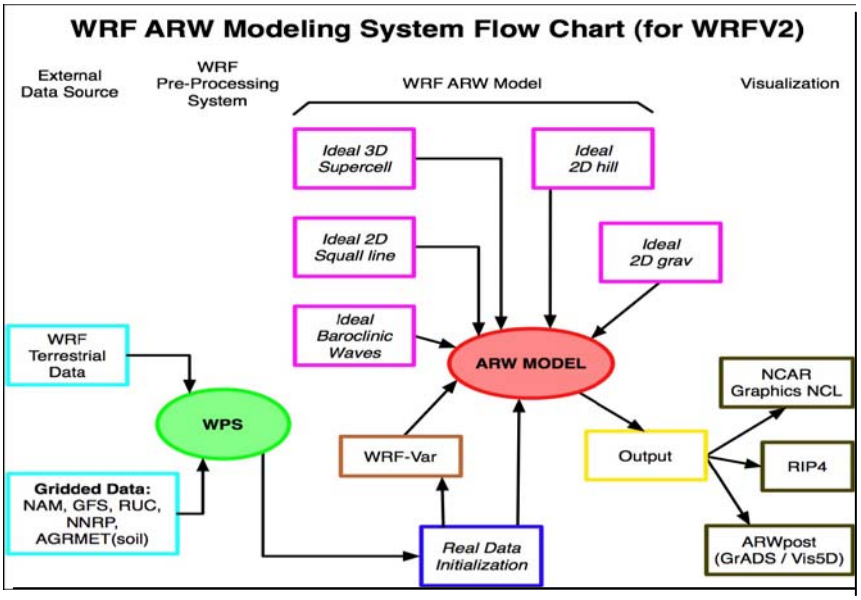

Fig. 5.4 WRF System Flow Chart Excerpted from
http://www.mmm.ucar.edu/wrf/users/tutorial/200807/WRF_Overview_Dudhia.pdf

5.3 Numerical simulation control experiment parameters setting

In this chapter, WRF ARW V2.2 compressible non-hydrostatic numerical model is adopted. In the experiment, 3-nested alternative and fixed grid form will be adopted. Resolutions of 3-nested domains are respectively 72, 24 and 8 km (see Figure 5.5). Longitude and latitude of the center is 25N and 120E. 3-nested grids are respectively domain 1 (55×40 grid points), domain 2 (100×79 grid points), and domain 3 (181×148 grid points), from the outer to the inner. The beginning time of integral for the experiment was 2008072512 UTC, the end time was 2008073000UTC, and total integral time 108 hours. During integral, there was information interaction between different resolution grids.

In the model, information on topography and surface status came from NCAR. Resolutions of 3 domain maps are respectively 5m, 2m and 30s (corresponding to 55km, 20km and 1km respectively). Relaxation boundary condition is adopted at coarse resolution side. Time change boundary condition is adopted in nesting region. For lower boundary, sea level temperature and multiplayer soil temperature are considered. Mercator projection is used in map projection.

Top height of pattern is 100hPa. Pattern is divided into 28 layers. Step size of integral is 90s. Parameters setting of main physical processes: micro-physical processes adopt alternative from Lin et al. (water vapor, rain, snow, cloud, water, ice, hail and so on). Long wave radiation adopts RRTM alternative, short wave radiation adopts Dudhia alternative. Land surface process adopts heat diffusion alternative. Cumulus convective parameterization adopts shallow convection Kain-Fritsch (new Eta) alternative.

Based on control experiment MYJ alternative, topography height of Taiwan Island is modified (see Table 5.3).

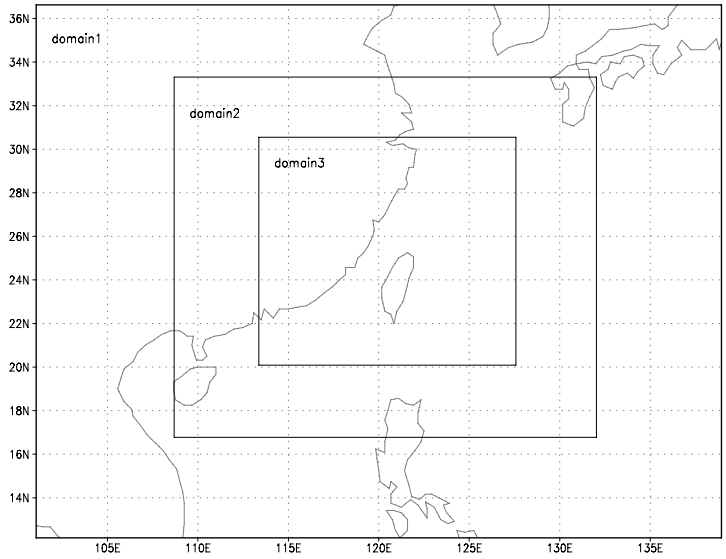

Figure 5.5 – 3-nested grids setting in WRFV2.2 model

Table 5.3 – Design of topography sensitivity experiment alternative

Alternative	SEN100	SEN50	SEN00
Taiwan topography	Original height	1/2 original height	Taiwan land leveling

5.4 Analysis of simulated results

Figure 5.6 and Table 5.4 give typhoon intensity change in both topography sensitivity experiment and true situation, from which, we can see, when Taiwan topography is reduced to 0, set as half of original height, and original height, the consumed intensity of cyclone during moving affected by Taiwan topography is 64% or 73% (intensity at original topography is 100%). However, when topography height changes from 0m to a half, change in air pressure is less. This means when topography exists, maybe owing to low pressure from topography, interaction between air pressure change and typhoon system results in a slower intensity change.

From Figure 5.7, we can see, when typhoon comes near Taiwan Island, affected by the topography, the surface wind field gradually increases in dissymmetry, wind speed decreases obviously. The higher topography in Taiwan Island, the earlier cyclone weakens, and the heavier dissymmetry of wind field is. From the figure, we also see, the place where wind speed is greater is located in sea-land interface at both sides of the central mountain, and wind direction is parallel to the mountains.

From Figure 5.8, we can see, during typhoon landing, east-west structure of typhoon without topography is almost symmetric, upper and lower of "eye" are consistent, and

"eye-wall" is upright and complete. That means, the system is still strong and weakening extent of typhoon after landing is less. When topography exists, as topography increases, "eye" is no longer obvious gradually, consistency of upper and lower is weakened, "eye-wall" is gradually tilted, not obvious, and "filling" extent of typhoon system increases gradually. From the above figure, we can also see, south wind speed on the right side of "eye" is obviously greater than north wind speed on the left side, and upper and lower are consistent. However, as topography is higher, south wind speed on the right side is gradually reduced. After topography is higher than a certain height, south wind speed on the right side at typhoon bottom becomes less than north wind speed on the left side. However, south wind speed on the right side at middle-high layer is greater than north wind speed on the left side, upper and lower are not consistent. Maximum wind speed always occurs at sea-land interface both sides of "eye" on the bottom.

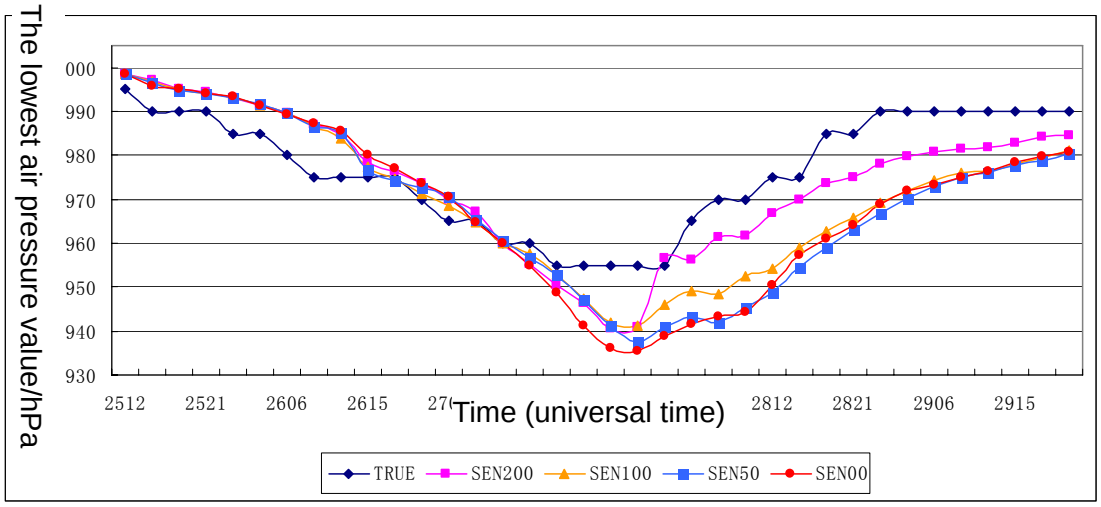

Figure 5.6 - Comparison between different topography sensitivity experiment simulating typhoon intensity and true situation

Table 5.4 – Intensity change when "Fungwong" passing Taiwan Island in topography sensitivity experiment and true situation

Time	TRUE	SEN100	SEN50	SEN00
27_18:00	955	942	941	936
27_21:00	955	941	937	936
28_00:00	955	946	940	939
28_03:00	965	949	943	941
28_06:00	970	948	942	942
28_09:00	970	952	945	943
Air pressure change	15	11	8	7
Weakening extent %	--	100%	73%	64%

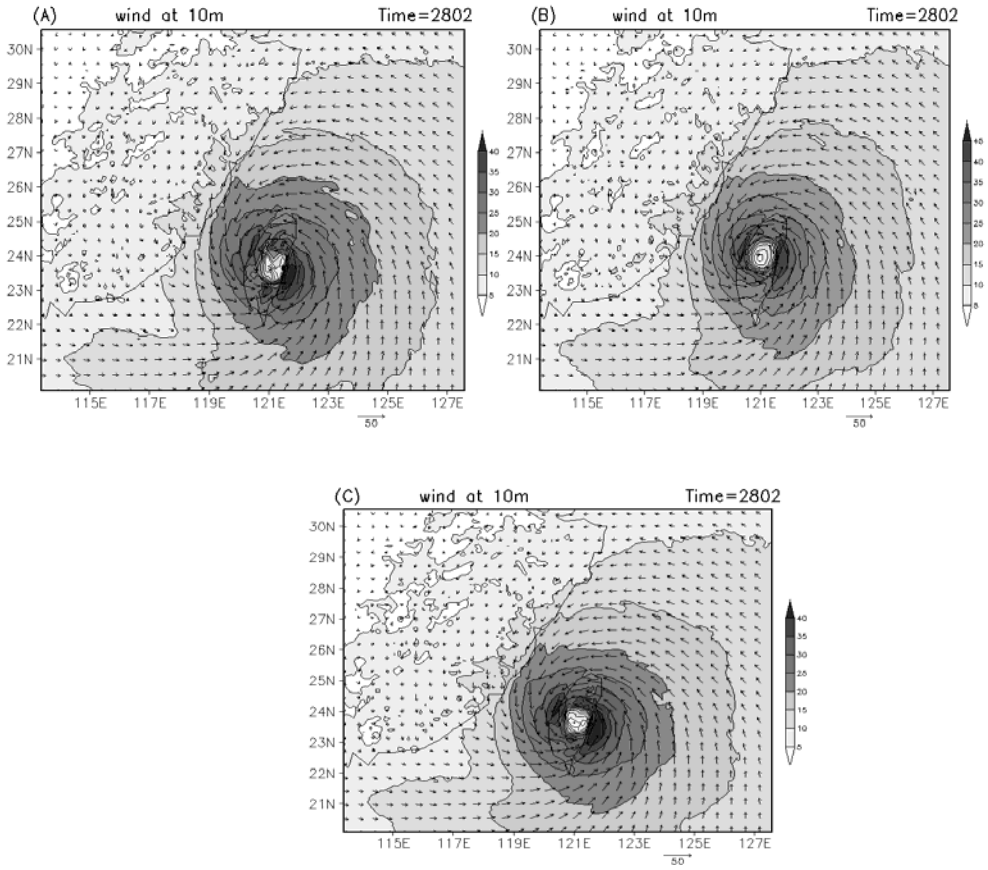

Figure 5.7 – Simulation of 10m wind field comparison during landing at 62h

(A- SEN100, B- SEN00, C- SEN50)

Generally, the relative vorticity of lower layer of typhoon circulation is positive, higher layers is negative. It means typhoon keeps or develops that relative vorticity difference between higher and lower layers is less than 0. The less total relative vorticity difference is, the more complete the structure is, and the stronger intensity of typhoon is. So this physical quantity can be used for judging intensity of typhoon. Figure 5.9 shows the relative vorticity difference field under the different topography conditions. From Figure 5.9, we can see, the less value area of relative vorticity difference is located near "eye", the higher topography is, the heavier dissymmetry of typhoon structure is, which will be not in favor of maintenance and development of typhoon. That further means topography is one of the most important factors affecting maintenance or development of typhoon.

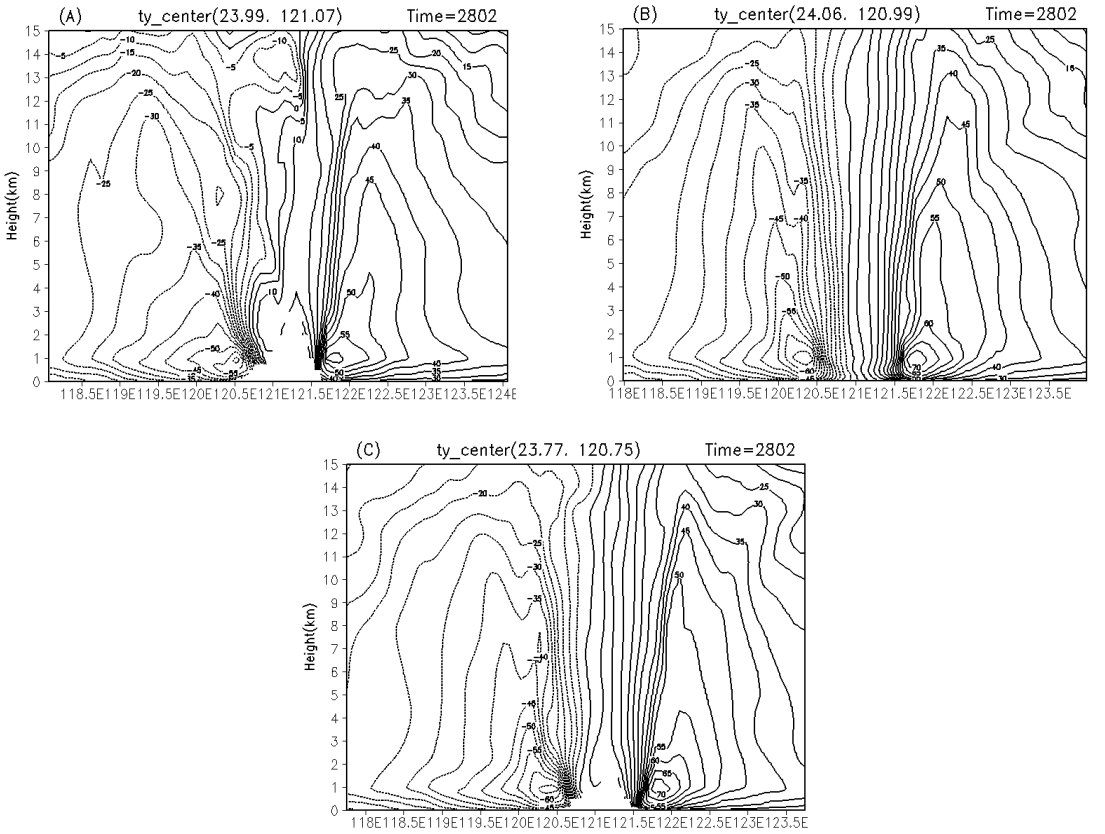

Figure 5.8 – Simulation of vertical profile of meridinal wind speed in the center of typhoon at 62h during landing

(A- SEN100, B- SEN00, C- SEN50)

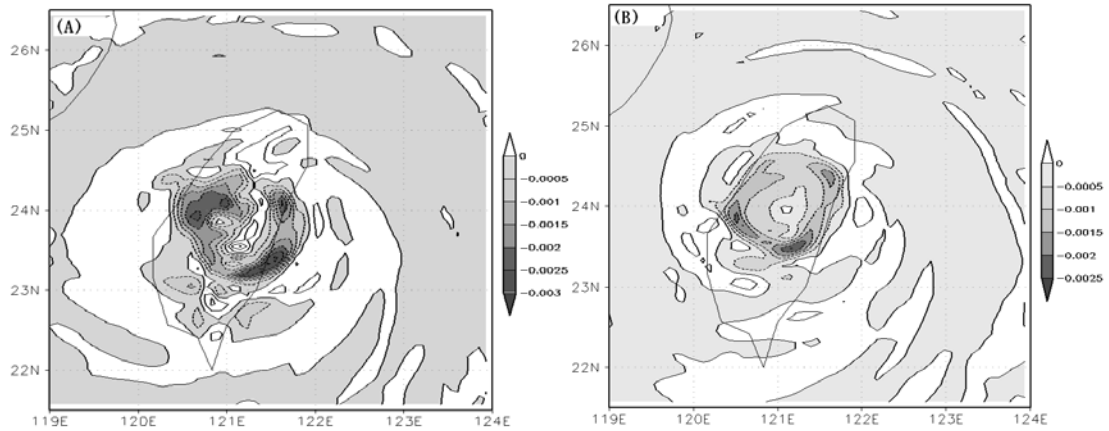

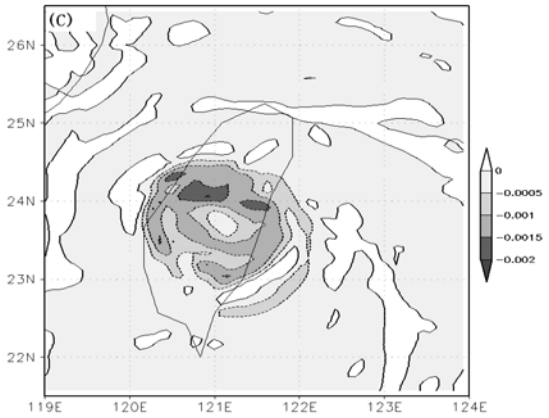

Figure 5.9 – Simulation of relative vorticity difference at 62h during landing (shadow portion less than 0)

(A- SEN100, B- SEN00, C- SEN50)

Summary

(1) From the analysis for the results of topography sensitivity experiment, we can see, existing of Taiwan topography makes intensity of typhoon weaken, and the higher topography is, the greater the weakening extent is.

(2) Typhoon moves more quickly without topography. Typhoon with topography is weakening from first 3 hours of landing, and the higher topography is, the greater the weakening extent of typhoon is.

(4) Based on the comparison and analysis for the air pressure field, hydrodynamic field and thermal field of the results of topography sensitivity experiment, we can see, existing of Taiwan topography affects hydrodynamic and thermal sources on which maintenance or development of typhoon relies, makes structure of hydrodynamic field and thermal field of typhoon dissymmetric, and the higher topography is, the more obvious dissymmetry is, the quicker and the severer “eye” filling is, the more incomplete the structure of “eye-wall” is.

6 RESULT 5 COMPILE AN ANTI-TYPHOON STRATEGY BOOK "EFFECT OF TYPHOON ON CHINA WIND POWER DEVELOPMENT AND SOLUTIONS"

Facing a quick development of wind power along the Chinese coastal and offshore areas, the wind power workers know that their knowledge on climate law of tropical cyclone is not enough, especially less understanding on extreme wind speed, sudden change of wind direction, abnormal turbulent of typhoon affecting wind farms, absence of detailed scientific analysis of destruction of tropical cyclone on wind farms, available and scientific solutions resisting typhoon disaster to be formed. *Effect of typhoon on China wind power development and solutions* is jointly written by typhoon experts and wind power experts in the project group in order to generally describe climate background of tropical cyclone activity and engineering design parameters relating to wind power development, introduce in details effect of typhoon on wind power development and the destruction mechanism of wind farm under typhoon, and systematically state technical solutions and scientific methods resisting typhoon. It will guide the managers of wind farms in effectively utilizing typhoon energy resources, correctly resisting typhoon and reducing loss brought by typhoon.

The authors' research fruits based on historic data and the latest observations are collected in this book with comprehensive contents, well organization, excellent pictures and language, easy to understand. In Appendixes, there is terminology including tropical cyclone, typhoon, typhoon eye and hurricane, typical satellite cloud pictures of tropical cyclone in developmental stage and some typhoon information websites for reference of managers and operators of wind farms.

The whole book is divided into 6 chapters.

Chapter 1 – Climate characteristics of tropical cyclone affecting mainland coastal and offshore areas in China

Chapter 2 – Characteristic analysis of tropical cyclone wind field

Chapter 3 – Effect of tropical cyclone on wind power development

Chapter 4 – Strategy resisting typhoon in coastal wind power development

Chapter 5 –Chapter 5 Typhoon-Resistance Improvement Measures for Wind Generator Set

Chapter 6 – Emergency management resisting typhoon in wind farms

6.1 Chapter 1 – Climate characteristics of tropical cyclone affecting mainland coastal and offshore areas in China

As the base of the whole book, the statistical analysis based on 60 years' (1949-2008) tropical cyclone data is shown in the following three aspects:

6.1.1 Basic characteristics of tropical cyclones over the northwest Pacific Ocean and tropical cyclones affecting offshore areas of China

The statistical analyses concentrate on the tropical cyclones over the northwest Pacific Ocean, tropical cyclones affecting offshore areas in China (15°N - 45°N, 105°E - 130°E) and coming into precautionary area (3 latitude spaces away from coastline), as well as frequency of tropical cyclones landing on the mainland China (see Table 6.1) and long-term variation characteristics (Figures 6.1 and 6.2). Both track and intensity characteristics of tropical cyclones over the northwest Pacific Ocean and tropical cyclones affecting the offshore areas in China for the different years are calculated (Figure 6.3).

Wind speed (m/s)	Wind force (scale)	Name	15°N - 45°N, 105°E - 130°E	Coming into precautionary area	Landing
≥51	≥16	Super typhoon	88	34	5
41.5－50.9	14～15	Severe typhoon	70	58	27
32.7－41.4	12～13	Typhoon	137	144	111
24.5－32.6	10～11	Severe tropical storm	125	110	119
17.2－24.4	8～9	Tropical storm	58	44	53
10.8－17.1	6～7	Tropical depression	101	38	46

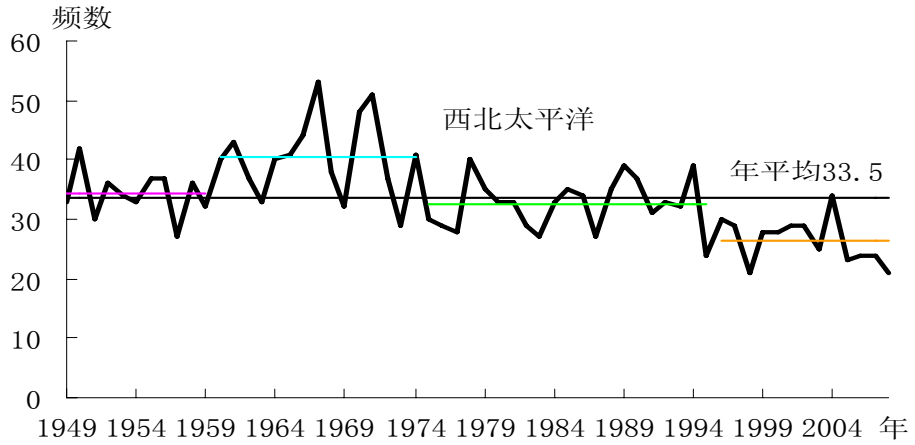

Figure 6.1 – Interannual and interdecadal variation in frequency of tropical cyclones over the northwest Pacific Ocean

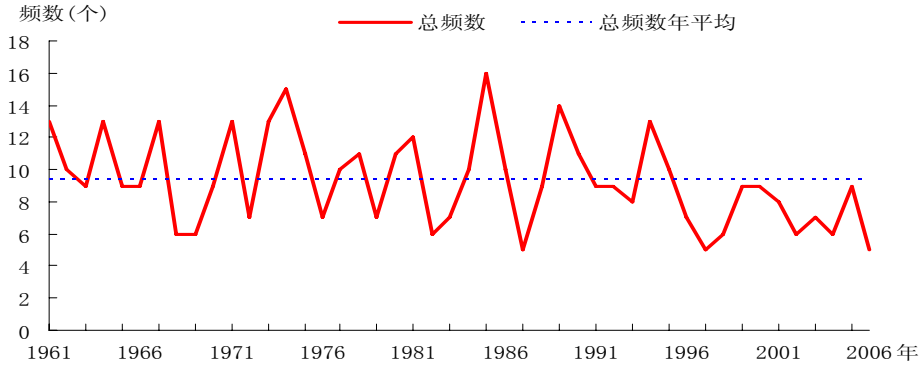

Figure6.2 – Interannual and interdecadal variation in frequency of tropical cyclones coming into precautionary area

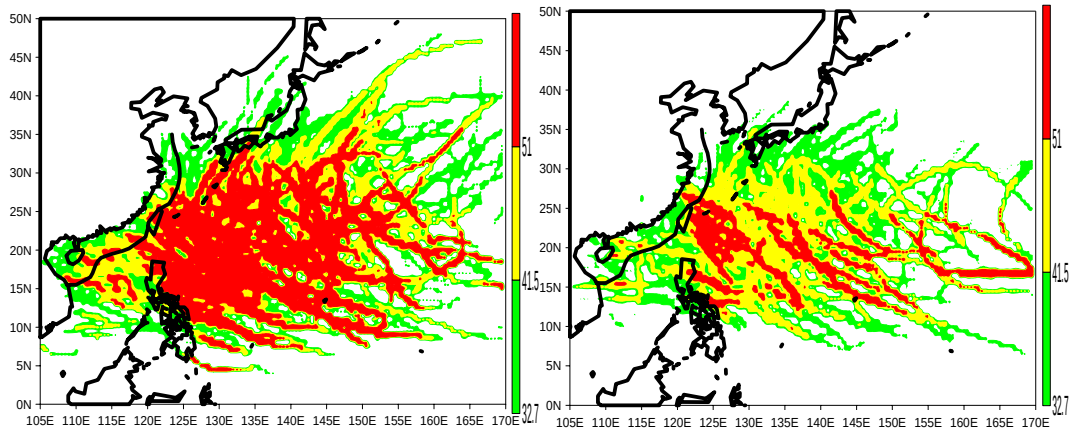

Figure 6.3 1960-1974 (left) and 1996-2008(right) TC tracks Maximum wind speed as once in 50 years on the sea

Based on the calculations of the wind field of tropical cyclones coming into 15°N - 45°N, 105°E - 130°E from 1961 to 2008 by means of dissymmetric typhoon wind field model, the gale data for every tropical cyclone at every 2 hours on 0.5° longitude and latitude grid point (see Figure 6.4) are obtained. Based on these gale data, the wind speed relating to cut-out wind speed of current mainstream wind turbines (20m/s, 22m/s or 25m/s), individual scales of wind speed (32m/s, 37.5m/s, 42.5m/s, 50m/s) matching the safety grade of wind turbine generators, and frequency of 7 wind force scales are obtained through the statistical analysis (see Figure 6.5). Based on these gale data, the gale (maximum wind speed of every tropical cyclone in its life cycle) sequence in the course of tropical cyclones on 0.5° longitude and latitude grid point is formed. Maximum wind speed as once in 50 years in the Chinese offshore area under tropical cyclones is calculated by means of Poisson-Gumbel composite extreme-value distribution function and Weibull probability distribution function widely used in the world (see Figure 6.6).

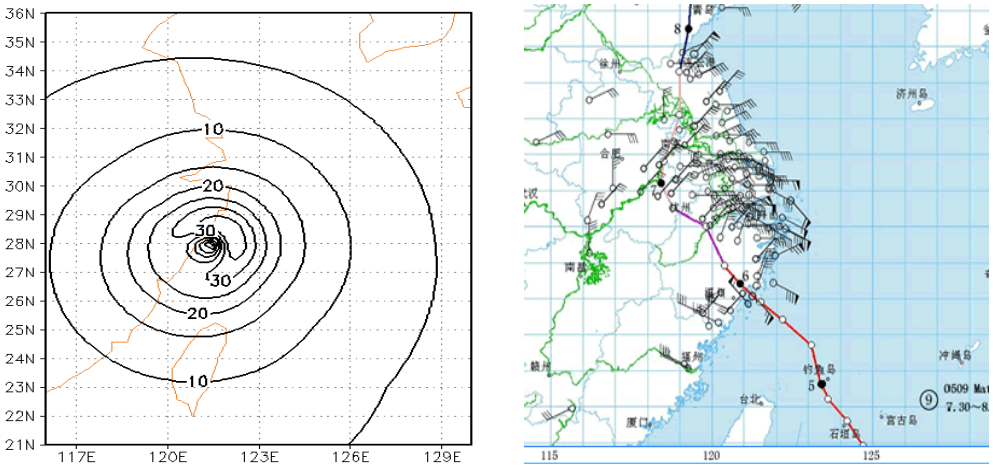

Figure 6.4 – Wind field and actual situation of typhoon Matsa calculated by means of dissymmetric typhoon wind field model

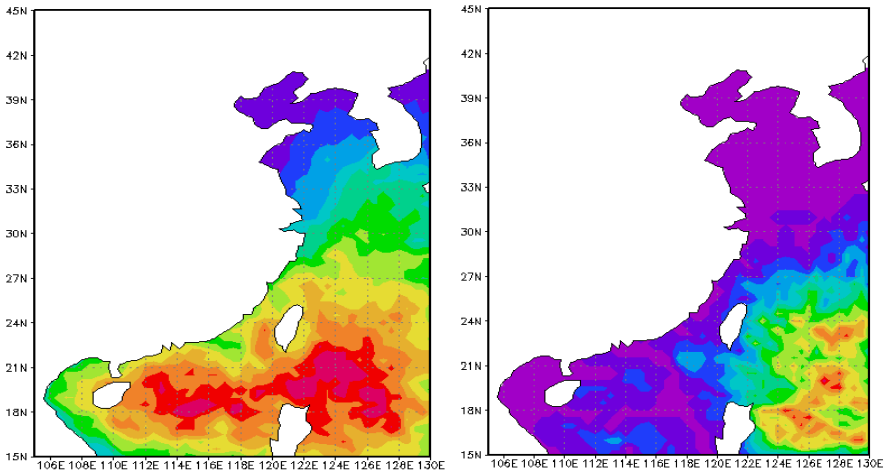

Figure6.5 15-25 m/s frequency ≥50m/s frequency

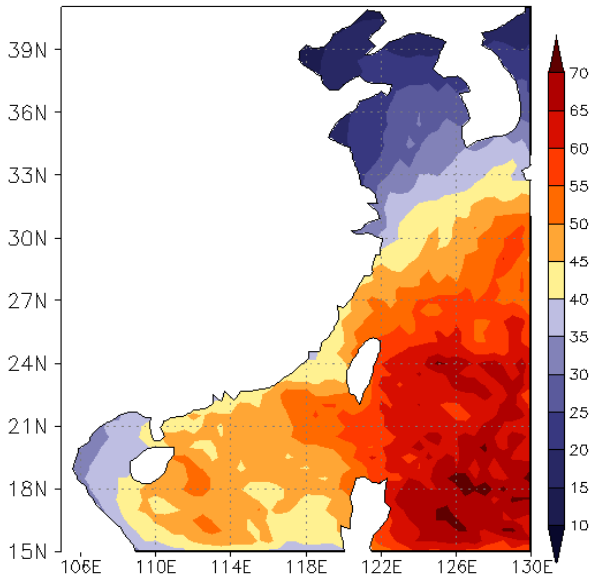

Figure 6.6 Maximum wind speed as once in 50 years under typhoon、

6.2 Chapter 2 – Characteristic analysis of tropical cyclone wind field

Based on recent years' data observed at more than 30 mast towers, a comprehensive explanation for characteristic parameters of tropical cyclone wind field relating to wind power development is provided, including the horizontal wind field on tropical cyclone ground and at 50m height (or 70m height), turbulence intensity of tropical cyclones in surface layer, sudden change of horizontal wind direction and vertical wind shear of tropical cyclones in surface layer.

6.2.1 Typical case study of TC

First 3 sections give 3 typical typhoon landing on the Chinese mainland in recent years, that is, Morakot, No.8 typhoon in 2009, landing on Taiwan, and landing on Fujian after passing through Taiwan Strait; Wipha, No.13 typhoon in 2007, directly landing at the place between Zhejiang and Fujian; and Goni, No.7 tropical storm in 2009, landing on Hainan Island, respectively. Analysis for wind field in a wide range, satellite cloud picture and ground (10m) horizontal wind field distribution characteristic of 3 tropical cyclones (Figure 6.8), wind variation characteristic of coastal mast towers at 50m height (Figure 6.9), and atmospheric pressure change characteristic is given for wind power workers to know the basic characteristics and wind field characteristics of tropical cyclones.

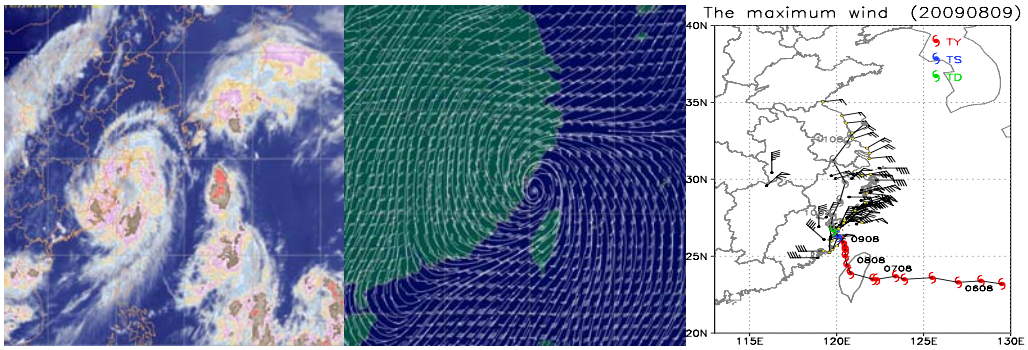

(a) (b) (c)

Figure 5.8 Meteorological satellites Cloud picture (a), MM5 numerical simulation for 925 hPa wind field (b) and actual situation (c) maximum daily wind speed measured at ground, Morakot on 8 Aug. 2009

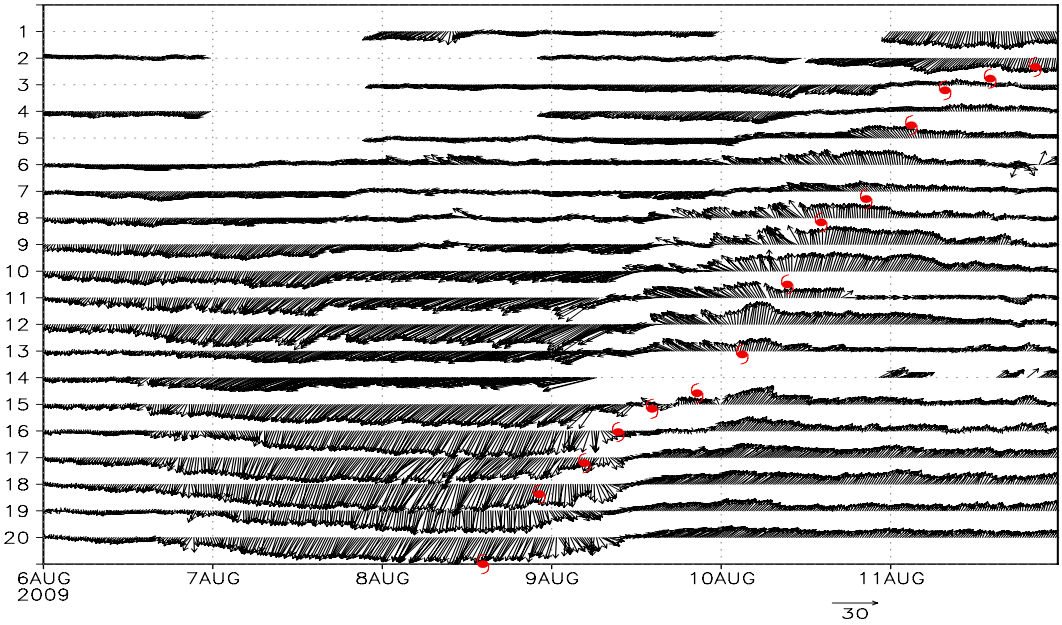

Figure 6.9 – Diagram of wind speed at 50m height vs. time of Morakot (ordinate expresses serial number of mast towers from south to north, length of arrowheads expresses wind speed, direction of arrowheads expresses wind direction, and red circles express landing time of typhoon)

6.2.2 Turbulence intensity and vertical wind shear of typical TC

Detailed analysis for general law of turbulence intensity, sudden change of horizontal wind direction and vertical wind shear of 3 typical tropical cyclones is given. Turbulence is a natural phenomenon widely existing but not being fully understood as yet. When sitting a local wind power farm, turbulence intensity is one of the most important indexes. Turbulence will directly affect performances and life of wind

turbine generators. Heavy turbulence intensity will reduce output power, may result in extreme load, finally it will destroy the wind turbine generators. In the center of typhoon landing or the area affected by the center, wind turbulence disturbance will make wind turbine systems generate random forced vibration. If turbulence intensity increases by 2 to 3 times, the calculated value of structural dynamic response or fluctuation wind load will increase by times, where turbulence intensity of main wind will increase by more than 2 times. Violent turbulence disturbance may be the main cause resulting in break of wind turbines. In the past, there were less analysis fruits because of limited data. In this chapter, most complete analysis for wind speed, wind direction, turbulence intensity and vertical wind shear of different topographies, different underlying surfaces, different wind directions and different distances away from the center of typhoon under tropical cyclones will be given. Figure6.10 expresses changes of wind speed, wind direction and turbulence intensity at different heights from Xiapu Dongchong mast towers near the center of Morakot, showing variation characteristics of wind speed, wind direction and turbulence intensity before, during and after typhoon landing. In the period of unsteady wind direction, obvious sudden changes in turbulence intensity are found, along with sudden fall of wind speed. However, there is stronger wind speed and less change in wind direction and turbulence intensity at Ningbo Cixi mast towers in the north farther away from Morakot (see Figure 6.10).

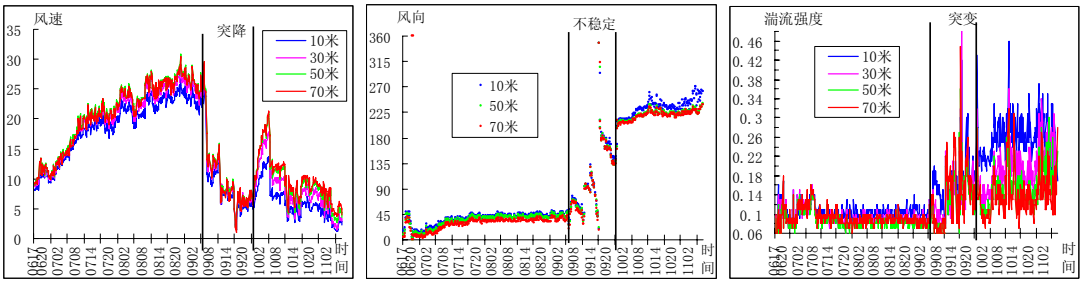

Figure6.10 – Changes in wind speed, wind direction and turbulence intensity from Xiapu Dongchong mast towers near the center of Morakot

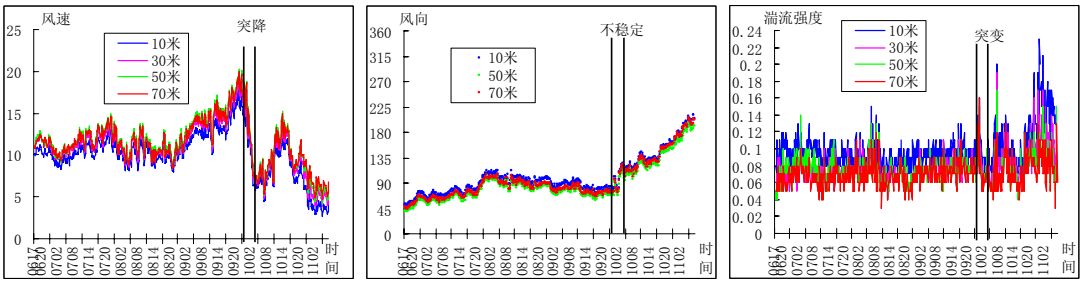

Figure6.11 – Changes in wind speed, wind direction and turbulence intensity from Ningbo Cixi mast towers in the north farther away from Morakot

Vertical distribution characteristics of wind in atmospheric surface layer, especially vertical distribution characteristics of gale under tropical cyclone, having direct effect on wind pressure, wind vibration and wind load of mast towers, should be important

basis for wind-resisting design and formulation and revision of wind load specifications. It is found in the analysis that wind shear at the periphery around typhoon only concerns underlying surface (Figure 6.12), vertical wind shear near typhoon landing point is more complex, not only concerning wind speed and underlying surface, but also typhoon circulation position where the mast towers are located (Figure 6.13).

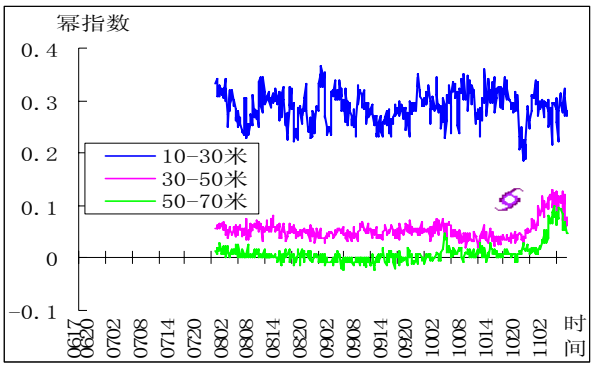

Figure 6.12 – Power law of wind shear from Qidong Dongyuan mast towers at the periphery around typhoon

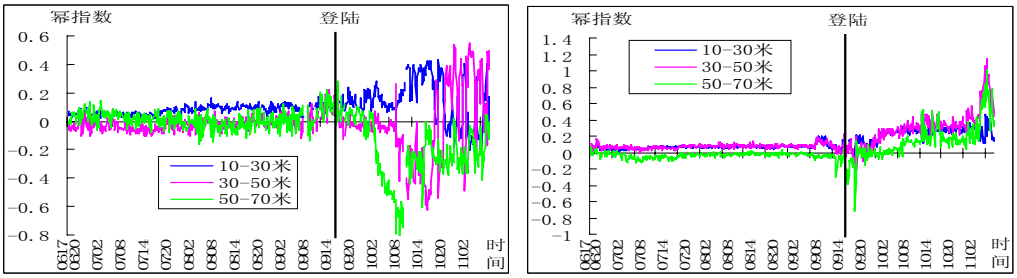

Figure 6.13 – Power law of 700m hill and seaside sand

By means of combining affecting process of 11 tropical cyclones, variation laws of their wind speed, wind direction, turbulence intensity and vertical wind shear are analyzed.

6.3 Chapter 3 Effect of tropical cyclone on wind power development

In this chapter, concepts of utilizable, defense-required and destructive tropical cyclones are brought forward, and mechanism of typhoon destructiveness on wind power equipment is analyzed. There are 3 portions:

1）. Analysis of effect of tropical cyclones on wind power development,

2）. Typhoon destructiveness on wind turbine generators and others

3）. The destruction mechanism of wind turbine generators under typhoon.

6.3.1 Analysis of effect of tropical cyclones on wind power development

Considering wind-resisting characteristics of wind generators in an individual wind farm and intensity of tropical cyclones affecting the wind farm, for the specific wind farm, the tropical cyclones affecting it can be divided into three kinds, i.e., utilizable, defense-required and destructive tropical cyclones. It must be pointed out that the same tropical cyclone may be destructive for the wind farms near the center of typhoon, and utilizable for the wind farms far away from the center of typhoon.

(1) **Utilizable tropical cyclone.** For a certain wind farm, if it is tropical cyclones below tropical storms directly landing and passing through the wind farm, or affected by the peripheric circulations near typhoon, i.e., the wind farm is located beyond force 10 wind circle, now wind speed in the wind farm will be about within the operating range of wind turbines, the wind turbines will be in full power state or near full power state. Such tropical cyclones will bring a good generating benefit to the wind farm, so called utilizable tropical cyclones.

(2) **Defense-required tropical cyclone.** If a wind farm is located within force 10 wind circle of typhoon or severe typhoon, wind speeds in the wind farm will all exceed the operating range and wind turbines will stop. Although the maximum wind speed may be less than maximum design wind speed, turbulence intensity of air flow will have gone beyond the design standard. Additionally, violent changes in wind direction during the typhoon landing period 23occur. Only appropriate resisting measures can avoid wind turbines damaging. Such typhoon is called defense-required tropical cyclones.

(3) **Destructive tropical cyclone.** When the center of severe or super typhoon goes near a wind farm, wind speeds exceed designed wind-resisting capacity, wind generating equipment will be heavily affected and damaged.

The center of Morakot landfall at coastal area of Xiapu County, Fujian Province in 2009, with maximum wind force of 12 (33m/s) at the center during the landing time. As a typical destructive tropical cyclone, Morakot bringing violent storm caused great human and material losses in Taiwan. For the wind farms in the south of Zhejiang Province and on the coastal area of Fujian Province, Morakot was a defense-required tropical cyclone. Wind speeds exceeded cut-out wind speed of wind turbines in coastal wind farms of the two provinces. In two days before and after typhoon landing, generated energy of a wind farm with installed capacity 100,000kW in Pingtan, Fujian Province, deceased by 420,000kW-hour. However, for the wind farms in the north of Zhejiang Province and in Jiangsu Province, Morakot was a rare utilizable tropical cyclone in this year. From 6 to 11 August, the wind farms were almost every day in full power state. Generated energy in 6 days reached about 2/3 of total generated energy in August.

6.3.2 Typhoon destructiveness on wind turbine generators and others

The destructions involve blades, hub pitch-controlled systems, nacelles, yaw systems, wind turbine tower frames and foundations, and other equipment. Blades connected to

spindles by hubs are the main components in wind turbines to transform wind energy into the mechanical energy, also the components being always damaged in typhoon disasters. Blade damages based on the extent of damage can be divided into three kinds: crack occurring in a blade, crack expanding up to blade profile shell destroyed, blade broken.

(1) Crack occurring in a blade of wind generator in the figure, shows no damaged failure in the main structure of the blade.

Crack on a blade of wind generator

This is because of maximum wind speed of typhoon not up to design value of 70m/s, and maximum bending moment from wind force not up to limit bending moment of blade structure. 9 blades of a wind farm in Guangdong were damaged by typhoon at transient wind speed of 50.7m/s, which shows some problems, it may exist in design or engineering of these blades, not suiting complex wind situations of typhoon (various wind speeds and directions) and combined load conditions caused by wind shear from a complex topography. Because of violent variations in wind direction during typhoon passing, wind does not always go in feathering direction that is favorable to blade force, it may go in the worst vertical direction which is unfavorable to blade force. Now the wind turbine may stop in emergency because of electrical power network off and be in braking state, thus, loads on blades will greatly increase. In air flow with maximum turbulence intensity, damaged blades owing to inadequate torsional rigidity will produce twisting vibration, resulting in structure instability and damage.

Shell damaged. Further expansion of torsional resonance or poor bonding strength between main beam of blade and shell will result in crack expanding and lump in covering from torsional resonance broken, so secondary destruction will occur.

Damaged V42 blade

Blade broken. Blades of a variable-pitch variable-speed wind turbine were broken at root by typhoon during each of typhoon Maemi and Saomai. When Saomai passed through Hedingshan wind farm, 3 blades of a D4 wind turbine were broken at root, the cause of which may be that strong wind damaged variable-pitch mechanism of hub, the changes of blade angle increased windward area of blades, resulting in 3 blades broken at root (see the following figure).

Broken D4 blade

(2) **Pitch-controlled system in hub.** When violent torsional resonance occurred with blades under gale, force on variable-pitch mechanism would greatly exceed designed value, some arms connecting blades to V-supports would be broken, or V-supports broken, blade position would be out of control, not in feathering position, some fans even ran away. During Maemi in 2003, variable-pitch mechanisms of some wind turbines were damaged. After gale, blades of variable-pitch wind turbines turned to feathering position of 90°. However, after the system was off, mechanical brakes generally acted, braking blocks enclasped braking disks on high-speed shafts, stopping fans rotating freely. Fixed fans in gale would result in too force on a certain blade, structure yielded and damaged in gale beyond survival wind speed.

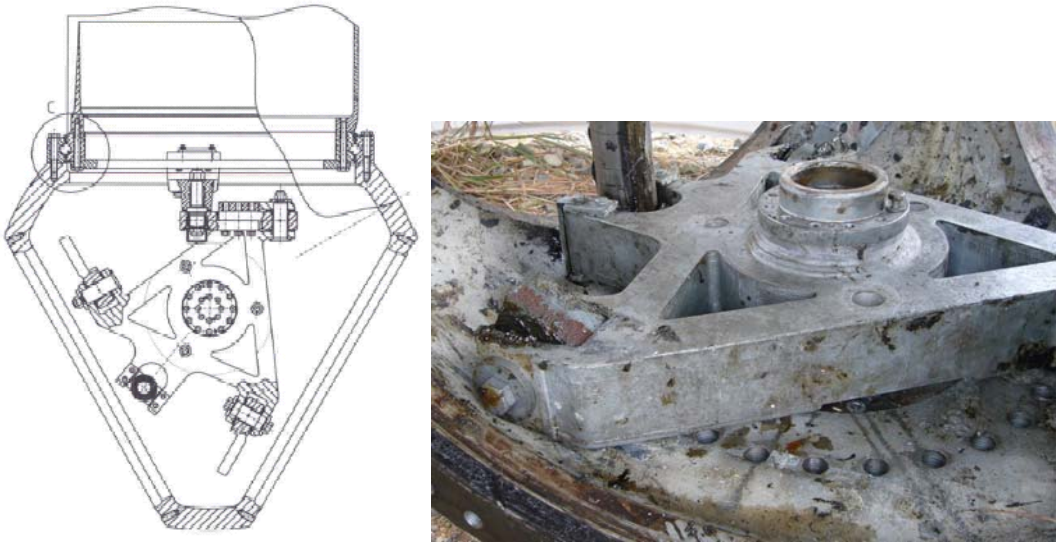

Damaged V-poking fork and connecting rod

(3) **Nacelle damaged.** Protective covers outside wind turbine nacelles are most damageable during typhoon. However, wind turbines differently designed would be with different destruction-resisting capacities. In the past, the wind turbines below 600kW adopting top-open and back-lifting structure were most damageable in typhoon. Although reinforcing measures had been taken for 11 open type wind turbines in Hedingshan wind farm before Saomai landing, besides damaged tower failure during typhoon, all open type nacelle covers were blown off.

250 and NTK41/500 wind generators

Fans of wind generators are connected to shafts through hubs. Shafts are fixed on nacelle pedestals with main bearing seats. During Saomai, gale caused wind generator nacelles to vibrate violently, resulting in main bearing seats displacement of shafts of seven V42 wind generators and loosing base feet displacement of seven V42 wind generators, of which the base feet of a wind generator broken, resilient shaft couplings between gear boxes and generators of 3 wind generators damaged. At the same time, acoustic absorption material inside nacelle wall, ventilation hoods for cooling air of generators, a great deal of control modules in top control cabinets and cooling systems of gear boxes damaged.

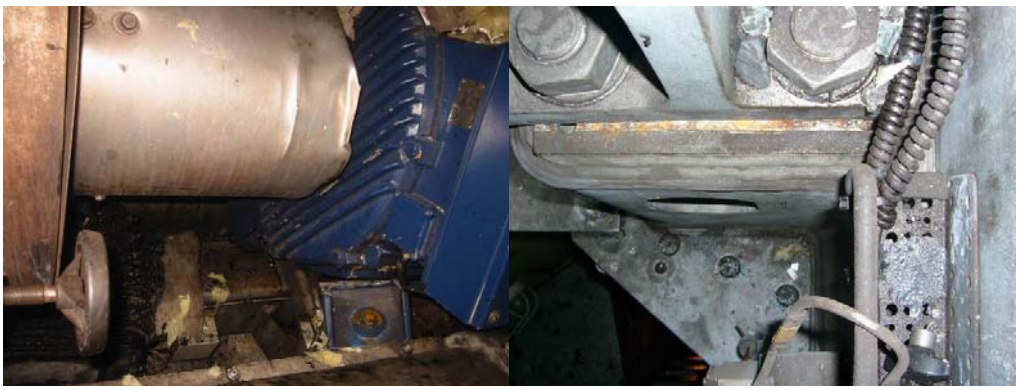

V42 generator base feet broken and main bearing seats displaced

(4) **Yaw system.** During typhoon landing, electrical power network is off and wind directions change, great wind action occurs on nacelles and fans sides. Only nacelles of wind generators with yaw hydraulic brake systems can be in place as the same as power cut. The nacelle position of most slider yaw systems or dampers with yaw bearings changes under gale. Generally, there are self-locking mechanisms for deceleration systems of yaw drive units, so gales forcing direction change make yaw systems of a great deal of wind generators heavily damaged in this course.

Broken teeth of yaw deceleration mechanism and yaw gear rim

Violent changes in wind direction generally occur during typhoon landing. At the same time, gales often cause line failure in wind farms and wind turbines off. For variable-pitch wind turbines, the load when side under wind is 30% greater than the load when front under wind according to the manufacturer's analysis.

(5) **Tower frame and foundation.** When maximum bending moment of typhoon on a wind turbine is larger than designed value of tower frame and foundation, the frame and foundation will yield and damage, resulting in the wind turbine damaged. Wind turbine tower frames include truss type and conic cylinder type. At present, most wind generators adopt conic cylinder tower frames. No matter which tower frames are adopted, tower failures will occur when wind speed is too great.

Broken wind turbine tower frame

Whole wind generator fell after foundation failure

(6) **Other equipment.** For 23 wind generators not fallen by Saomai, all anemometers were blown off, lightning rods of individual wind generators were blown inclined. Aluminum alloy skylights of fourteen V42s were blown damaged. Violent nacelle vibration made a great deal of electric components and control modules in top control cabinets out of their sockets and damaged.

(7) **Transmission line.** During front attack of severe typhoon, access systems and lines inside farms often fail and trip, a great deal of broken rods, fallen rods, or broken wires

will be found, causing great losses for transmission systems. During Saomai, 10 of 17 steel towers in 7km long 35kV network connection line fell, 17 towers of 10kV line fell, and broken wires, damaged cross arms were countless in Hedingshan wind farm. The main causes of tower failures in steel tower lines are as follows:

1) In line design in China coastal area, generally Zhejiang I weather region 35 m/s or Zhejiang II weather region 30 m/s is considered. The wind speed of landing typhoon exceeded design limits and actual wind-resisting capacity of the line.

2) Line towers of mountainous wind farms are generally located on upwind mountain ridges and wind gaps, whole steel towers and conductors are under too heavy wind pressure, so towers would be broken or fall. Some failure tower lines operated for many years, there was less allowance of towers, lack of maintenance.

3) Spacing distances on two sides of failure towers are generally large-and-small, i.e., large spacing on one side and small spacing on the other side. In supper severe typhoon, greatly different landscape level forces act respectively on two sides of iron tower in line direction, resulting in torsion and falling. This is the main cause of iron tower falling.

4) Because of weak cross bars and layering bars, fall-resisting capacity of some assembled foundations cannot meet the requirements of resultant bending moment of landscape resultant force of tower bodies and resultant force of earthing conductors on the root of towers, resulting in some pulling up. This is one of important causes of iron tower falling. Too great wind force tears stay suspension loops, pulls out tower disks, resulting in torsion and falling of towers.

Causes of broken earthing conductors and by-pass jumpers:

1) Aluminum cores of the conductor at 10cm of by-pass jumper layering tension clamp outlet of neutral phase conductor of the iron tower were broken, insulators of jumper strings and by-pass jumpers repeatedly and drastically shook conductors so that aluminum cores fatigued and were broken. This means the tower structure has to be perfected.

2) During gale, tension by-pass jumpers swayed to a great extent so that electric distance away from tower bodies was small. This means there are some defects in anti-windage yaw of tension by-pass on exterior angle side for these towers.

3) Gale blew off foreign bodies so that earthing conductors were cut or too great wind load resulted in broken cores or wires of earthing conductors.

(8) **A great deal of rain always is brought along with typhoon landing, resulting in secondary disasters**. 1) Flood. Flash flood from gale and rainstorm will break roads and bridges, strictly affecting wind farms. 2) Geological hazard. 3) Storm surge. When typhoon landing near **Astronomical** tide, **Astronomical** tide ， storm tide and flood will come together.

6.3.3 The destruction mechanism of wind turbine generators under typhoon

(1) Cause analysis for damaged blades: 1) too large wind speed, too large turbulence intensity. 2) some causes in design and manufacture of blades.

(2) For different control strategies of wind generators (speed loss, variable pitch), there are different structural strengths.

(3) Control strategies of wind generators: active yaw, braking when power off. Sudden change in wind direction occurs during typhoon landing. Gale may blow in the most unfavorable direction vertical to blade surface. Now wind turbines may stop and be in braking state because of power network off or other emergent cases. That could greatly increase load on blades and whole machines (by 30%).

(4) Cause analysis for wind generator tower frame falling: 1) wind speed was too large so that wind pressure on wind generators exceeded maximum design value (for wind generator foundations and tower frames). 2) strength distribution in integral design of wind generators (foundation > tower frame > nacelle > blade).

Relation between electric power network off and damaged wind turbines: after network off, yaw systems of wind generators could not yaw in time along with wind direction of typhoon. Mechanical braking increased force on blades for fixing fans.

6.4 Chapter 4 Strategy resisting typhoon in coastal wind power development

Based on analysis from chapter 1 to chapter 3, some technical solutions against tropical cyclones relating to coastal wind farms construction are brought forward. They mainly include: type selections for wind turbine generators, type selections for transmission and transformation equipment, new technology application, and improvement of backward equipment in existing wind farms.

6.4.1 Type selection for wind turbine generators and accessory equipment in areas affected by tropical cyclones

(1) Type selection analysis for wind turbine generators

On the whole, the transmission and transformation equipment and lines of existing wind farms can not meet the requirements of providing uninterrupted power for wind turbine generators, resulting in equipment damaged.

Typhoon rotates counter-clockwise. At beginning, it is northeaster, and quickly turns into southwester after landing. If wind turbines are in feathering during northeaster and power-off, not capable of following wind direction, when wind direction turns into

southwester, included angle between wind turbine generators and wind direction will be within 0 to 180, negative pressure will turn into positive pressure, blades will be damageable. So, not only wind speed but also wind direction should be considered in coastal and offshore wind energy development and utilization.

In southeast coastal area of China, existing standard wind turbine generators can meet weather conditions of part of farm sites. In areas of south Zhejiang and north Fujian, as well as east Guangdong, where severe typhoon often occurs, S-grade wind turbine generators should be designed in order to suit local weather conditions. Before such wind turbine generators exist specially for these areas, farm site selection must be careful.

Under the condition of making sure normal power supply of transmission and transformation equipment, existing standard type can be used in many regions to reduce investment to a great extent and ensure safety and high efficiency in equipment operation.

Considering all parameters and economy of fixed-pitch and variable-pitch wind turbine generators, it is recommended that variable-speed constant-frequency variable-pitch wind turbine generators with mature technology, excellent performances, and high efficiency utilizing wind energy should be adopted in wind farms of the above mentioned areas, which will facilitate technical reform in future and existing in the condition of tropical cyclones.

6.4.2 Improvement of wind generating technology in areas affected by tropical cyclones

Complex topographic conditions cause frequently changed wind direction, unstable wind speed, large vertical wind shear in height range of wind turbine generators, and heavy turbulence intensity. These bring severe challenge to wind turbine generators in present conditions.

In coastal or offshore areas, severe salt fog corrosion and humidity will affect wind turbine generators and stability of power supply, especially during severe typhoon, all unfavorable factors may occur together and produce overlay, bringing severe challenge to service life and survival environment of wind turbine generators.

For the design wind speed of existing the highest standard wind turbine generators, 70 m/s transient wind speed once in 50 years and 50 m/s maximum wind speed in 10 minutes are adopted, and normal power supply conditions of electric power network is considered. During typhoon, power supply of network to wind turbine generators cannot be ensured, in addition to complex coastal topographic conditions, abnormal turbulences and severe wind shears may occur, which will form fatal blows to wind turbine generators.

Destructions of wind turbine generators by typhoon are mainly because of power interruption for wind turbine generators, the wind turbine generators are in emergent stopping state of yaw system and blade bake system braking. Power supply interruption will cause variable-pitch wind turbine nacelles not to go windward as required,

fixed-pitch wind turbine nacelles not to go crosswind, and blades not to be free. Thus states sustaining will result in damage of the weakest among blades, nacelles and tower cylinders, especially, when a tower cylinder is earlier than blades to be not capable of bearing load from typhoon, worst state will occur that whole wind turbine generators are damaged. In order to enhance the capacity of resisting worst environment for wind turbine generators during typhoon, based on analysis on damage reasons of damaged equipment in resent years, some technical improvement advices are now brought forward:

(1) Wind measuring devices. Wind speed and direction are like a baton for automatic control system of wind turbine generators. Therefore, excellent performance and reliability of wind measuring devices in generators will be the guarantee of wind energy utilance increase and safety operation of generators.

(2) Brake system. Braking of wind turbine blades is a system combining blade locking system, relying mainly on pneumatic braking of blades supplemented by mechanical braking. High-speed shafts of gear boxes keeping braking for a long time will result in damage of gear boxes, blades and yaw systems. Under the preconditions of not changing the original safety chain and failure mode of the generators, blades shall be made completely in feathering and blade wheels free. During typhoon, because of urgent gale and heavy rain, electric power network may fail, power supply to wind turbine generators is interrupted, some protections do not work. When yawing does not work after power off, high-speed shafts of gear boxes in braking state for a long time will result in damage of gear boxes, blades and yaw systems because huge energy from gale cannot be eliminated.

(3) Structure and strength of blades. Extreme load should be considered. Special profile should be designed and standard grade should be heightened. New blade structure, material and fibrous layering mode should be researched to make sure blade strength and flexibility, and to prevent resonance. Problems on poor shear strength in glass fiber reinforced plastic should be solved. In addition of making sure pneumatic performances of blades and cost, adhesive area and strength should be considered. Vacuum rate should be adjusted.

(4) For tower frames and yaw mechanisms, resonance frequency and extreme load should be considered to increase strength and flexibility of tower frames. Effective vibration reducing measures should be taken. Manufacturing technologies should be improved to avoid stress concentration and to increase design life and high wind speed resisting capacity of tower cylinders.

(5) Control for wind turbine generators. Vibration monitoring for blades, gear boxes, tower frames and nacelles should be enhanced to reduce fatigue load of equipment and increase designed service life of equipment. Automatic adjustment for rotary speed, power output, sector management for the positions with high turbulence intensity and wind speed as well as other functions should be considered. Severity degrees of failures should be classified, consequent results should be analyzed. By reducing operation state step-by-step, impact to equipment will be decreased in order to prolong service life of equipment efficiently.

(6) Equipment and line for power transmission and distribution as well as power supply guarantee. Emergency standby electric power inside farms should be equipped for control, yaw and dynamic systems of wind turbine generators to make sure uninterrupted power supply to wind turbine generators. In order to utilize investment efficiently, control in group for yaw and hydraulic driving power supply of wind turbine generators in whole farm can be performed so as to reduce capacity of standby electric power.

(7) Remote monitor for wind turbine generators and transmission and transformation equipment. Operation state of every set of equipment is monitored,analysis and summing-up real-time. Information and data should be established as basis for existing equipment and future wind farms.

(8) Order agreements, delivery acceptances, iron towers assembling and other procedures should be strictly checked. Negative deviation limit should be clarified in order agreements. Spot-check rate should be no less than 5% in delivery acceptance. Re-inspection should be performed in iron tower assembling construction. Spot-check and re-inspection should be well reported.

6.5 Chapter 5 Typhoon-Resistance Improvement Measures for Wind Generator Set

When a variable-pitch wind generator set experiences typhoons, the blades will undertake more repeated fluctuating load because of the frequent change in wind direction and turbulence, no matter whether they are in the normal working position or in a feathering pitch. Pitch control system is the bearing link in this load, and when pitch control system becomes problematic blades or generator set will be damaged destructively. Therefore, it is suggested that a constant-pitch wind generator set should be chosen so as to avoid the great economic loss due to the deconstruction of pitch system, when a typhoon attacks wind power fields. In this chapter, the typhoon-resistance improvement measures for a constant-pitch wind generator set will be stated.

6.5.1 Improvement of part bearing capacity

According to the typhoon data at a wind power field in the recent years, the wind generator set is improved through fixing an instantaneous wind speed of 80 m/s for the foundation and tower, while for blades an instantaneous wind speed of 75 m/s is fixed; and the economic and technical feasibility also should be considered.

(1) Improvement of foundation and tower

In case of Wind 1a, the designed redundancy factor is up to 1.485.

If instantaneous wind speed=75 m/s, the designed redundancy factor is 1.41.

If instantaneous wind speed=80 m/s, the designed redundancy factor is 1.31.

(2) Improvement of blades

If instantaneous wind speed=75 m/s for the improvement design, over-designed glass-fibre cloth will be used to replace common glass cloth, the main bearing area of the blades will be partially improved, and the fatigue load and limit load of the blades will be improved by 15%, compared with the former blade 1a.

●Main improved parts

Blade area

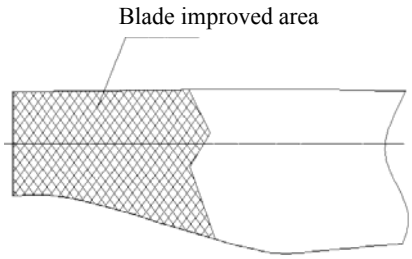

Bearing layer of main area

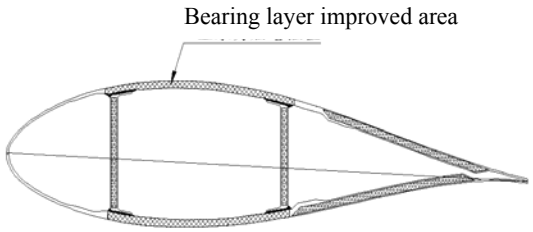

● Appropriate improved parts

Leading edge area

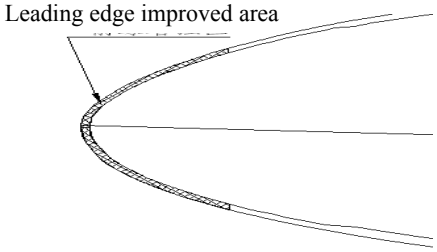

Tailing edge area

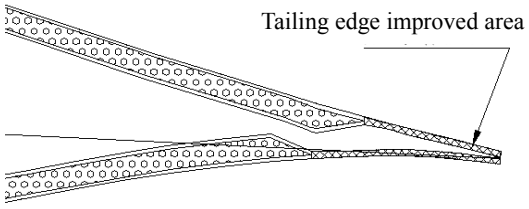

(3) Improvement of main shaft braking torque

The braking torque of main shaft is designed for improvement on the basis of instantaneous wind speed=75 m/s, and the throttle valve should be adjusted in

hydraulic system so as to make the braking time controlled in the optimal range.

(4) Improvement of yaw braking torque of main axle

On the basis of instantaneous wind speed=75 m/s, a yaw brake is re-chosen or the number of brakes increases if the brake pattern will not be changed。

(5) Improvement of yaw bearing

Exclusive yaw bearing and enlarged connection bolts for HD1000S wind generator set are designed to resist a wind speed of 75 m/s.

The cost for the improvement of nacelle cover, fairing and other connections is low, and they can be improved on the basis of instantaneous wind speed=80 m/s. Of course, glass steel connections and connecting components should be improved at the same time.

6.5.2 Active protective measures

Control system increases “Typhoon State” patterns. They are operated for:

- Main mechanic braking state;
- Impeller 90˚-yawing, cross wind, locked;
- Blade-tip brake off-throwing.

What is different from the “protection from strong wind” pattern of wind generator set when wind speed is more than 25 m/s is that the impeller in this pattern will track the main wind direction with 90 degree crosswind yawing. “Typhoon state” pattern is characterized by that the unstable typhoon direction will not be tracked after the 90 degree yawing of the impeller from the main wind direction and the impeller is stable during the typhoon.

(1) Main shaft mechanic baking

There are two state choices of main shaft mechanic baking, i.e. releasing or braking. That the main shaft brake releases the impeller for loose running can effectively protect the gear box, but if the impeller runs loosely without any load it will surely stall due to racing in the state of typhoon, leading to the deconstruction of blades and wind generator set. The accurate time of stalling due to racing can not be calculated,

but the stalling due to racing will occur sooner or later if the rotating acceleration is changed abruptly with the change in wind direction and the increase in wind speed.

Main shaft mechanic baking can make the driving gear in the gear box undergo constantly-changing torque, probably leading to gear-teeth broken. It is stipulated in GB/T 19073 that the gear bending strength safety index should be no less than 1.4, while the gear bending fatigue strength safety index should be no less than 1.7. In DIN 3990, it is stipulated that static load should be three times nominal power for calculation and the gear bending strength should be no less than 1.4. In AGMA 6006, it is stipulated that the index of 1.3 should be used for calculation and the gear bending strength should be no less than 1.56. At present, all the gear boxes made and designed in gear box factories should meet the requirements of the three above standards at the same time. Gear shape should have enough resistance to tooth-breaking.

Therefore, the choice of main shaft mechanic baking state is more effective than that of loose braking state for the protection of wind generator set.

Normally-closed brake is selected for a constant-pitch wind generator set, i.e. main shaft braking will be through spring force when power is off. The working principle is fit for the protective program of generator set to the most. However, the brake in a variable-pitch wind generator set is normally open. The brake is open when power is off. Impeller might race in a wind direction state to cause serious damage. This is the reason why the typhoon-resistance capacity of a variable-pitch wind generator set is less than that of a constant-pitch wind generator set.

(2) 90˚-yawing of impeller

There are two choices after 90˚-yawing of a impeller: the impeller tracking main wind direction for yawing and the impeller not tracking main wind direction and keeping it fixed after yawing. Under a typhoon state, the impeller is locked and fixed for yawing, which is beneficial to the protection of wind generator set.

(3) Blade-tip brake off-throwing

Under a typhoon state, wind direction is variable and unstable. When the impeller yaws from the main wind direction at a degree of 90 and is in the locked state, blade-tip brake off-throwing will reduce the rotating torque maximum of the impeller in the entire typhoon period. The load reduction of impellers and gear box is beneficial to the protection of wind generator set.

Under a typhoon state, blade-tip brake off-throwing will cause the carbon fibre axle connected with blade-tip to bear greater load and the safety of the carbon fibre axle should be examined and checked.

6.5.3 Specification for the controlling program of "Typhoon State" pattern

(1) Autonomously enter "Typhoon State" pattern

a. In the control system "Typhoon State" is coded and the program is in the state of priority. Activation condition: the mean wind speed is more than the fixed values (minimum: 25 m/s, maximum: 50 m/s, implied speed: 32 m/s) in 15 seconds.

Executive programs:

- The impeller yaws from the main wind direction at a degree of 90 and is in the locked state, and the real-time tracking typhoon is not carried out.

- Main shaft self-starting (braking wheel is locked);

▲ Blade-tip self-starting (blade-tip off-throwing).

When instantaneous wind speed is ≥ 25 m/s, wind generator set will get into the "protection from strong wind" program, whereas when wind speed is the conditional wind speed of "Typhoon State", the program will autonomously changed into "Typhoon State" pattern.

b. According to the situation of wind generator set after a typhoon, man-restarting should be adopted. It can be manually returned by operators with more than 80% authorization through SCADA or WKA and logged out of "Typhoon State" pattern.

c. If wind generator set is out of power before entering into "Typhoon State" pattern, the wind generator set will get into "protection offline" pattern, the difference of which from "Typhoon State" pattern is that the impeller is not necessarily in the state of the 90˚-yawing from the main wind direction.

(2) Manually enter into "Typhoon State" pattern

If the wind power field is equipped with emergency power, the control system autonomously enter into "Typhoon State" pattern. On the basis of this, the index for "emergency power" should be increased. This index can be manually fixed by

operators through SCADA or WKA one by one. After “emergency power” state is reached, autonomous activation wind speed is ≥ 25 m/s for strong wind protection program. When the wind speed reaches the conditional wind speed of “Typhoon State”, it will be autonomously turned into “Typhoon State” pattern to restart the program, which is the same as the autonomously-entering into “Typhoon State” pattern.

6.6 Chapter 6 Emergency management resisting typhoon in wind farms

Based on above four chapters, emergency management ideas and measures for typhoon protection will be brought forward in this chapter aiming to disaster characteristics of wind farms affected by typhoon for reference of all local wind farms to prepare emergency plans for typhoon protection. According to four stages in emergency management for typhoon protection, four aspects will be described in this chapter:

1）. Preparation of emergency plans for typhoon protection,

2）. Precaution before tropical cyclones,

3）. Emergency measures when tropical cyclones are coming, and

4）. Assessment after disasters and production recovery.

6.6.1 Preparation of emergency plans for typhoon protection

Always keeping in mind “human-centred development” and “disaster risks and harm reduction”, following policy of “priority to precaution, combination of precaution and emergency, and always preparation”, and carrying out the principle of unified command, response in level, priority to locality and cooperation. Emergency plans for typhoon protection should be scientific and maneuverable.

6.6.2 Precaution before tropical cyclones

According to typhoon precaution matters from meteorological offices, typhoon warning signals can be divided into four levels, represented respectively with blue, yellow, orange and red color.

(1) Typhoon blue warning signal standard: It may be or have been affected by tropical cyclones within 24 hours, average wind force in coastal areas or land reaches above scale 6, or gusts above scale 8, and may go on.

(2) Typhoon yellow warning signal standard: It may be or have been affected by tropical cyclones within 24 hours, average wind force in coastal areas or land reaches above scale 8, or gusts above scale 10, and may go on.

(3) Typhoon orange warning signal standard: It may be or have been affected by tropical cyclones within 12 hours, average wind force in coastal areas or land reaches above scale 10, or gusts above scale 12, and may go on.

(4) Typhoon red warning signal standard: It may be or have been affected by tropical cyclones within 6 hours, average wind force in coastal areas or land reaches above scale 12, or gusts above scale 14, and may go on.

In order to prevent major serious accidents from typhoon and other accidents exerting significant influences on society, reduce extent and degree of losses from accidents, make sure safety operation in power farms, and ensure economics safety, stability and safety of employees' lives and properties, wind farms prepare prescriptions against typhoon disaster suitable to the wind farms, based on operation features of wind turbines, following typhoon precaution regulations of meteorological offices.

6.6.3 Emergency measures when tropical cyclones are coming

When preparing emergency measures for typhoon protection, wind power companies shall implement emergency and rescue work according to rescue policies of "relying on people, relying on collectivity, engaging in production, and mutual assistances and mutual relieves".

In order to perform typhoon emergency and rescue work high-efficiently, wind power companies shall regularly organize drillings of emergency plans for typhoon protection. Specific requirements are as follows:

(1) At least one practical drilling a year for every emergency plan shall be organized in a wind farm.

(2) After every practical drilling, complete and correct evaluation for practical effects of the whole drilling shall be organized for summarizing, appraising, modifying and perfecting the plans so as to make sure science, practicability and maneuverability of the emergency plans.

6.6.4 Emergency preparation for typhoon

Generally, facilities destruction in wind farms by typhoon is mainly destructions of roads, transmission lines and wind turbines. The destructions of wind turbines can be divided into mechanical and electrical portions. Nacelle covers of wind turbine generators, yaw systems, variable-pitch mechanisms and anemometers are often destroyed by super wind force and varied wind directions. The following preparations for typhoon emergency shall be well performed:

(1) Purchase living foods and materials for typhoon and flood prevention to make sure needs of production site.

(2) The Chief on duty shall mainly check related office equipment and articles in Center Control Building for normality.

(3) The Deputy to Chief on duty shall check all doors/windows and lighting system of Center Control Building.

(4) Team Leaders on duty shall check living water system for normality, quantity of living water fro sufficiency, in order to make sure normal water supply during flood and typhoon prevention.

(5) Drivers on duty shall completely check vehicles.

(6) Staff shall be organized to review and check power transformation equipment, wind turbine generators and casing transformers, as well as drainage of site, roads and highways of all wind farms before typhoon and flood.

(7) Based on damages of nacelle sheds and covers of wind generators in wind farms for many years, wind farms shall continuously sum up experience and lessons to prevent similar accidents occurring again.

(8) Before typhoon comes, fire pumps shall be tested and checked again to make sure pumping in time if necessary.

(9) Canteen staff in wind farms shall well perform all preparation before typhoon or flood comes.

(10) After a wind farm start company's emergency plans and the farm's implementation rules, all related people in the wind farm shall be informed. Director of the wind farm, professional safety inspectors, and members of overall teams shall be on the site for typhoon defence.

6.6.5 Emergency measures under different states of typhoon

(1) Upon reaching typhoon prevention warning state standard, the company shall declare to enter the warning state. The first responsibility person of the company shall hold a special meeting of the typhoon prevention leading group, knowing information, communicating states, analyzing and forecasting possible dangers, deploying work on typhoon prevention, checking working conditions of staff at all levels on duty and at posts, and arranging rush repair tasks. According to practical needs, the company leaders shall immediately organize certain working groups to enter dangerous areas, checking, supervising, coordinating and directing work of typhoon prevention.

(2) Upon reaching typhoon prevention emergency state standard, the company shall declare to enter the emergency state. The first responsibility person of the company shall hold a special meeting of the typhoon prevention leading group, knowing information, communicating states, analyzing and forecasting possible heavier dangers, deploying work on typhoon prevention, checking working conditions of staff at all levels on duty and at posts, and arranging rush repair tasks. The company leaders shall immediately organize certain working groups to enter dangerous areas, checking, supervising, coordinating and directing work of typhoon prevention.

(3) Upon reaching typhoon prevention heavy emergency state standard, the company shall declare to enter the heavy emergency state. The first responsibility person of the company shall hold a special meeting of the typhoon prevention leading group, knowing information, communicating states, analyzing and forecasting possible heaviest dangers, deploying work on typhoon prevention, checking working conditions of staff at all levels on duty and at posts, and arranging rush repair tasks. The company

leaders shall immediately organize certain working groups to enter dangerous areas, checking, supervising, coordinating and directing work of typhoon prevention.

6.6.6 Measures during typhoon surprise

(1) During severe weather when typhoon is making a front surprise or landing on near area, all emergency rescues and disaster relief work in a wind farm must be arranged in order of priority, considering the view point of ensuring persona and equipment, acting according to practical circumstances and never taking risks.

(2) All typhoon-fighting persons, with the exception of persons on duty staying in Center Control Building, shall rest and await orders in staff dormitories, and only if necessary start to the site for wind turbines reposition, inspection tour, rush repairs and so on.

(3) During typhoon, the team leader on duty in janitor's room of Center Control Building shall arrange for persons to monitor, interrogate and inspect site states round the clock, monitor equipment in service and weather changes, report practical situations in time to the field commander and the team leader on duty.

(4) The field commander and the team leader on duty shall arrange all tasks according to practical situations when conditions permit, regularly organize persons for inspection tour, making inspection tour for field and roads of all wind farms and resetting generating equipment, repairing and replacing damaged wind generators, performing remote control and repair for similar frequently starting/stopping DEWIND wind turbines from too great wind speed in order to make sure automatic wind adjustment, making power-off rush repair for 10kV line with earthing failure, handling individual unexpected accidents.

6.6.7 Assessment after disasters and production recovery

In case risks of typhoon and any accident occur, after the accident, besides cooperation in accident investigation according to the requirements of State Administration of Works Safety and State Electricity Regulatory Commission, the wind power company shall form an accident investigation group for the accident investigation.

(1) **Assessment after disasters.** After the typhoon-fighting work, the wind power company shall assist the insurance agent in determining the nature of losses and making quantitative assessment. The results of assessment shall be kept in the archives. At the same time, a person shall be specially assigned to follow the insurance agent with claim settlement, supervise and urge the insurance agent for fund in place quickly.

(2) **Production recovery.** Production shall be recovered as soon as possible to minimize losses.

Chapter 1 "Climate characteristics of tropical cyclone affecting China mainland coastal and offshore area" and Chapter 2 "Characteristic analysis of tropical cyclone wind field" were written by Zhang Rongyan, Zhang Xiuzhi, Li Qiang and Xing Xuhuang. Chapter 3 "Effect of tropical cyclone on wind power development" was written by Wu Jincheng. Chapter 4 "Strategy resisting typhoon in coastal wind power

development" was written by Liang Zhiqiang. Chapter 5 "Emergency management resisting typhoon in wind farms" was written by Qu Haibin. The manuscript was unified, modified and finalized by Yan Junyue, Zhang Xiuzhi and Yang Xiaosheng, and checked and approved by Zhu Ruizhao.

7 SUMMARY

Expected targets have been successfully fulfilled with the following innovative achievements in the project:

- Statistic analysis of the tropical cyclones landing on China mainland has been conducted in 8 regions, and the times of landing of the tropical cyclones in coastal areas of Zhejiang Province and those in the north of Fujian Province has obviously increased with the times. An obviously decrease in times of landing thereof has taken place in offshore areas in the north of Zhejiang Province, and that in central and southern Fujian Province and the costal areas on the east of Pearl River estuary almost remains unchanged over the time, while a declining momentum has taken place in western Guangdong Province, Leizhou Peninsula and Hainan islands area.

- The maximum in-process wind series of the tropical cyclones at the mesh points 50km×50km in offshore areas of China have been calculated by the asymmetrical wind field model of typhoon, and the distribution of the maximum wind speeds of the strongest wind in 50 years and the frequencies of the occurrence of wind speeds in various operational levels of the wind turbines. .

- The horizontal wind fields, the vertical shear of winds, strength of turbulent flow during 19 periods under the influence of tropical cyclones have been analyzed with the data of 85 wind towers and a great deal of ground meteorological data, and the characteristics of variation in the vertical shear of winds and strength of turbulent flow in case of various distances to the center of the tropical cyclones, various terrains, various lower surfaces and wind directions.

- It can be seen that typhoon moves quickly in case of no terrain factor with the meso-scale numerical model WRF and test of terrain sensibility. The terrain of Taiwan causes typhoon to weaken about 3 hours before landing, and the power and source of heat of typhoon on which it depends for maintenance or development are influenced by the terrain there after landing of the typhoon, which renders the power and structure of thermal field asymmetrical. The higher the terrain is, the more obvious the asymmetry is, the faster and fiercer the “eye area” is filled and the more incomplete the structure of the “eye wall” is.

- "Influences of Typhoon on Offshore Wind Power Development in China and Countermeasures" addresses the scientific issues and demands of coastal and ocean wind power development, and conducts gradual in-depth presentation of the climatic characteristics of the tropical cyclones influencing coastal areas and offshore areas of China mainland and expounds the characteristics of the wind field of tropical cyclones and analyzes the influences of tropical cyclones on wind power development, countermeasures against typhoon in costal wind development and emergency control of typhoon wind power fields through integrating the experience of the typhoon experts and wind power experts. In addition, it features novel contents, a well-knit structure with both illustrations and texts of both knowledgeability and readability.